IMPROVING INTELLIGENCE OF ROBOTIC LOWER-LIMB PROSTHESES TO ENHANCE MOBILITY FOR INDIVIDUALS WITH LIMB LOSS

A Dissertation
Presented to
The Academic Faculty

By

Krishan Bhakta

In Partial Fulfillment
of the Requirements for the Degree
Doctor of Philosophy in the
George W. Woodruff School of Mechanical Engineering
College of Engineering

Georgia Institute of Technology

December 2021

IMPROVING INTELLIGENCE OF ROBOTIC LOWER-LIMB PROSTHESES TO ENHANCE MOBILITY FOR INDIVIDUALS WITH LIMB LOSS

Thesis committee:

Dr. Aaron Young, Advisor
School of Mechanical Engineering
Georgia Institute of Technology

Dr. Ye Zhao
School of Mechanical Engineering
Georgia Institute of Technology

Dr. Anirban Mazumdar
School of Mechanical Engineering
Georgia Institute of Technology

Dr. Young-Hui Chang
School of Biological Sciences
Georgia Institute of Technology

Dr. Frank Hammond III
School of Mechanical Engineering
Georgia Institute of Technology

Date approved: December 6, 2021

The mindset isn't about seeking a result — it's more about the process of getting to that result. It's about the journey and the approach. It's a way of life. I do think that it's important, in all endeavors, to have that mentality.

Kobe Bryant

This work is dedicated to my family, for I would not be where I am without them.

ACKNOWLEDGMENTS

I want to thank everyone that has made this journey possible. I would not be where I am without the help of everyone that has made this such an enjoyable experience. I want to thank my family for the constant support and unconditional love you have always given me. To my parents, who never let me feel that anything was out of reach. To my siblings, for always having my back and pushing me to be better.

To Dr. Aaron Young, thank you for giving me an opportunity to be part of an amazing research lab. Thank you for all the support and guidance throughout the years. Thank you to all my committee members for playing pivotal roles to help me improve and become a better researcher.

Thank you to everyone in the EPIC, POWER, and DART labs. I have made lifelong friends and this would not have been possible with you. Thank you for all being on the rollercoaster with me.

To Jonathan, my work husband, thank you for teaching me to always be humble and have a passion for learning. You have helped me tremendously throughout the years, and I am lucky to call you my friend.

To Diana, thank you for your support and positive energy. You always were ready to lend a hand, no matter what it was. So thank you!

To the prosthesis team, thank you for all the laughs, memories, and support I received during this journey!

To Ben, thank you for being an awesome friend! You helped me realized that you can always have a good time, so thank you!

To Inseung, this journey would not have been possible without you. Thank you for your enthusiasm and always willing to help out when needed.

To Dawit, to being always kind and always willing to help me in whatever I needed, so thank you!

To Kinsey, thank you for everything you have done for me. You have made me a better person and none of this would have been possible without you.

To all my undergraduate students over the years, thank you for all your hard work and help. Without this, I would not be in the position I am now. So thank you!

To all the subjects who participated in our studies – I cannot thank you enough for all your time and patience you gave us over the years.

TABLE OF CONTENTS

LIST OF TABLES

LIST OF FIGURES

SUMMARY

The field of wearable robotics is an emerging field that seeks to create smarter and intuitive devices that can assist users improve their overall quality of life. Specifically, individuals with lower limb amputation tend to have significantly impaired mobility and asymmetric gait patterns that result in increased energy expenditure than able-bodied individuals over a variety of tasks. Unfortunately, most of the commercial devices are passive and lack the ability to easily adapt to changing environmental contexts. Powered prostheses have shown promise to help restore the necessary power needed to walk in common ambulatory tasks. However, there is a need to infer/detect the user's movement to appropriately provide seamless and natural assistance. To achieve this behavior, a better understanding is required of adding intelligence to powered prostheses. This dissertation focuses on three key research objectives: 1) developing and enhancing offline intent recognition systems for both classification and regression tasks using embedded prosthetic mechanical sensors and machine learning, 2) deploying intelligent controllers in real-time to directly modulate assistive torque in a knee and ankle prosthetic device, and 3) quantifying the biomechanical and clinical effects of a powered prosthesis compared to a passive device. The findings conducted show improvement in developing powered prostheses to better enhance mobility for individuals with transfemoral amputation and show a step forward towards clinical acceptance.

CHAPTER 1
INTRODUCTION

1.1 Motivation

The need to develop smarter prostheses is becoming a more prominent issue, as recent projections indicate that the number of individuals with lower-limb loss will increase significantly over the next couple of decades [1]. These individuals ambulate with a variety of gait abnormalities and as the result of using compensatory strategies, many develop asymmetric joint biomechanics, chronic leg and back pain, joint degradation, increased energetic demands, and higher risk of osteoarthritis [2, 3, 4, 5, 6, 7]. These impairments cause significant disabilities and decrease quality of life. The steady increase of lower-limb amputations stem from a variety of reasons such as trauma, vascular disease (i.e. diabetes), congenital limb deficiencies, and cancer across a wide age range of individuals [8]. The rehabilitation process for an individual suffering an amputation is very taxing and current available technology may not restore complete function compared to a pre-amputation state. Hence, there is a significant need to advance lower-limb prostheses to dampen the negative effects of amputation on the health outcomes of potential prosthesis users.

Current solutions of lower limb prostheses can be divided into three major groups: passive, semi-active (i.e. variable damping), and powered/active devices [9]. The most abundant type of prostheses currently available in the marker are passive, which lack the ability to generate net positive power over a gait cycle, which leads to an increased demand in user effort [10]. Although, passive devices serve the purpose of providing weight-bearing support, they are unable to enable efficient gait biomechanics on different terrains [11]. The best commercial devices to date, include onboard microprocessors to

modulate stiffness/damping responses in respect to the environment. These semi-active devices allow for improvement on purely passive devices by adapting to different terrain, but still lack the ability to generate net positive work throughout the gait cycle which is necessary for walking upstairs and at incline [10]. There have been research investigations in modulating foot properties to allow for the optimal stiffness profiles during walking which have yielded improved comfort to the user [12]. Powered prostheses are a promising new technology that may help lower limb amputees function at higher levels in their daily lives because of their ability to adjust to different terrain and provide appropriate assistance when required [13, 14, 15, 16].

Active devices can generate net positive work and exert torques that cannot be achieved with passive systems. Recent advances on the integration of microprocessors/microcontrollers, sensors, and actuators coupled with innovative mechanical design have helped in the understanding of creating smarter prosthetic technology [13, 16]. Lastly, in order for powered prostheses to become the prominent technology, good mechanical hardware is required. Considerations of weight, power requirements, and adaptability to users is critical to improve amputee quality of life. Many different types of prostheses have been created to address this need [14, 15, 17, 18, 13, 19, 20, 21]. Furthermore, prosthesis emulator systems have been established as an alternative method for quickly testing out control paradigms without the need for building custom hardware [21]. Still, there exists a gap, powered prostheses are constrained to laboratory settings with no flexibility to be used in more realistic environments (i.e. home and community ambulation). Recent advances in mechanical hardware have led to the culmination of multiple prosthetic platforms that can be used across research groups to effectively compare control strategies and accelerate the process of having this technology disseminated for clinical use. In parallel, these advances have led to improvements in better mobility as well as reductions in energy expenditure [22, 9, 23]. A gap is still seen in the field of implementing these new devices into clinical settings across a variety of

users in a robust and reliable manner. Although, these devices have the capability of full actuation, this implies increased complexity from a control perspective. The need for further comparison between powered and passive prostheses is required to ensure clinical acceptance of these devices. To achieve this goal, sophisticated, robust, and reliable control systems must be developed to recognize user needs and provide seamless assistance.

As the name suggests, powered prostheses have the ability to aid the user at different parts of the gait cycle (i.e. typically called the mid-level control tier). In the past decade, many different mid-level control laws have been investigated including trajectory control (i.e. echo control), discrete control (i.e. impedance control paired with a finite state machine), continuous control (i.e. non-linear or phase-variable), and bio-inspired control (i.e. electromyography (EMG)-based or model based control) [24, 25, 26, 27, 28, 29, 30, 31, 32, 33]. Although a multitude of studies have been conducted, it is still unknown which control strategy is effective across a wide range of walking tasks. However, there is a growing consensus that both intrinsic and sensory feedback signals improve the efficacy of these environmental-adaptive controllers. A challenge in the field is how to avoid manual user-specific tuning of control parameters across terrains. Investigating how scaling-enabled controllers can modulate assistance over different terrains will increase the chance of having these intelligent prostheses be clinically deployed. The idea of using machine learning and sensor fusion techniques in real-time can be explored to estimate environmental variables in a more continuous fashion which allows for more natural, seamless control.

Commanding and adjusting the control parameters for these powered devices is a much needed and active area of research. The end goal is to have a controller that can adapt and modulate assistance to enhance human performance across many different tasks. Since walking is a highly dynamic task, the need to understand what/where the user is doing as well as understanding the context of the environment is crucial to update the

controller. Different strategies have been introduced in the literature to estimate the user's state and environment [34, 35, 33, 36, 37, 38, 39, 9]. Most strategies will use a mechanical sensor such as an inertial measurement unit (IMU) to determine the user state [40, 41]. However, these approaches do not yield robust results for more dynamic tasks and are limited by slow update rates and inaccurate estimations. Recent literature has shown that implementing machine learning (ML) based strategies show good promise in making these powered robotic devices autonomous and implementable in real-time. Specifically in the case of powered prostheses, several research groups have studied how to improve high-level controllers (i.e. intent recognition algorithms) to replace current methods of transitioning between ambulation modes such as using a key fob or performing unnatural movements [34, 35, 33, 36, 37, 38, 39]. Multiple intent recognition strategies have been explored in the last several decades. There have been key innovations made in the last decade for improving mode identification or classification for these devices. The first major study to accomplish offline mode classification was Huang et al. in 2009, where phase-specific classifiers were used on EMG sensors embedded within the socket of the passive prosthesis [42]. This showed better results compared to a single window of information that was fed to one classifier. Building upon this work, Varol et al. showed the first real-time user-dependent using only mechanical sensors on a powered knee and ankle prosthesis [36]. In 2014, Young et al. developed time-history methods that improved steady state classification errors compared to no time-history methods [43]. Hargrove et al. implemented the first-real time user dependent classifier that used both EMG and mechanical sensors paired with the previously developed time history methods [38]. Two key findings were found in a study conducted in 2016, where Young et al. created mode-specific classifiers as well as the first implementation of a user-independent system [39]. Utilizing mode-specific classifiers reduced the number of classes each model would have to predict for specific tasks (ex. LW and SA only). The implementation of a user-independent system allowed for training models on a pool of subjects and evaluating

on a novel subject. Simon et al. in 2017 showed that delaying the transition decision by 90 ms between modes did not affect the user but also allowed for richer information for a mode classifier to detect a mode change which vastly improved the overall classification accuracy [44]. An additional challenge is that the powered prosthesis is not directly attached to the user's motor system. The controller must infer, indirectly, the intent of the user within the context of the environment and then, aid the user in the desired movement. Providing feedback or having volitional control of the prosthesis through a neural interface is key to interpret the user's intent during locomotion [45, 46, 47, 48, 24, 49].

In the context of powered prostheses, there have been limited research studies exploring methods of detecting environmental variables such as walking speed and ground slope. However, methods have been developed for wearable sensor systems (i.e. IMUs) and exoskeleton devices. Direct integration of a foot IMU's information was used to calculate walking speed in healthy individuals [50]. Sup et al. in 2011 took a similar method but applied to estimating slope on a powered prosthesis [51]. Improvements upon these methods have been made. Specifically, a study looked at coupling direct integration methods with kinematic modeling [52]. Kang et al. in 2019 looked at the effect of utilizing EMG information to improve both speed and slope estimation using a hip exoskeleton [53]. Few studies have explored this with individuals with transfemoral amputation. Dauriac et al. in 2019 estimated walking speed with a single shank IMU with individuals with transfemoral amputation; this study explored both direct integration and kinematic modeling approaches seen in prior literature [54].

Another issue for developing reliable high-level controllers is the lack of intuitive human and robot interaction, which can lead to under-utilization or even abandonment of this type of technology. Currently, it is unknown how to effectively design and utilize intelligent but reliable control systems that can enhance the user experience when using a powered prosthesis. Machine learning is becoming a more prominent tool that can be used to estimate what the user is trying to accomplish and adapt to more versatile and dynamic

motions. A critical need to be addressed is to have these algorithms be dependable in real-time as well as generalize across different users.

In order for this type of technology to be translated to clinical settings, a thorough analysis must be performed to understand the functional benefits of the powered prosthesis compared to commercially available prostheses. Furthermore, a recent review paper argues that metabolic analysis over common community ambulation tasks is necessary to advance the field by making comparisons between prosthetic devices [55]. Both biomechanical and clinical measures of powered prostheses must be evaluated in order to show improvement compared to passive devices. A challenge with current state-of-the-art robotic prostheses is the user acceptance of these devices. Comparative surveys (i.e. prosthesis evaluation questionnaire (PEQ) or lower extremity functional scale (LEFS)) conveying user perception and effort of wearing powered prostheses is a must. Additionally, a gap exists in the field, if these powered devices do not provide an intuitive method of control, users will opt for traditional but reliable prostheses regardless of the drawbacks. Hence, investigating how to properly implement intent recognition systems into current robotic prosthetic technologies will yield wide acceptance of these devices.

1.2 Objectives

In order to improve individual's quality of life for those with amputation, enhancing mobility is a must to achieve independence in common ambulatory activities. Even though there have been many key findings made, there are still key research gaps present. First there have been many dependent offline studies but there is a lack of exploring user independent strategies. Although it has been seen that user dependent models can be run in real-time, there have been no real-time user independent systems that have been tested using solely mechanical sensors. Third, there have been no studies exploring how well these user dependent and independent models can generalize to different grades of context (i.e. stair heights or ground slope angles). Most studies have used methods which require

at least 1 gait cycle before they can make an estimate, and not many intent recognition systems try to infer user intent in a continuous fashion. Lastly, there has been no real-time tiered intent recognition system where a controller first predicts an ambulation mode and then within continuously estimate an environmental variable like ground slope. The main objective of this dissertation is to create a deployable real-time intent recognition system that can infer the user's intention during different ambulation modes and environmental contexts. This dissertation focuses on better understanding and applying intelligence to a control system embedded on an active lower-limb prosthetic device. This works looks to expand current literature and improve clinical outcome measures such as symmetry and energy expenditure for individuals with transfemoral amputation. The work entails the investigation of using sensor fusion techniques coupled with machine learning to improve control strategies in powered prostheses to promote better human-robot symbiosis. My central hypothesis is that continuous state and environment estimation using mechanical and wearable body sensors coupled with implementing machine learning techniques can enhance robotic prosthetic controllers to seamlessly sync robotic assistance with the user compared to passive devices. In this dissertation, I focus on 4 main research aims: 1) offline machine learning analysis of mode classification, 2) offline continuous machine learning analysis of walking speed, 3) real-time implementation of a tiered mode/slope system and walking speed estimator to scale parameters across contexts, and 4) comparison of biomechanical profiles between the powered vs passive prostheses across level walking, stairs, and ramps.

Aim 1: Develop, optimize, and validate machine learning (ML) algorithms to predict ambulation mode using sensor fusion and signal processing techniques. Based on the collection of mechanical sensors onboard the prosthesis, the main goal is to make a mode classifier that can predict the difference between level ground, ramps, and stairs. This information could help these high-level controllers to enable individuals with amputation to seamlessly transition between locomotion modes. Furthermore, I

hypothesized that more complex and customizable algorithms, like XGBoost, will improve the accuracy of the classification and scale across different grades of terrain by learning patterns that are not described by simple methods, especially when using inputs from multiple sensors. Secondly, I hypothesized that adding extra mechanical sensors can help to improve the performance of both user-dependent and user-independent classifiers.

Aim 2: Establish and validate a ML framework that can perform continuous speed determination utilizing embedded sensors. Another aspect of making powered prostheses more clinically relevant is the ability to estimate what environmental context you are in. Furthermore, having the ability to continuously estimate the terrain can allow for adaptive control strategies to be employed to scale assistance in a meaningful way. The hypotheses here are (a) that the inclusion of more sensors will yield in an improvement of model accuracy and (b) that optimization of ML algorithms using signal processing and sensor fusion techniques will reduce the speed of prediction in real-time.

Aim 3: Validate intent recognition systems in real-time coupled with scaling parameters across environmental contexts. Dynamically changing the appropriate control law based on amputee's intent (mid-level) is still not fully understood and not generalizable across users. Current methods are not capable of changing intrinsic control parameters to modulate assistance. Hence, I investigated how the use of scaling control parameters across different terrain can improve the functional benefit of the prosthesis. Furthermore, taking the information learned from Aims 1 & 2, I developed and validated a real-time intent recognition system that predicted mode first, and subsequently estimated slope angle and walking speed while directly adjusting scaling parameters at the mid-level. There are three main hypotheses in this study: 1) real-time error will perform worse compared to offline error, 2) the relative improvement in error from offline to real-time is worse for independent models compared to dependent models, and 3) User independent models will in general perform worse than user dependent models across different machine learning tasks.

Aim 4: Compare and validate prosthetic performance by comparing biomechanical & clinical measures to current commercially available passive prostheses. Individuals with transfemoral amputation typically have to use compensatory strategies (i.e. increased intact side hip work) to compensate for the lack of mechanical output on their prosthetic side. There is a gap in the field of understanding how the biomechanics of both the intact and prosthetic side change when utilizing a powered vs. passive device and how they compare to the results of healthy able-bodied individuals. I hypothesized that powered prostheses could reduce energy costs & improve symmetry between intact and prosthetic side compared to their everyday passive devices.

1.3 Innovation

This work is innovative in the lower limb prosthesis control field in the following three ways: 1) no known studies have done user-independent real-time (online) intent recognition traversing different types of terrains such as level walking and ramps for a

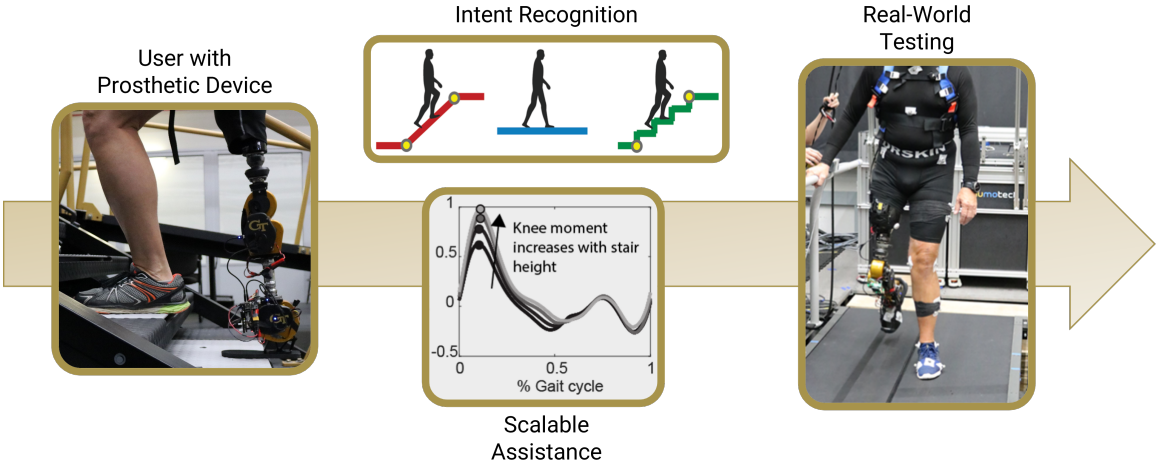

Figure 1.1: Flow diagram of how to implement these devices into the community more. Utilizing a powered prosthesis, the overall goal is to identify user intent, and then adjust control strategies for assisting the user appropriately during real-world community ambulation. The primary research goals are to create new frameworks of intent recognition systems that can be used either discretely or continuously to decipher user needs. Lastly these intent recognition systems must be deployed in real-time to show proper validation that these devices can be better than currently available technology.

powered knee/ankle prosthesis. 2) None of the intent recognition strategies proposed so far incorporate a tiered high-level controller which predicts ambulation mode and secondly estimates an environmental context variable (i.e. walking speed or inclination angle) 3) Finally, we provide in-depth biomechanical evaluation of using these active prosthetic controllers compared to passive devices.

1.4 Dissertation Outline

This document is organized into six chapters. Chapter 2 covers the methods of mode classification that were employed in this dissertation. The content described shows a novel machine learning algorithm (i.e. XGBoost) being used as well as showing results of its generalizability to multiple stair heights and inclination angles. The emphasis of this chapter is to create a guide of how to collect, process, and build a machine learning pipeline that can predict user intent in the form of mode classification. This chapter covers **Aim 1** and contains excerpts from:

- Bhakta et al. Machine Learning Model Comparisons of User Independent & Dependent Intent Recognition Systems for Powered Prostheses. IEEE Robotics and Automation Letters. 2021. DOI: 10.1109/LRA.2020.3007480.

Chapter 3 focuses on establishing a machine learning framework that can perform continuous speed determination for real-time applications on knee/ankle prostheses. Furthermore, there is a more in-depth comparison of user dependent and independent systems utilizing an expansive embedded sensor suite on a powered prosthesis Lastly, there is a validation of these techniques in static and dynamic speed tracking scenarios to emulate real-world scenarios that may be encountered in common ambulatory activities. This chapter covers **Aim 2** and contains excerpts from:

- Bhakta et al. Evaluation of Continuous Walking Speed Determination Algorithms and Embedded Sensors for a Powered Knee & Ankle Prosthesis. IEEE Robotics and

Automation Letters. 2021. DOI: 10.1109/LRA.2021.3068711.

Chapter 4 covers the investigation of deploying an embedded real-time intent recognition system on a powered knee and ankle device. The chapter provides improvements made to both the mid-level and high-level control paradigm typically employed on a robotic device. The first part of the chapter describes the tuning of impedance parameters and how scaling these parameters as a function of the environment is needed to make these devices more adaptable to various terrains. Secondly, there is a systematic comparison of deploying user dependent and user independent models in real-time to predict ambulation mode and then estimate both slope angle and walking speed. This chapter covers **Aim 3** and contains excerpts from:

- Bhakta et al. Impedance control strategies for enhancing sloped and level walking capabilities for individuals with transfemoral amputation using a powered multi-joint prosthesis. Journal of Military Medicine. 2020. DOI: https://doi.org/10.1093/milmed/usz229.
- Bhakta et al. Multi-Context Real-Time Intent Recognition for Powered Lower-Limb Prostheses (Preparing Manuscript)

Chapter 5 takes a more holistic view of the problem and looks to compare the biomechanical effects of using a powered vs passive prosthesis. The work contained in this chapter shows an in-depth analysis of the kinematic, kinetic, and energy profiles for both ramps and stairs. These results highlight the fact that providing appropriate and timely assistance profiles is key to enhance human performance metrics such as symmetry and to reduce work done by the intact side during these tasks. This chapter covers **Aim 4** and contains excerpts from:

- Camargo et al. Stair ambulation with an active knee and ankle prosthesis: a step forward towards biologically inspired biomechanics. (Under Review)

Lastly, Chapter 6 contains concluding remarks and conclusions of the dissertation with comments on future research directions. This works hopes to serve as a benchmark and framework to develop future intent recognition systems that can allow these devices to bridge the gap between research studies versus clinical settings. This dissertation aims to provide valuable information to add intelligence to these powered prostheses to be more useful for individuals with transfemoral amputation.

CHAPTER 2
OFFLINE MODE CLASSIFICATION OF USER INDEPENDENT & DEPENDENT INTENT RECOGNITION SYSTEMS

2.1 Background

Over the last two decades there have been many advancements in powered prosthetic technology that can aid users with lower-limb amputation and restore their locomotive abilities [13, 14, 56]. However, best practices for effectively coupling powered prostheses to individual users remain elusive. A recent challenge in creating smarter controllers is understanding how to recognize and adapt to user intent. Controllers which seamlessly decipher user intent and provide appropriate assistance will have greater viability in clinical scenarios.

Recent projections indicate that the number of individuals with lower-limb loss will increase significantly over the next several decades [1]. The steady increase of lower-limb amputations warrants the need to develop more advanced technology to allow users to ambulate more naturally and over terrains that they would often encounter in the community, such as stairs and ramps. Current solutions are mainly passive, which lack the ability to generate net positive work over a gait cycle. Hence, users develop compensatory strategies to walk which include having higher intact limb-joint moments that may lead to joint degradation, pain, and osteoarthritis [5, 6, 3, 7]. Powered prostheses may help to reduce some of these compensatory strategies, but still require more advanced and reliable controller designs [57].

Recent advances on the integration of microprocessors, microcontrollers, sensors, and actuators coupled with innovative mechanical design have paved the way toward further advancing smarter prosthetic technology. These powered devices show promise in being

able to help lower-limb amputees function at higher levels in their daily lives because of their ability to accommodate and provide appropriate assistance on different terrain which may in turn improve overall quality of life [38]. Robust and reliable implementation of controllers capable of accurate intent recognition (i.e. recognizing the desire to change between ambulation modes) is a non-trivial requirement given the high variability that frequently presents itself within given clinical populations.

Prosthetic control strategies have been explored to understand what techniques can be utilized to develop smarter algorithms [9]. Many research groups have focused on single lower-limb joint devices, and the lower limb prosthetic market to date only includes single joint (knee or ankle) powered technology [58, 59]. However, when more than one biological joint is missing, such as in a transfemoral amputation, an additional challenge is to ensure that two independently powered prosthetic joints can be controlled in a synchronous and stable manner. The most common prosthetic control strategies typically employ a three-tier controller paradigm: high-level, mid-level and low-level control [26, 9].

The high-level controller is responsible for detecting and deciphering user intent (i.e. determining locomotion mode or estimating environmental variables). The mid-level controller generates a desired profile at each joint throughout the gait cycle using either torque or position laws. The low-level controller's responsibility is to ensure that the actual torque output from the motor and transmission matches the desired torque. The focus of this chapter was to enhance the high-level controller as it is critical that these predictions have high accuracy given their direct impact on the behavior of the other two tiers, triggering actions of the prosthesis that depend on ambulation mode. Hence, the complete response of the powered prosthesis heavily depends on the determination of the user's ambulation mode. Manual triggers to transition between different locomotion modes are non-intuitive and presents a cognitive burden to the user while walking.

Machine learning or pattern recognition techniques have been shown to classify the

ambulation mode in powered prostheses from mechanical sensors [36, 34, 43, 60, 61] and neuromuscular signals [33]. These techniques have shown levels of accuracy that demonstrate potential for the application in intelligent control of detecting ambulation modes. Simon et al. implemented a mode-specific classifier that utilized a delayed mode transition decision of 90 ms while achieving an error of less than 0.5% [44]. However, as has been demonstrated in stability and error recovery studies, the response of such a system is highly sensitive to classification errors [37]. Traditionally, these implementations use methods that are relatively simple such as linear discriminant analysis (LDA) based on Bayesian theory [62, 34, 39, 43]. This offers the advantage of ease of use and fast training but are limited in capturing complex data dependencies. In addition, most of the methods have been used in a subject dependent setting, where they require training for everyone that wears the device, failing to capture patterns that are generalized across different users. Overcoming this challenge could reduce the burden of gathering lots of training data and may facilitate the adoption of smarter prostheses. In a previous study we proposed one of the first attempts of a method to produce subject independent classification that reduced the error levels to a range that allowed its use to control a prosthetic device [39]. However, we consider that additional development is needed to improve such systems, in particular with respect to a limitation that is consistently found in the literature: which is that all the training data is collected on a single ramp grade/stair height and tested on the same conditions. Furthermore, in most prior studies, classification accuracy have only been reported for a single height/incline in the training set. For real-world applications, these methods do not adequately represent community ambulation which has a larger variation in terrain, and as such, an intent recognition system must have the capability of adapting to different stair heights and inclination angles. However, this is a much more complex problem for a machine learning algorithm and is still an under-explored area of research.

Recent results in machine learning literature show the practical advantage of the

gradient tree boosting method in classification problems with tabular data in complex classification scenarios [63, 64, 65, 66, 67]. Amongst different implementations, the open source package XGBoost [68] has been established as a robust solution in a wide range of problems, dominating competitions such as Kaggle [69]. XGBoost is a supervised machine learning algorithm based on gradient boosting and ensemble learning techniques. This method allows representation of the learning problem as gradient descent on an arbitrary differentiable loss function. This technique uses clever penalization of individual trees by including an additional regularization term in the loss function to combat overfitting and to improve the classification or regression output compared to its predecessors. This algorithm was selected for multiple reasons which include: 1) additive tree models that can be seen to adaptively determine the size of local neighborhoods (i.e. improves the flexibility of the fit to the data), 2) weight functions are updated at each subsequent iteration of creating the tree while taking the bias-variance tradeoff into consideration during fitting, and 3) approximating complex functional relationships using additive tree models [68, 63, 70] . In addition, this model is easily usable and efficient when training on different tasks. This decision tree boosting algorithm also allows us not to be constrained with the assumptions of Bayesian classifiers in which a certain covariance structure is specified. In the realm of exoskeletons and prostheses, several groups have implemented ensemble algorithms in gait classification tasks [71, 72, 73, 74]. To the authors' knowledge, this is a new algorithm that has not been implemented in the field of lower-limb powered prostheses.

One novel aspect of this chapter compared to prior literature is having an expanded mechanical sensor set embedded on the prosthesis which includes 6-axis IMUs on the foot, shank and thigh, a 6-axis load cell, and joint encoders at the knee and ankle. Furthermore, our experimental paradigm allows for a unique data set to test generalizability across multiple stair heights and ramp inclination angles, and lastly exploring the use of a new algorithm for wearable robotics (XGBoost) on classifier

performance. Thus, our first hypothesis is that more complex algorithms like XGBoost will improve the accuracy of the classification and scale across different grades of terrain by learning patterns that are not described by more simple methods, especially when using inputs from multiple sensors. Secondly, we hypothesized that adding extra mechanical sensors could help to improve the performance of both user-dependent and user-independent classifiers. This chapter provides meaningful information for future development of user-intent recognition systems that can be clinically relevant.

2.2 Experimental Methods

2.2.1 Powered Knee & Ankle Device

In this chapter, we utilized a powered knee and ankle prosthesis that features two independently controlled joints at the knee and ankle, providing powered assistance in the sagittal plane; a more detailed presentation of the prosthesis can be found in a previous paper [20, 75]. Briefly, the prosthesis includes six embedded mechanical sensors: two joint incremental encoders (US Digital E5) to measure knee and ankle kinematics, a 6-DOF (degree of freedom) load cell (SRI M3714C2) to measure ground reaction forces and moments, and three 6-axis (accelerometer & gyroscope) inertial measurement units (YOST 3-Space LX embedded) (IMUs) (Figure 2.1). All sensors were collected at 100 Hz except for IMUs, which were sampled at 250 Hz. A three-tier control paradigm was implemented in this protocol. The low-level controller was responsible for minimizing error between the desired and actual torque profiles. The mid-level controller was an impedance controller paired with a finite state machine. Furthermore, the gait cycle was discretized into four states (early stance, late stance, swing flexion, and swing extension) for each ambulation mode [26]. Detailed approaches of how impedance parameters were tuned were based on previous literature [76, 26]. The high-level controller is responsible for predicting transitions between different ambulation modes (i.e. user intent) and estimating features of different terrain. The focus of this chapter was to demonstrate a

method of developing a user intent recognition system that could be utilized on wearable robotic devices.

2.2.2 Protocol Design

Eight individuals (7 males/1 female, age: 49.63 $\pm$ 13.68 years, height: 1.77 $\pm$ 0.07 m, mass: 87.31 $\pm$ 16.47 kg) with unilateral transfemoral amputation (4R/4L) were recruited and provided informed consent in accordance with the Georgia Institute of Technology Institutional Review Board. The prosthetic device was configured to each user by a certified prosthetist for appropriate comfort and alignment. The prosthetist guided the subjects in adjusting their gait to overcome any exaggerated or over-compensatory

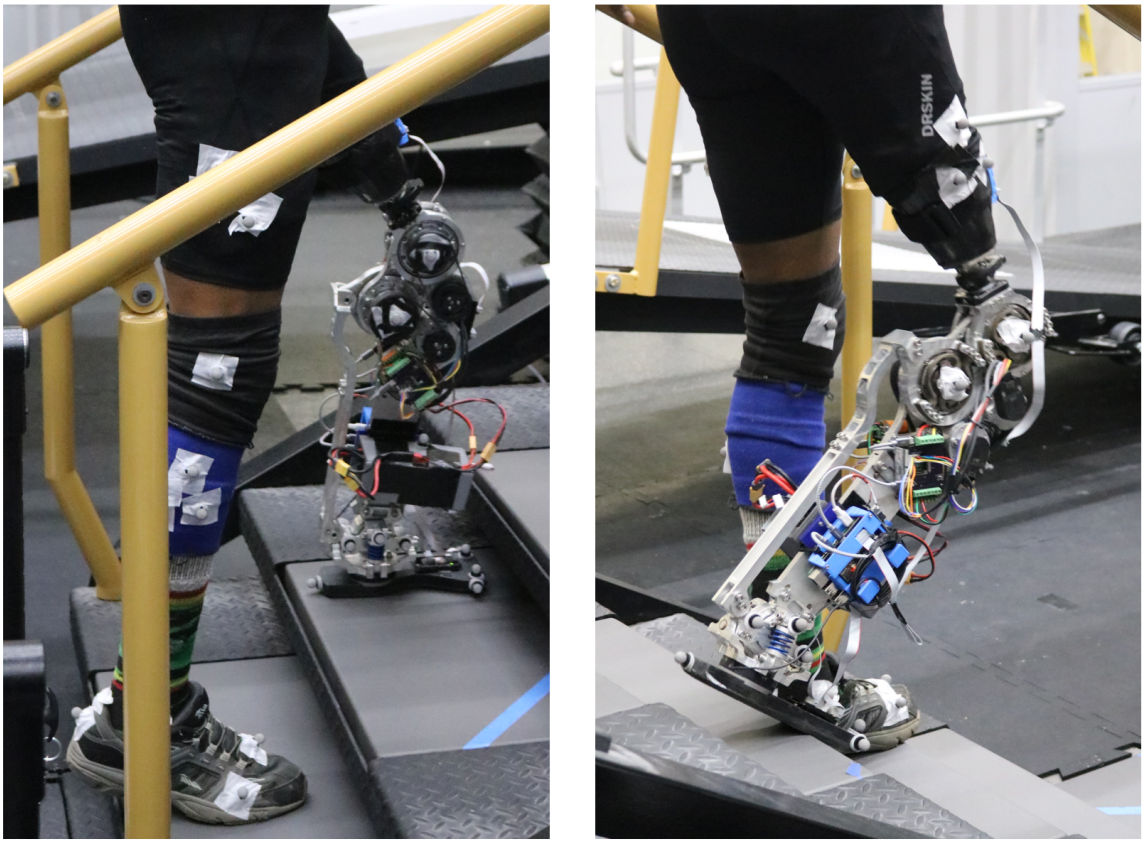

Figure 2.1: Experimental setting in which one individual with transfemoral amputation is completing a stair ambulation trial across our custom-built terrain park. The terrain park is adjustable and can be modified between different stair heights and inclination angles. Embedded sensors on the prosthesis which include two joint encoders, one 6-DOF load cell, and three 6-axis inertial measurement units are useful in deciphering user intent.

movements. When the prosthetist was satisfied with the tuning process, we conducted our collection of ambulation circuits. Users were asked to complete 2 types of ambulation circuits (ramp circuit: level walking (LW), ramp ascent (RA), & ramp descent (RD), stair circuit: level walking (LW), stair ascent (SA), & stair descent (SD)) of each preset condition in our in-lab terrain park area using our powered prosthesis. Our custom built terrain park was adjusted and set to 4 different presets for which 4 ramp trials occurred at 7.8°, 9.2°, 11.0°, and 12.4°and 4 stair trials at 10.2 cm, 12.7 cm, 15.2 cm, and 17.8 cm. Hence a total of 32 trials were collected from each subject across all the different modes. Ambulation mode labels were generated using our finite state machine. Steady state steps (SS) were identified if the previous gait event (heel contact or toe-off) remained in the same event. While transitional steps (TS) were identified if the previous gait event on the previous mode was different on the next mode (e.g. LW_LateStance to SA_SwingFlexion – was labeled as SA).

2.2.3 Data Processing and Feature Extraction

To ensure an appropriate input of data to train our mode classifiers, a general workflow was implemented to investigate and compare multiple machine learning algorithms for predicting locomotion mode (Figure 2.2). We had 6 embedded sensors on the prosthesis (2 encoders, 3 IMUs, and 1 load cell). We had 2 channels from each encoder and 6 channels from each IMU and the loadcell. We extracted 5 feature types (minimum, maximum, mean, standard deviation, and ending value) resulting in a total of 140 features (28 channels x 5 feature types = 140 total features) for a given window [36, 33, 43]. We ran two sequential forward simulations to see if certain feature types and channels were needed. It was found that removing any given feature type did not result in a decrease in classification error. Similar results were seen in the channel simulation. Hence, to be conservative, all the features were kept, since there was no evidence of overfitting from these simulations. The experimental data was neither based on timing or % gait cycle, but

rather the 6-DOF loadcell to transition between phases of each ambulation mode as seen in previous studies [26]. Gait decisions were made at toe off (weight under a threshold) and heel contact (weight exceeding a threshold) to create reliable time points for transitioning the device between ambulation modes. A normalization scheme was applied first at the sensor level by dividing the load cell signal by each subject's respective weight. Furthermore, a z-score normalization was explored across all sensors on the feature level, with the load cell showing the best improvement compared to non-normalized data.

2.2.4 Locomotion Mode Classifiers

Initially, five algorithms were chosen for performance comparison in mode classification. These algorithms were linear discriminant analysis (LDA), quadratic discriminant analysis (QDA), Naive Bayes (NB), neural networks (NN), and XGBoost. The Bayesian classifiers were selected as being the current standard in the field of low-error classifiers. We ran a performance comparison across these Bayesian techniques in which LDA showed the lowest error. LDA has also been seen in prior work to be the gold standard to compare against [77]. Hence, the model comparison was reduced to 3 models: LDA, NN, and XGBoost. For each phase, a specific classifier was trained to capture the optimal transition point. Depending on the gait mode transition, the time during the gait cycle in which the classifier must make its decision is inherently gait phase specific. This strategy of transitioning is not unique and many groups have used a similar phase dependent scheme to change between gait modes based on gait events, and we adopt a similar approach here [43, 26, 44, 14].

2.2.5 Algorithm Optimization

Hyperparameter optimization of NN and XGBoost was completed to ensure model architectures were appropriate for generalizing our mechanical sensor information for the task of mode classification; LDA did not require any additional tuning. Scripts were

Table 2.1: Final mode classification optimized parameters

	NN	XGBoost
DEP	Layers: 1 Nodes: 50 Optimizer: $Adam$ Learning rate: 0.001 Activation function: $relu$ Batch size: 32	Max depth: 1 Lambda: 0.5 Min split loss: 0 Learning rate: 0.3
IND	Layers: 3 Nodes: 10 Optimizer: $Adam$ Learning rate: 0.001 Activation function: $tanh$ Batch size: 128	Max depth: 3 Lambda: 1 Min split loss: 0.1 Learning rate: 0.3

written for all models and case studies (dependent, independent, remove-one-height/incline) and an initial window size of 250 ms was selected. We started with a directed search of unique hyperparameters for each algorithm. The subset of parameters resulting in the lowest average error between steady state and transitional error was selected until all of the parameters were swept. In XGBoost, the set of hyperparameters explored included: the learning rate used to influence the convergence to a solution, the maximum allowable tree depth, the regularization term to control the sensitivity, and minimum gain required to further split on a node in the tree (Table 2.1). In the NN, the set of hyperparameters included: layers and nodes to determine adequate size of the network needed, optimizer and learning rate to influence the convergence to a solution, and activation function and batch size to limit model complexity.

After model optimization, a window size sweep was performed from 50 ms to 500 ms in increments of 50 ms, with the evaluation metric of taking the average of the steady state and transitional error together. The optimal window size was found to be 250 ms. Specifically, the transitional error had a minimum at 250 ms, with larger error associated with smaller or larger windows; while steady-state error was reduced the most at 250 ms and held approximately constant with larger window sizes.

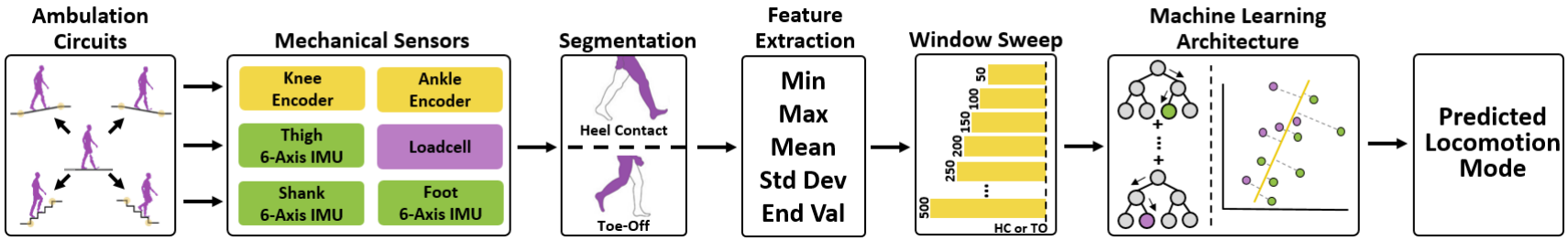

Figure 2.2: The machine learning workflow used to predict user locomotion mode is shown. Users were asked to perform ambulation circuits which involved walking in 5 locomotion modes - LW, RA, RD, SA, and SD. Joint encoders that measured angular position and velocity, 6-DOF loadcell that measured ground reaction forces & moments, and IMUs that measured acceleration and rotational velocities were first segmented into two phases - heel contact and toe-off. The next algorithm consisted of transforming the data into several features (minimum, maximum, mean, standard deviation, and ending value) for a fixed window size. Next, a window size sweep was performed to find optimal window length to predict locomotion mode based on transitional error. The features were then passed through each machine learning algorithm (LDA, NN, and XGBoost) to predict locomotion mode. NN and XGBoost had to undergo an extra step of hyper-parameter tuning. In NN, layers, nodes, optimizer, learning rate, activation function, and batch size were swept. In XGBoost, learning rate, maximum tree depth, regularization term, and minimum gain were swept. After an optimized set of parameters were chosen, models were trained for our 6 different case studies to predict locomotion mode.

2.2.6 Model Evaluation

Several steps were taken to prevent overfitting of each model. First, six different case studies were explored: dependent (DEP), independent (IND), remove-one-height dependent (RM-1-H-DEP), remove-one-height independent (RM-1-H-IND), remove-one-incline dependent (RM-1-I-DEP), and remove-one-incline independent (RM-1-I-IND). The DEP case study was similar to previous literature where data was trained on each individual subject and evaluated using a remove-one-trial cross validation. The IND case study was also taken as a traditional method of training on all users except for one which in turn became the test set. Thus, in these first two cases, both the train and test set had examples from the same stair height and ramp incline conditions. The RM-1-H-DEP and RM-1-I-DEP conditions were trained with all of the ramps and stairs conditions except for the unknown height or incline that served as the test set. This procedure was repeated until each height or incline was included in the test set. Lastly, the RM-1-H-IND and RM-1-I-IND conditions were trained with all the data except for all of the subjects' data at a specific height or incline and the removed subject's data. These were then tested on the removed subject's specific height or incline that was not in the train set. Similar to the RM-1-DEP cases, this procedure was repeated until each height or incline was swept. Our error criteria for evaluating the model's performance can be seen in the following equations (Equation 2.1, Equation 2.2, Equation 2.3), where SS is steady state steps, TS is transitional steps, HC is heel contact, and TO is toe off. This error was then averaged across subjects for both the steady state and transitional errors.

$$SS\_error = 1 - \frac{SS\_correct\_HC + SS\_correct\_TO}{SS\_total\_HC + SS\_total\_TO} \tag{2.1}$$

$$TS\_error = 1 - \frac{TS\_correct\_HC + TS\_correct\_TO}{TS\_total\_HC + TS\_total\_TO} \tag{2.2}$$

$$sensor\_error = 1 - \frac{SS\_error + TS\_error}{2} \tag{2.3}$$

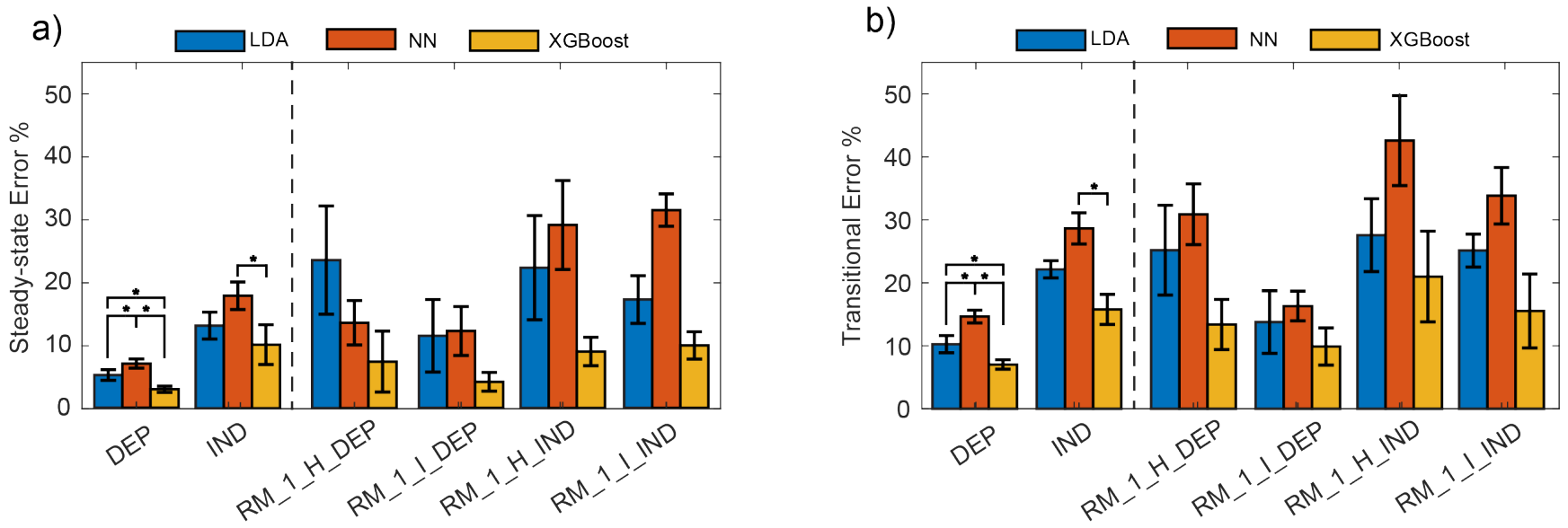

Figure 2.3: Three different models (LDA/NN/XGBoost) were compared for the classification of ambulation mode in ramps, stairs and level-ground, resulting in XGBoost outperforming other models. The y-axis shows the performance metric, consisting of the error in classification during steady state walking within a mode and the error of transitioning between modes. The x-axis show the six conditions of evaluation: subject dependent (i.e. training and testing on the same subject), subject independent (i.e. training on all subjects but the testing subject), and remove-1 condition for the stair height and ramp inclination for both a) dependent and b) independent. Error bars represent $\pm$ standard error of the mean. Asterisks indicate statistical significance ($p<0.05$).

2.2.7 Statistical Analysis

We conducted a one-way repeated measures analysis of variance (ANOVA) to compare the model performance across only the DEP and IND conditions (α = 0.05). The independent variable was the machine learning model (LDA/NN/XGBoost). A Dunn–Bonferroni post-hoc correction was used to compute the statistical differences between each condition (Minitab 19.0, USA).

2.3 Results

2.3.1 Model Comparison

In the DEP case for steady state error, XGBoost (2.93% $\pm$ 0.49%) was found to be the best model compared to LDA (5.20% $\pm$ 0.85%) and NN (7.01% $\pm$ 0.73%)($p<0.05$). Similar results were found in the transitional error case, where XGBoost (7.03% $\pm$ 0.74%) had the lowest error compared to LDA (10.26% $\pm$ 1.36%) and NN (14.66% $\pm$ 1.02%)($p<0.05$). In the IND case for steady state error, XGBoost (10.12% $\pm$ 3.16%) was found only to be statistically different than NN (17.89% $\pm$ 2.19%). Similar trend was seen in the transitional error, where XGBoost (15.78% $\pm$ 2.39%) was found to be only statistically different than NN (28.65% $\pm$ 2.48%).

2.3.2 Remove-One-Preset Comparison

From the model comparison above, XGBoost was selected as our best model, and the results for Figure 2.3 are only displayed for this model. Across all of the remove-one-incline conditions, the transitional and steady state error rates were consistent across incline rates. However, for remove-one-stair height conditions, the transitional and steady-state error rate decreased with large stair heights. The average steady error for user-dependent classifiers across both preset conditions was 4.59% $\pm$ 2.05%, while the transitional error was 7.60% $\pm$ 2.57%. The average steady error for user-independent classifiers across both

preset conditions was 6.54% $\pm$ 1.92%, while the transitional error was 17.26% $\pm$ 4.92% (Figure 2.4).

2.3.3 Sensor Contribution

A sequential forward sensor selection using the XGBoost algorithm revealed that in both DEP and IND cases, the inclusion of all sensors yielded the lowest error ($p<0.05$). In this

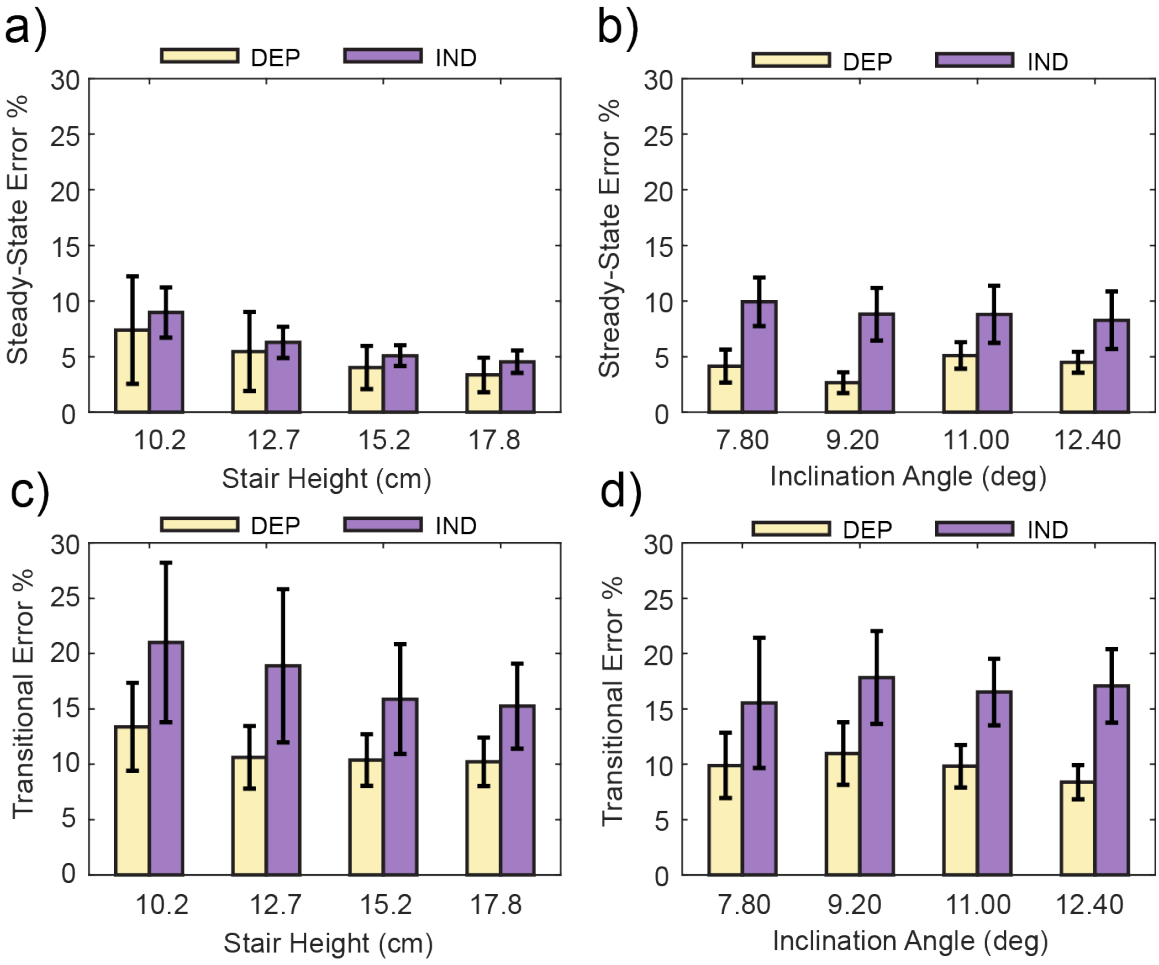

Figure 2.4: XGBoost showed the best performance across all case studies. It can be seen that this model can generalize to different stair heights and inclination angles with relatively low error. The y-axes show the error for each condition - a) RM-1-H-DEP, b) RM-1-I-DEP, c) RM-1-H-IND, and d) RM-1-I-IND, while the x-axes show the 4 preset conditions for the 2 types of ambulation circuits. Results are presented for both DEP and IND cases to show how well the algorithm behaves under different validation strategies. Error bars represent the $\pm$ 1 standard error of the mean.

analysis, each sensor's features were independently tested. In the first iteration, we took one of the sensors and its features (6 total sensors, 140 total features: 6-DOF loadcell – 30 features, foot IMU - 30 features, shank IMU – 30 features, thigh IMU – 30 features, and joint encoders – 20 features) and determined which sensor, when removed from the training set of the model, would yield the highest test error implying that this was the most useful sensor needed for the mode classifier. If selected, the sensor was kept in the feature space, while the remaining sensors were tested again in another iteration; this continued until all sensors were swept. The error metric used was the average of the steady state (SS) and transitional (TS) errors to determine what combination of sensors would yield the lowest error (Eq. 3). Across both steady state and transitional errors, the forward sensor selection algorithm chose the load cell as the best sensor that contributed the lowest error across both test (DEP and IND) cases. (Figure 2.5).

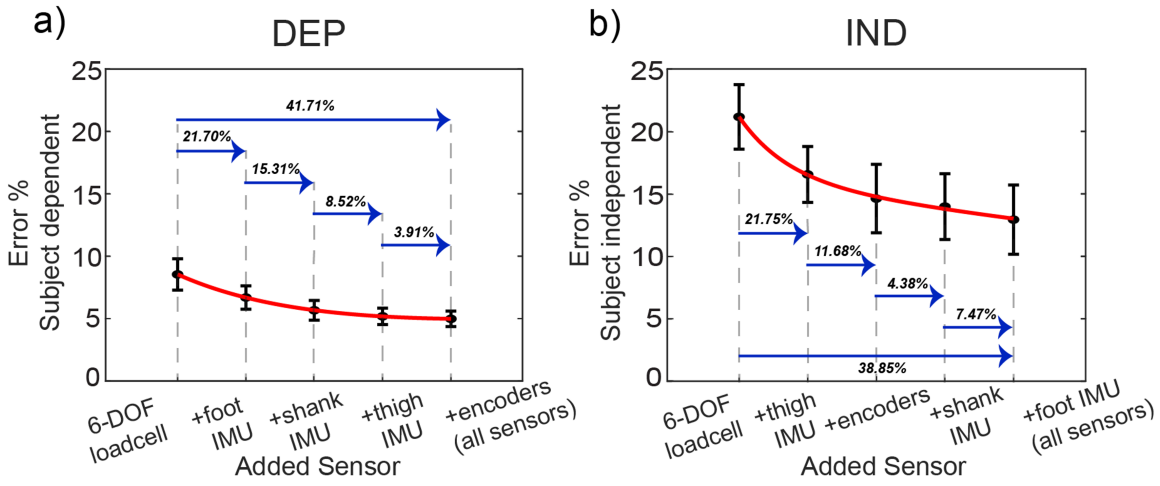

Figure 2.5: The XGBoost algorithm was evaluated incrementally for each sensor that was selected on a sequential forward feature selection process. This was implemented for both a) subject dependent and b) subject independent models. In both cases, the loadcell was the most favorable sensor for locomotion mode classification. For example, in a) the first bars show the model trained with only the features of the loadcell (6 channels x 5 feature types = 30 features), the second bars show adding the foot IMU (30 previous features from loadcell + 30 new features, and so on until all the features were trained upon - 140 total features). The y-axes show the sensor error (Equation 2.3) for each condition, while the x-axes show the added sensor to the pool on each iteration. Error bars represent the $\pm$ standard error of the mean.

2.3.4 XGBoost Confusion Matrices

We created several confusion matrices to show how the model performed across individual modes. Note LW data was present in both classifier types. We concatenated across subjects and combined steady state and transitional errors to show how XGBoost performed in classifying each mode. In the DEP case, XGBoost correctly classified 3170/3227 (98.23%) level walking (LW) steps, 592/633 (93.52%) ramp ascent (RA) steps, 594/643 (93.84%) ramp descent (RD) steps, 400/421 (95.01%) stair ascent (SA) steps, and 268/299 (89.63%) stair descent (SD) steps. Overall, across all modes in the DEP case, XGBoost correctly classified 5024/5223 steps (96.19%). In the IND case, XGBoost correctly classified 3098/3227 (96.00%) level walking (LW) steps, 516/633 (81.52%) ramp ascent (RA) steps, 457/643 (71.07%) ramp descent (RD) steps, 391/421 (92.87%) stair ascent (SA) steps, and 233/299 (77.93%) stair descent (SD) steps. Overall, across all modes in the IND case, XGBoost correctly classified 4695/5223 steps (89.89%).

2.4 Conclusions

In this chapter, we explored two key features in enhancing the locomotion mode classification performance by 1) comparing different model complexities of current state-of-the-art models to XGBoost and evaluating the performance of these algorithms across users and different stair heights and inclination angles, and 2) understanding whether the user-independent classifiers with the addition of extra sensors could achieve similar performance to the dependent classifiers.

As we explored the effect of model complexity across different case studies, XGBoost outperformed both LDA and NN in the steady state error across independent and dependent models ($p<0.05$), while only outperforming NN in the transitional case ($p<0.05$). Therefore, our first hypothesis was partially accepted in that the most complex algorithm (XGBoost) performed the best, but simply adding complexity did not yield

benefits as LDA still outperformed more complex NN in certain situations, and is rejected that more complex algorithms are better for improving performance. Thus, an optimal level in complexity can reduce classification error. Across all case studies performed, XGBoost showed best performance which is one step closer to creating algorithms that can generalize across multiple grades of terrain. Note that RM-1-cases were generally

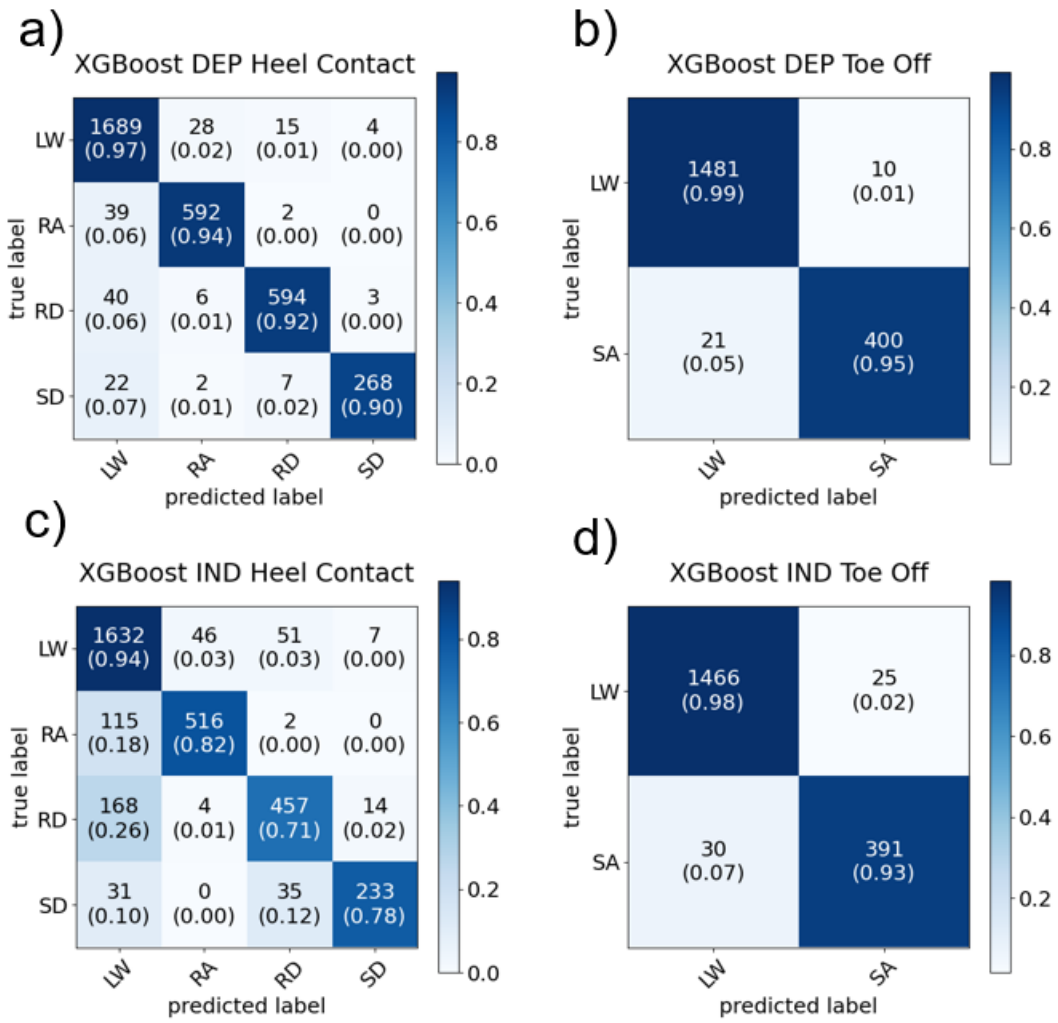

Figure 2.6: Confusion matrices for our best model (XGBoost) to show individual classification accuracies for each mode and phase type - a) DEP HC classifier, b) DEP TO classifier, c) IND HC classifier, and d:) IND TO classifier). The results show that in the DEP case, XGBoost had a 96.19% classification accuracy and that in the IND case, XGBoost had a 89.89% classification accuracy. The y-axes show the true label while the x-axes show the predicted label.

more difficult for a machine learning algorithm to predict modes compared to a DEP or IND setup. This is because the classifier must generalize to a ramp incline or stair height that does not exist in the training data. Our goal was to understand if these algorithms could learn on limited data and generalize to unknown environmental conditions.

Although sensor (Figure 2.5), channel (not shown) and feature type (not shown) selection were analyzed, no sensors/channels or feature types all were useful for reducing user-independent classification errors. Our second hypothesis on the addition of sensor information was accepted. It was shown that the inclusion of sensors continually improved model performance across both DEP and IND cases. Results indicated that the 6-DOF loadcell was the most essential sensor. Additional analysis could be performed to determine the influence of specific feature components from each sensor to minimize the amount of information that is extracted from the sensors while maintaining model performance.

We believe that direct comparisons cannot be made to prior literature due to our dataset's unique inclusion of multiple stair heights and inclination angles which do not exist in previous studies. Hence, we found other literature methods that created intent recognition systems; LDA and NN was commonly used as a baseline and we applied that same method to make an equal comparison to our dataset. The results indicate that XGBoost shows potential in generalizing across subjects when employing a user independent intent recognition system. We observed that XGBoost had some difficulty in differentiating between LW and RA (Figure 2.6). Future work should look into combining these modes as one label as seen in prior work to see if there is an improvement in model performance [39, 44]. Similar results were seen in Young et al., where steady state and transitional errors of 8% and 13% were achieved but required more complicated dynamic bayesian networks (DBN - useful methods that incorporate time history information using current observations and prior probabilities) and mode specific architectures which are much more challenging to implement than the methods presented here [34, 39].

One limitation of our conducted study is the small number of subjects (N=8) especially when trying to create a user independent system. The purpose of each ambulation circuit was to capture the behavior of traversing different terrain types from level walking to allow for inclusion of both steady state and mode transitional steps. However, the amount of training data is relatively small. For every ambulation circuit, there are only 4 transitional steps compared to 12-16 steady state steps. Future work is still required to address the issue of achieving smaller transitional errors with a small training dataset. Lastly, our analysis was limited in that it was just an offline analysis. Previous studies have indicated that implementing these models in real-time must be done properly in order to avoid the dangerous outcomes of misclassification errors [36, 38, 37]. To make these algorithms prevalent in prosthetic controllers for clinical applications, real-time validation of these models is imperative.

CHAPTER 3

OFFLINE EVALUATION OF CONTINUOUS WALKING SPEED DETERMINATION ALGORITHMS UTILIZING EMBEDDED SENSORS

3.1 Background

Lower-limb loss is a continually increasing issue, warranting the pursuit of advanced technologies to aid in restoring natural gait functionality over a variety of terrains [1]. Most commercially available prosthetic solutions are passive; while the simplistic mechanisms make them easy to implement clinically, they are linked to significantly lower walking speed ranges and compensatory ambulation strategies [6, 7]. Powered prostheses may reduce these compensatory strategies and increase both self-selected walking speed and range of comfortable walking speeds, but more advanced and intuitive control strategies are required before such devices can be widely adopted.

Powered prosthetic technology has seen significant advances in the last two decades, allowing for the restoration of natural gait function [13, 38]. However, intelligent and intuitive control of these devices remains difficult. While sound performance has been achieved in steady-state, unperturbed ambulation, more complex functionalities such as mode transitioning and dynamic ambulation have yet to see conclusive advances. Many of these dynamic control problems require fast and accurate gait parameter determination - such as walking speed - to function at a usable level.

Gait parameter determination is a common metric used in mobility evaluation and gait speed is an essential metric to understand the level of mobility of individuals that are impaired with gait pathologies. While not an all-encompassing measure, decreased walking speed correlates strongly with impaired mobility in clinical applications [78]. Walking speed and associated energy expenditure can also be used to asses physical and

cardiovascular fitness in amputees [79].

The most common prosthetic control strategies typically employ a three-tier controller paradigm: high-level, mid-level, and low-level control [9]. Determination of walking speed, handled by the high-level controller, could be used to inform the mid-level controller to apply a more optimal torque profile across speeds. Implementation of real-time parameter scaling may positively impact patient mobility as well as increase the range of comfortable walking speeds, both significant advantages over passive prostheses. Ultimately, these adaptations may be more intuitive and comfortable for the user and promote a broader and more dynamic range of use cases.

Previous studies have applied wearable sensors (ex. inertial measurement units) that measure acceleration and gyroscopic information to gait parameter determination (e.g., walking speed). There are typically three techniques of determining walking speed: 1) direct integration (typically the gold standard), 2) kinematic gait modeling, and 3) regression modeling or machine learning. Although direct integration methods are simple to compute, they tend to drift over time. Correction methods (i.e., zero velocity updates) have yielded improved results. Previous studies have utilized a single foot IMU to estimate walking speed and achieved an RMSE of 0.05 m/s [50]. Other studies have also applied direct integration methods using an inverted pendulum model in which they achieved an RMSE of 0.07 m/s using a shank IMU[80]. Kinematic models have also been evaluated but are less accurate without subject dependent calibration [80, 81, 82, 52]. However, each of these methods was severely limited by a maximum of one prediction per gait cycle, making it much more difficult for the method to respond quickly to changes in non-steady state walking. For this reason, machine learning and simple regression models have recently gained traction as a leading method of estimating walking speed [83, 84, 85, 86, 87, 88]. However, applying these methods to populations beyond healthy individuals has not been extensively explored; preliminary investigations into individuals with amputation have been conducted [89, 90, 54]. Our approach aims to address the gap in the

field, by creating an algorithm capable of accurate and fast real-time determination of walking speed on a powered prosthesis.

In this chapter, we evaluated the efficacy of multiple machine learning algorithms in determining walking speed of individuals with transfemoral amputation. We developed a machine learning pipeline and validated its performance by achieving low error and delay in determining walking speed, especially for dynamically changing situations. Furthermore, in the remove-one-subject validation, these methods can achieve similar errors to direct integration methods, but with the advantage of continuous real-time determination of walking speed. A sensor-level analysis showed that the inclusion of more sensors can reduce the overall error of determining walking speed. The novel aspects and contributions of this chapter are: 1) establishment of a ML framework that can perform continuous speed determination for real-time applications on knee/ankle prostheses, 2) development and comparison of user dependent and independent systems, 3) utilization of an expansive embedded sensor suite on a powered prosthesis (three 6-axis IMUs on the foot, shank, and thigh, a 6-DOF load cell, and two joint encoders at the knee and ankle), and 4) validation of these techniques in static and dynamic speed tracking scenarios. We aimed to provide meaningful information for the future development of clinically relevant gait parameter determination systems.

3.2 Experimental Methods

3.2.1 Protocol Design

In this chapter, we employed a powered knee and ankle prosthesis that features two independently controlled joints at the knee and ankle, providing powered assistance in the sagittal plane; more details of the prosthesis can be found in previous papers [20, 75]. The prosthesis includes six embedded mechanical sensors: two joint incremental encoders (US Digital E5) to measure knee and ankle kinematics, a 6-DOF (degree of freedom) load cell (SRI M3714C2) to measure ground reaction forces and moments, and three 6-axis

(accelerometer & gyroscope) inertial measurement units (IMUs) (YOST 3-Space LX embedded). All sensors were collected at 100 Hz except for IMUs, which were sampled at 250 Hz. The focus of this chapter was to demonstrate a walking speed determination system that could ultimately be used to tune assistance parameters dynamically during ambulation.

Six individuals (6 males, age: 50.83±10.22 years, height: 1.76±0.06 m, mass: 83.82±12.06 kg) with unilateral transfemoral amputation (4R/2L) were recruited and provided informed consent in accordance with the Georgia Institute of Technology Institutional Review Board. The prosthetic device was configured to each user by a certified prosthetist for appropriate comfort and alignment. The prosthetist instructed the subjects to correct their gait to overcome any exaggerated or over-compensatory movements. When the prosthetist was satisfied with the tuning process, users were asked to complete a total of 10 walking trials (Figure 3.1) on a force instrumented Bertec treadmill (Columbus, Ohio): 9 static speed trials (1 minute each), each collected at a speed from between 0.5 m/s and 0.9 m/s in 0.05 m/s intervals, and a single dynamic trial lasting approximately 112 seconds. In dynamic trials, speeds were changed every 20 seconds, allowing a 4 second continuous transition to the next speed, covering speeds between 0.5 m/s and a subject-selected maximum speed (5 subjects chose 0.9 m/s; 1 subject chose 0.85 m/s).

3.2.2 Data Processing and Feature Extraction

To ensure an appropriate input of data to train our walking speed models, a general workflow was implemented to investigate and compare multiple machine learning algorithms. We extracted 8 features (minimum, maximum, mean, standard deviation, start value, ending value, signal magnitude area, and signal energy), resulting in a total of 224 features (28 channels x 8 feature types) for a given window [36, 33, 43]. Phase segmentation relied on the transition criterion of our finite state machine to separate the

gait cycle into early stance, late stance, swing flexion, and swing extension phases, as seen in previous studies [26].

3.2.3 Walking Speed Models

Three algorithms were chosen for performance comparison in walking speed determination: linear regression (LR), extreme gradient boosting (XGBoost), and neural networks (NN). Linear regression is a simple method that attempts to model the

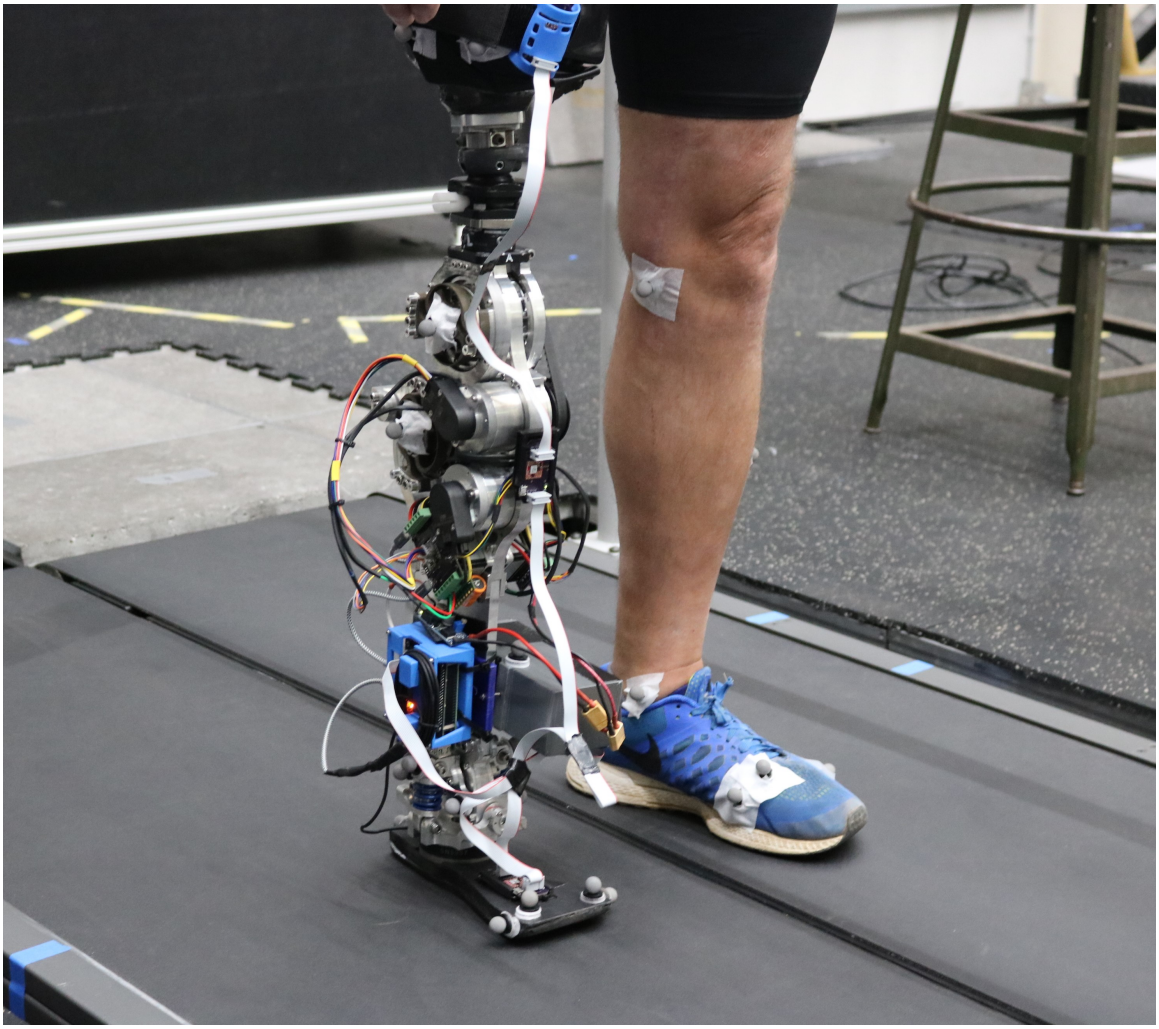

Figure 3.1: Experimental setting in which one individual with transfemoral amputation was completing a walking speed protocol for 1 minute at one of nine equally spaced speeds ranging from 0.5 m/s to 0.9 m/s. Embedded sensors on the prosthesis include two joint encoders, one 6-DOF loadcell, and three 6-axis inertial measurement units were used in determining walking speed.

relationship between two variables using a linear fit. A neural network is a biologically inspired network of connections in which each neuron can adapt with its associated weights that can be used in predictive modeling to draw conclusions about a problem from complex and sometimes unrelated set of features. XGBoost is an optimized gradient tree boosting library that can solve a problem in an efficient and parallelized structure [68]. This method is especially useful for learning problems that are nonlinear and complex in nature. Linear regression is the simplest to use and offers the advantage of easy to train and fast training but can be limited in capturing more complex behaviors. Extreme gradient boosting was selected for multiple reasons which include: clever penalization of trees to overcome overfitting, uses weighted functions to create additional trees with respect to a bias-variance tradeoff, and also utilizes a differentiable loss function to reach a global minimum, which in turn makes this algorithm easy to use and flexible to different problems [68, 63]. Neural networks were selected due to their inherent ability to capture more complex data patterns and has also been a gold standard in many machine learning tasks. A phase sweep was performed to determine the optimal phase configuration for each individual regressor to train on, including 1-Phase (full gait cycle), 2-Phase (stance/swing), and 4-Phase (early stance/late stance/swing flexion/swing extension) models. 4-phase was shown to be the optimal phase configuration: for each phase of walking, a separate regressor was trained on data from that specific phase to capture phase dependent signal information. In this method, speed determinations were generated continuously throughout the gait cycle, switching between models during the appropriate phase based on the state machine. This allows for continuous determination of gait speed at a clock rate of 50 Hz, a significant improvement over the delay incurred by direct integration methods, which require at least one stride to update the determination.

3.3 Algorithm Optimization

Hyperparameter optimization is a critical step in improving an algorithm's capability of performing better at the task. It should be noted that the parameter search should not be only to capture the best possible configuration but also make the model generalizable to unknown data [91]. Hyperparameter optimization of the NN and XGBoost models were completed to ensure model architectures were appropriate for generalizing our mechanical sensor information for the task of walking speed determination; LR did not require any additional tuning. Scripts were written for all models and case studies (dependent, independent, remove-one-speed, and dynamic) and an initial window size of 250 ms was selected. For each subset of parameters, the parameter resulting in the smallest phase-specific RMSE was selected until all of the parameters were swept (Table 3.1)). It should be noted that for each configuration setup, different validation scenarios were used to understand how well the algorithm could generalize (see Model Evaluation). Furthermore, the selection of the hyperparameter space was similar to the recommended default values of each algorithm [91]. In XGBoost, the set of hyperparameters explored included: the learning rate used to influence the convergence to a solution, the maximum allowable tree depth, the regularization term to control the sensitivity, and the number of estimators utilized to learn the data. Note, the early stopping functionality was utilized to prevent overfitting of the model. In NN, the set of hyperparameters included: layers and nodes to determine the adequate size of the network needed, optimizer and learning rate to influence the convergence to a solution, and activation function and batch size to limit model complexity.

After model optimization, a Kalman filter was implemented to take advantage of the time-series nature of the regression task. Process noise and window size were swept simultaneously; process noises were varied from $1.0e-6$ to 0.5, and window size was swept from 50 ms to 1000 ms to determine the optimal time-dependent parameters for the

Table 3.1: Final walking speed estimation optimized parameters

	NN	XGBoost
Parameter Ranges	**Layers:** 1-3 **Nodes:** 10, 20, 30, 40, 50 **Optimizer:** $Adam, SGD,$ & $RMSprop$ **Learning rate:** 0.001, 0.005, 0.01 **Activation function:** $sigmoid$ & $tanh$ **Batch size:** 32, 64, 128	**# of Estimators:** 50, 100, 150, 200, 300 **Max depth:** 1, 3, 6, 9 **Lambda:** 0, 0.5, 1, 2, 4 **Learning rate:** 0.01, 0.05, 0.1, 0.3, 0.5
DEP	**Layers:** 1 **Nodes:** 40 **Optimizer:** $Adam$ **Learning rate:** 0.001 **Activation function:** $sigmoid$ **Batch size:** 128	**# of Estimators:** 300 **Max depth:** 6 **Lambda:** 0.5 **Learning rate:** 0.1
IND	**Layers:** 3 **Nodes:** 10 **Optimizer:** SGD **Learning rate:** 0.001 **Activation function:** $sigmoid$ **Batch size:** 128	**# of Estimators:** 300 **Max depth:** 3 **Lambda:** 1 **Learning rate:** 0.3

Kalman-filtered model performance. The evaluation metric was the smallest phase-specific RMSE. The optimal window size was found to be 500 ms for all cases and models, while process noises where independently optimized for each phase configuration.

3.3.1 Model Evaluation

Several steps were taken to prevent overfitting of each model. First, six different case studies were explored: dependent (DEP), independent (IND), remove-one-speed dependent (RM-1-S-DEP), remove-one-speed independent (RM-1-S-IND), dynamic dependent (DYN-DEP), and dynamic independent (DYN-IND). The DEP case study was similar to previous literature, where data was trained on a particular subject and evaluated

using a 5-fold cross validation. The IND case study was also taken as a traditional method of training with a remove-one-subject validation, which in turn became the test set. Thus, in these first two cases, both the train and test set had examples from all static speeds. The RM-1-S-DEP and RM-1-S-IND conditions were trained with all of the static speeds except for the unknown speed that served as the test set. This procedure was repeated until each speed was included in the test set. Lastly, the DYN-DEP and DYN-IND conditions were trained with all the static data, and tested on the subject's dynamic trial. In dynamic cases, average model delay was calculated during a change in speed as the average horizontal (time) distance between the ground truth line and the model prediction to characterize how quickly the model responds to changing speed. All cases were coupled with a Kalman filter, which was optimized on the DYN-DEP and DYN-IND cases, then applied to the remaining cases. The RMSE was recorded for each unfiltered phase-specific model, as well as the Kalman filtered RMSE over each phase-specific model and also over the entire gait cycle. The variety in collected errors allows for the efficacy of the Kalman filter to be independently determined, as well as comparisons to determine the optimal phase combination for walking speed determination.

3.3.2 Statistical Analysis

We conducted three separate two-way repeated measures analysis of variance (ANOVA) to compare the model performance across the DEP and IND conditions for each validation method (Static, RM-1-Speed, Dynamic) , where the independent variables were the models (LR/NN/XGBoost) and types (DEP/IND) (Figure 3.2A). In the phase comparison, a three-way ANOVA was performed with independent variables of models, types, and phases (early stance/late stance/swing flexion/swing extension) (Figure 3.2B). Finally, in the sensor selection, two separate two-way ANOVA were run, with model and sensors (thigh IMU, shank IMU, foot IMU, load cell, encoders) as the independent variables. In each analysis, α = 0.05 and a Bonferroni post-hoc correction were used to compute the

statistical differences between each condition (Minitab 19.0, USA).

3.4 Results

3.4.1 Model & Phase Comparison

From the model comparison described above, all ML models performed similarly in the standard DEP and IND cases, LR performed best in the RM-1-S cases, and XGBoost performed best in the DYN cases. Figure 3.2 displays the model evaluation using Kalman filtered RMSE over the entire gait cycle. In the DEP and IND cases, no model performed statistically significant from the others. XGBoost achieved the minimal DEP error at 0.014±0.001 m/s, while NN achieved minimal IND error at 0.070±0.007 m/s. DEP models were shown to perform better than IND models ($p<0.05$). In the RM-1-S cases, XGBoost performed worse than LR and NN and DEP models outperformed IND models ($p<0.05$). LR performed optimally in the RM-1-S cases achieving errors of: RM-1-S-DEP 0.034±0.001 m/s; RM-1-S-IND 0.068±0.008 m/s; finally, no statistically significant differences were observed between models or cases for the dynamic validation cases. XGBoost performed the best in the dynamic case, with errors of DYN-DEP 0.067±0.005 m/s; DYN-IND 0.070±0.014 m/s.

A phase comparison of each ML algorithm was also performed to understand if there are specific locations during the gait cycle that would improve the determination of walking speed. The model output was combined with a Kalman filter for five different cases (Figure 3.2B). The results show for the best phase to select in the DEP case was the early stance phase with an RMSE of 0.014±0.001 m/s for XGBoost. In the IND case, late stance shows the best for a subject-independent model with LR achieving an RMSE of 0.060±0.007 m/s. DEP models outperform IND models ($p<0.05$), and swing extension performed worse than early stance and late stance ($p<0.05$). Kalman filtering over the entire gait cycle led to errors of 0.014±0.001 m/s (DEP) and 0.068±0.009 (IND). These results indicate that walking speed determination error varies over the gait cycle, and in

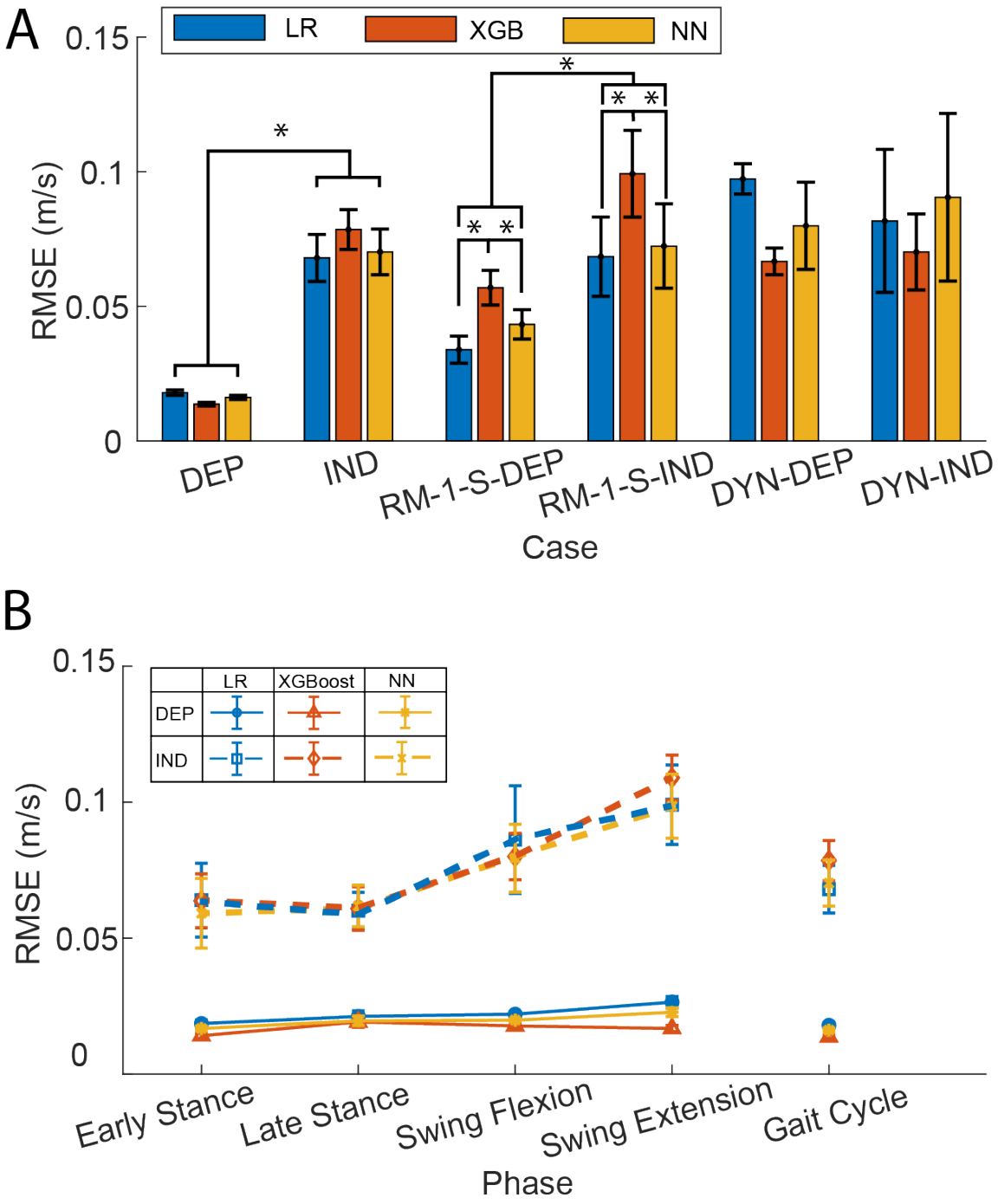

Figure 3.2: (A) Three models (LR/NN/XGBoost) were compared for walking speed determination. The y-axis shows the average RMSE across subjects, evaluated for each Kalman filtered model. The x-axis shows the six conditions of evaluation: subject dependent i.e., training and testing on the same subject, subject independent i.e., training on all subjects but the testing subject, remove-1-speed conditions for both DEP and IND, and dynamic conditions for both DEP and IND. Error bars represent $\pm$ standard error of the mean. Asterisks indicate statistical significance ($p<0.05$). (B) A phase comparison was performed to understand if using a regressor at a specific section of the gait cycle could improve results on static speed determination. The average RMSE across subjects is plotted against phase.

the IND case predicting selectively in certain phases can lead to a reduction in error.

3.4.2 Remove-One-Speed & Dynamic Tracking Validation

LR was the best performer in the RM-1-S-DEP and RM-1-S-IND comparison. Figure 3.3(A,B) displays the RMSE as a function of removed speed, where all models used a phase configuration of the entire gait cycle. All models performed similarly across the removed speeds in which the algorithm was interpolating (removed speed 0.55-0.85 m/s), but had substantially worse performance (an average error percentage increase of 64.8% in the DEP case and 42.6% in the IND case) when removed speeds required the algorithm to extrapolate (0.5, 0.9 m/s).

DEP Dynamic tracking performance, shown in Figure 3.3(C) was similar across models, with LR achieving a slight edge at 0.057 ± 0.006 m/s. LR performed stronger than other models in the IND case, Fig. 3(D), achieving 0.058 ± 0.007 m/s. Time delay was calculated to determine each model's responsiveness to changes in speed. NN achieved the minimum average time delay in the DEP case of 132 ms. LR followed at 207 ms, and XGBoost performed worst with a delay of 241 ms on average. In the IND case, XGBoost performed best with a time delay of 264 ms. NN and LR obtained delays of 339 ms and 384 ms, respectively. These delays are much shorter than one stride, the minimum time required to update most direct integration methods.

3.4.3 Sensor Selection

A sequential forward sensor selection revealed that in the DEP case, the inclusion of all sensors yielded the lowest Kalman filtered error; however, in the IND case, error leveled off and eventually increased as the final sensors were added. Figure 3.4 shows continually decreasing error in the DEP case, with the thigh IMU being the most important sensor; XGBoost was capable of achieving 0.025 ± 0.002 m/s from only this sensor. Adding the shank IMU and encoders added significant information, reducing XGBoost error to

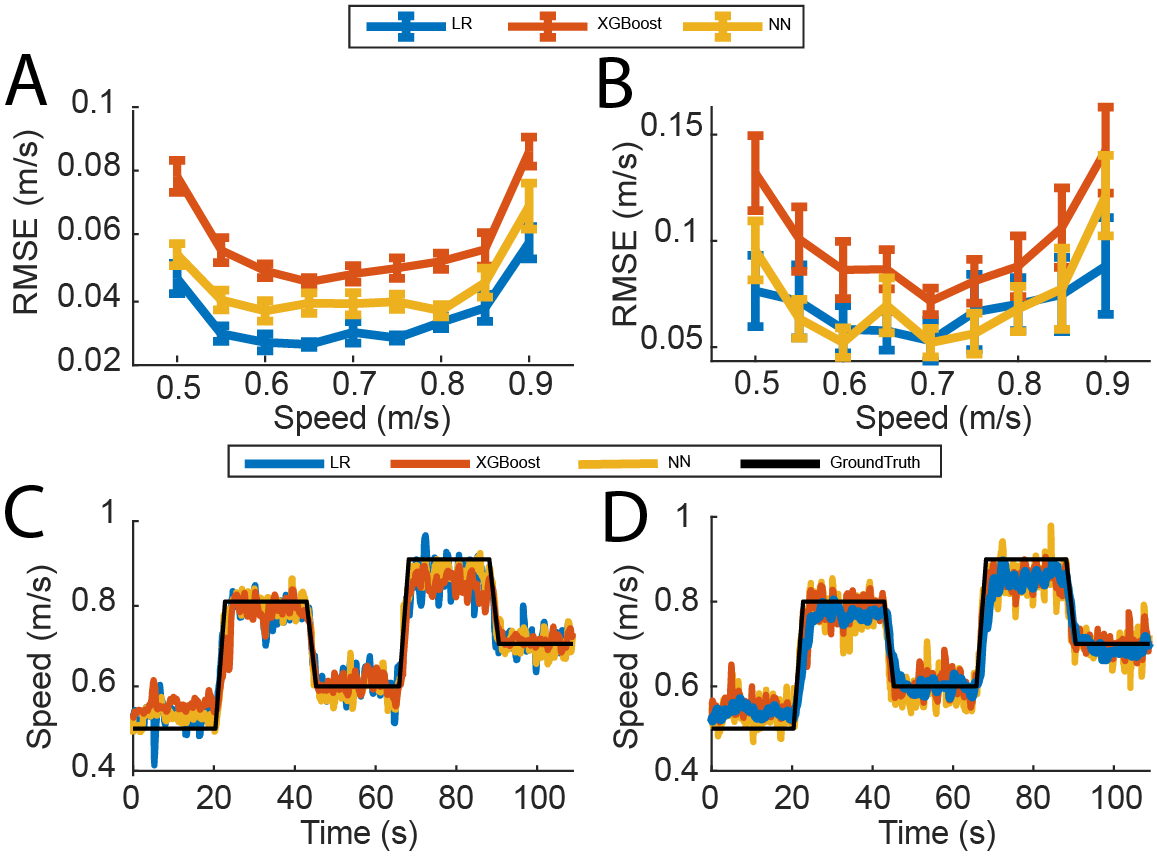

Figure 3.3: (A) DEP and (B) IND RMSE errors plotted across speed for the RM-1-S cases, with error bars representing the $\pm$ standard error of the mean. In (C) DEP and (D) IND dynamic trial tracking profiles are shown for each model with the solid black line indicating treadmill speed, with speed on the y-axis and time on the x-axis.

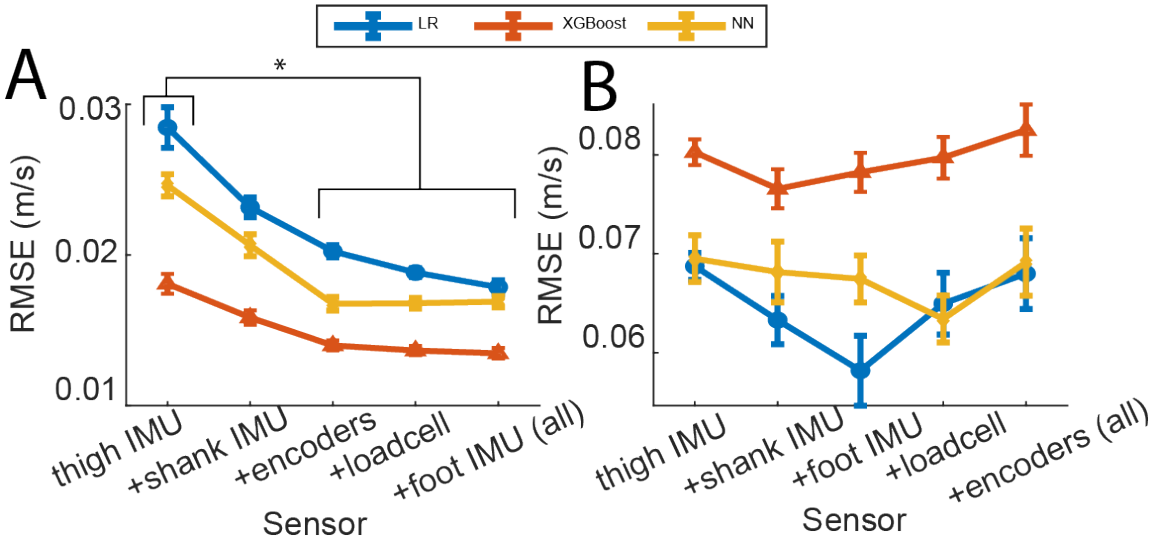

Figure 3.4: The optimal ML algorithm was selected to determine the sensor order using a sequential feature selection process. This was implemented for the remaining (A) subject dependent and (B) subject independent models. In both cases, the thigh IMU and shank IMU were the most favorable sensors for walking speed determination. The y-axes show the average RMSE across subjects for each condition, while the x-axes show the added sensor to the pool on each iteration. Error bars represent the ± standard error of the mean.

0.016±0.001 m/s. Further sensor addition contributed less to error reduction; in the DEP case, the thigh IMU was statistically more significant than each of the encoders, loadcell, and foot IMU ($p<0.05$). The thigh and shank exhibit a similar relationship for XGBoost in the IND case, combining for optimal unfiltered error of 0.083±0.002 m/s; further sensor addition was seen to increase error.

3.4.4 Comparison of Computational Costs

An analysis was performed to understand the computational resources needed to run these algorithms in real-time. We measured the processing time it took to perform feature extraction and prediction using the 3 different models on a commercially available microprocessor (i.e. Raspberry Pi 4 Model B+ (4GB) with default settings). Linear regression showed the smallest computational time with 17.5±2.9 ms, followed by XGBoost with 19.8±4.4 ms, and lastly NN with 21.2±4.7 ms. The authors realize that hardware is different for many devices, but hope this can serve as a benchmark test to

ensure that our proposed algorithm may be viable to embed on a powered prosthesis in real-time.

3.5 Conclusions

In this chapter, we explored two aspects in enhancing walking speed determination. In each case study, our results were either strongly competitive or better than results achieved by direct integration or kinematic models in literature. Our RMSE errors are comparable to prior literature values while predicting at higher rates; Sabatini et. al achieved 0.05 m/s using direct integration methods on a foot IMU [50]; Li et. al achieved 0.07 m/s using combined direct integration and kinematic model methods employed on a shank IMU [80]; and Dauriac et. al obtained 0.09 m/s using a kinematic model on a prosthesis mounted shank IMU [54]. Our minimum DEP error with XGBoost of 0.014$\pm$0.001 m/s was lower than these numbers, while the NN's IND performance of 0.070$\pm$0.007 m/s was competitive with these strategies as well as other machine learning approaches [82, 84, 83, 85, 53]. Our system notably has more sensors than comparable studies in literature, but these sensors tend to be standard on robotic knee/ankle prostheses.

Our method not only showed that these algorithms are suitable for static speeds, but were able to handle other validation cases such as remove-1-speed and dynamic tracking profiles. The RM-1-S cases demonstrate moderate robustness of the models to compensate for missing data towards the center of the training range (LR DEP 0.025$\pm$0.001 with 0.65 m/s removed), while they struggle to extrapolate to data outside of the training range (LR DEP 0.057$\pm$0.005 with 0.9 m/s removed), as seen in Figure 3.3(A, B). Additionally, the low error rate and tracking delay of our models also allows for real-time continuous output of walking speed, compared to a minimum one stride delay inherent in direct integration methods. The benefit of this continuous prediction was best highlighted by the dynamic tracking case, where our models achieve low delays (NN DEP 132 ms, XGBoost IND 264 ms), showing promise in real-time applications. This validation highlights that these

models may serve as a solution to determining walking speed in more dynamic environments outside of the lab setting. Furthermore, the sensor selection showed the inclusion of additional sensors beyond a single IMU reduced errors in the subject dependent case. The thigh IMU was the most important sensor, followed by the shank. The remaining sensors all behaved similarly, with diminishing impacts on error reduction.

Specific calibration and location choices must be implemented to integrate directly from the IMUs, which can be non-trivial and time consuming. A potential benefit of ML methods over direct integration is an increased robustness to variation in the location and calibration of wearable sensors when placed on the user or prosthesis. One limitation of our protocol was the small number of subjects (N=6) as the recruitment and training of patients was non-trivial. It is plausible that the user independent system could be improved by including more subjects [39]. Gathering enough data could be the largest disadvantage of this approach. Compared to other methods that have addressed estimating walking speed via tracking user cadence and integrating IMUs which require no prior data collection is a large benefit. However, a balance tradeoff of achieving higher accuracies and the amount of data required should be considered. In this approach, the users walked for $\approx$10 minutes in order to train a model. Additionally, by creating user-independent models, the need for gathering more data may be alleviated, as the model can generalize to patterns seen in other subjects. The authors believe that exploring how to make effective user-independent models that can be embedded in powered prostheses is a critical need. Furthermore, our study was limited to an offline analysis. Previous studies have indicated that implementing these models in real-time is a must for robotic controllers to be utilized for clinical applications [38, 37, 53]. Our results demonstrates that walking speed determination can be done continuously throughout the gait cycle, which, if implemented in real-time, allows for control parameters to be updated instantly compared to waiting for a delayed system (e.g. waiting for the next stride), as would be necessary with direct integration systems [80, 50, 54]. Future work will look to perform studies with an online system that incorporates real-time assistance

scaling based on estimated parameters.

Based on the results presented in this chapter, we can conclude that determining walking speed is feasible, but a major milestone is needed to ensure that this approach can be useful for the wearable robotic field; whether these algorithms can be utilized in more real-world scenarios such as overground walking and uneven terrain. While there was a limitation of training these algorithms with treadmill data, future studies will be needed to ensure that these methods can be accurate and efficient in other situations. The hardest challenge is being able to determine what the walking speed will be when the user is starting/stopping to walk and during turning. We believe that the methods proposed in this chapter is a step in the right direction to determining walking speed in more dynamic situations since they allow for continuous real-time output throughout the gait cycle.

CHAPTER 4
MULTI-CONTEXT REAL-TIME INTENT RECOGNITION FOR POWERED LOWER-LIMB PROSTHESES

4.1 Background

Developing real-time intent recognition systems are critical for powered prostheses to adapt to different terrains and allow for smooth symbiosis with the user. Transitioning currently available powered prostheses between modes and environmental contexts are cumbersome – they require users to slow down, stop, manually trigger a change, or even perform an exaggerated movement to get the leg to behave in the correct mode [92]. To maximize the benefits of these devices, control systems must be able to identify the terrain correctly to provide the appropriate prosthesis response. Patient safety is critical in lower-limb applications, since a misclassification of mode or wrong torque commands could lead to increased fall risk. The first real-time intent recognition system for powered prostheses was developed by Varol et al. where a user-dependent classifier was trained only on mechanical sensors [36]. Since then this work was expanded to adding classifiers that predicted ambulation mode using EMG and mechanical sensors coupled with time history methods. In 2018, Spanias et al. created an adaptive pipeline that would take a baseline DEP model and add EMG information over long periods of time [37]. The results of the study were also implemented in real-time. Recent work by Woodward et al. showed that by making a real-time adaptive framework that enhanced a baseline IND model had similar results compared to a user-dependent system, but with a substantial reduction in training time [93].

The accurate classification of ambulation modes and estimation of walking parameters is a challenging problem that is key to many applications in wearable robotics. Direct

knowledge of user's current state can enable assistive devices to adapt to dynamic conditions; furthermore it can provide clinicians with more detailed patient activity information. This chapter describes the development process of a real-time combined locomotion mode classifier and environmental parameter estimator using machine learning and wearable sensors. A detailed analysis of the different results, show trends for how future intent recognition systems should be developed.

The novelty of this real-time intent recognition system is that it is the first tiered user-independent system to be run using solely mechanical sensors on a powered prosthesis. If the system correctly identifies the ramp modes, it will subsequently make a prediction of slope which will update the scaling equations implemented at the mid-level controller. The main difference here is that compared to the training session before, the researcher would have to manually trigger the device into the correct mode. In this system it will automatically change the locomotion mode when it predicts a new mode using its embedded microprocessor. It allows for the user to seamlessly walk between modes with any exaggerated motions. There are three main hypotheses in this study: 1) real-time error will perform worse compared to offline error, 2) the relative improvement in error from offline to real-time is worse for IND models compared to DEP models, and 3) User IND models will in general perform worse than user DEP models across different machine learning tasks.

4.2 Methods

4.2.1 Powered Robotic Knee & Ankle Prosthesis

Our study utilized the Open Source Leg (OSL), a powered knee and ankle prosthesis, that was open-sourced and designed by the Neurobionics Lab at the University of Michigan. The primary benefit of using this device allows for control strategies to be tested and compared as it is a common platform that many researchers can use without the hassle of designing different hardware unique to each lab [17, 18]. The prosthesis features two

independently controller joints that provide powered assistance in the sagittal plane to the user. The device allows for quick and easy adjustments to fit any user's socket configuration as well as an able-bodied adapter. A more detailed description of the prosthesis can be found in the literature [17, 18]. Briefly, the prosthesis contains six embedded sensors: two joint encoders to provide kinematic information, one 6-DOF loadcell (SRI M3564F) to measure forces and moments exerted onto the device by the user and environment, and 3 inertial measurement units to capture acceleration and gyroscopic information. The shank IMU is directly measured from the Dephy ActPack (Dephy Inc.), while the thigh and foot IMU's are recorded using external sensors (Lord Microstrain 3DMGX5-25) mounted on the residual limb and device respectively. All sensors were collected at 100 Hz. A Raspberry Pi 4 was utilized as the main processor to control the leg. The focus of this chapter was to develop a multi-context real-time intent recognition system that could be deployed for a tiered control paradigm of predicting mode and continuously estimating an environmental variable such as ground slope angle or walking speed.

4.2.2 Protocol Design

Offline Collection

Ten individuals with unilateral transfemoral amputation were recruited and provided informed consent in accordance with the Georgia Institute of Technology Institutional Review Board. The prosthetic device was configured to each user by a certified prosthetist for appropriate comfort and alignment. The prosthetist guided subjects in adjusting their gait to overcome any exaggerated or over-compensatory movements as needed. When the prosthetist was satisfied with the tuning process, we began our formal collection. The experimental protocol was split into two separate sessions: offline collection and real-time collection. Furthermore, each collection was split into two types of protocols: mode/ramp circuits and treadmill walking. Ten individuals participated in the tiered mode/ramp

protocol and nine individuals participated in the walking speed protocol. During the offline collection, users were asked to complete 12 ramp ambulation circuits over 4 different presets consisting of level walking (LW), ramp ascent (RA), and ramp descent (RD) steps and 3 overground level walking (LW) circuits. Our custom built terrain park was adjusted and set to 4 different presets for which 4 ramp trials occurred at 7.8°, 9.2°, 11.0°, and 12.4°respectively. Users were also asked to complete 9 walking trials on a force instrumented Bertec treadmill (Columbus, Ohio): 7 static speed trials (60 seconds each), each collected at a speed ranging between 0.3 m/s and 0.9 m/s in 0.1 m/s increments, and two dynamic trials (one 120 seconds (staircase) and one 90 seconds (triangle)). Although certain subjects could walk faster In the dynamic profiles, speeds were changed with varying acceleration profiles to capture real-world scenarios of transitioning between speeds. Note the offline protocols designed here followed the experimental protocols seen in Aims 1 & 2, but the key difference was that this data was collected on our Open Source Leg (OSL).

4.2.3 Real-Time Collection

During the real-time collection (6 individuals participated), users were asked to complete 10 ramp ambulation circuits and 3 overground level walking circuits for each condition. There were 3 novel presets (7, 9, 11 deg) evaluated and 2 presets (9.2 and 11.0) that were collected from the offline day Two conditions were tested: evaluating how well a user-dependent (DEP) tiered mode and slope intent recognition system compared to a user-independent (IND) system. A total of 26 trials were collected for each subject (≈325 steps). In the second part of the real-time collection, 3 conditions were tested: user-dependent (DEP), user-independent (IND), and semi-independent (SEMI). In each condition, users were asked to walk on the treadmill under 2 different dynamic profiles, for a total of 6 walking trials. The first dynamic profile was similar to the offline day (staircase), and the second was a novel speed profile (trapezoid). Additionally user outcome measures were

collected such as stance time spent on the prosthetic leg.

4.2.4 Scaling Across Contexts

At the mid-level controller, an impedance control law was utilized. Equations were used that smooth the behavior between phases. These phases were determined by our finite state machine which splits the cyclic behavior of walking into 4 unique phases. A previous study was done to analyze the effects of which parameters change across subjects in 3 different ambulation modes: level walking, ramp ascent, and ramp descent. The results from this study indicated that only 5-7 parameters change across subjects (see Figure 4.1) [76]. However, these equations did not scale as a function of environmental context such as slope angle, walking speed, or stair height. In this aim, scaling equations were developed to appropriately scale impedance parameters as a function of these environmental variables. In level walking, push-off was scaled with walking speed, where the ankle stiffness and equilibrium angle were changed in late stance. In ramp ascent, knee extension was scaled with slope angle, where the knee stiffness parameter in early stance was changed (see Figure 4.2). Finally, in ramp descent, the knee flexion torque was scaled with slope angle, where the damping coefficients were changed in the stance portion of the gait cycle. Similar scaling equations could be implemented for stair ascent and descent.

Mode	Phase	Ankle Parameters			Knee Parameters			Trigger Thresholds			
		k (Nm/deg)	b (Nms/deg)	θ (deg)	k (Nm/deg)	b (Nms/deg)	θ (deg)	T1 (deg)	T2 (% $F_{vertical}$)	T3 (deg/s)	T2 (% $F_{vertical}$)
Level Walking	*Early Stance*	EQ2	0.25	0	3	0.1	0	5.0 - 6.0	20.0 - 25.0	0.3	50
	Late Stance	EQ2	0.1	EQ3: $p_{start} = 0$ $p_{final} = -17$ to -23	EQ3: $p_{start} = 3$ $p_{final} = 1$	0.05	EQ3: $p_{start} = 0$ $p_{final} = 63$				
	Swing Flexion	2.6	0.1	1.75	1.4	0.1	63				
	Swing Extension	2.1	0.525	1.75	1.4	0.2	0				
Ramp Ascent	*Early Stance*	EQ2	0.25	0	3	0.15	0	6.5	Same as LW	0.4	50
	Late Stance	EQ2	0.1	Same as LW	EQ3: $p_{start} = 3$ $p_{final} = 1$	0.15	EQ3: $p_{start} = 0$ $p_{final} = 63$				
	Swing Flexion	2.6	0.1	1.75	1.4	0.1	63				
	Swing Extension	2.1	0.525	1.75	1.6 [1.4 to 2.0]	.20 [.15 to .25]	0				
Ramp Descent	*Early Stance*	3.5	0.25	0	2	.45 [.4 to .5]	EQ4 [.8 to .97]	Same as LW	Same as LW	0.3	40
	Late Stance	2.5	0.1	EQ3: $p_{start} = 0$ $p_{final} = -11.5$	EQ3: $p_{start} = 2$ $p_{final} = 1$	Previous Value	EQ3: p_{start} = Previous value $p_{final} = 25$				
	Swing Flexion	2.4	0.1	3	1.2	0.1	45				
	Swing Extension	2.4	0.1	3	2	0.15	0				

Figure 4.1: The final set of impedance parameters across participants for LW, RA, and RD. Green highlights the subject-specific tuning parameters. Baseline values and the associated tuning range in brackets are displayed for each green highlighted portion.

4.3 Data Preparation

4.3.1 Machine Learning Pipeline

The DEP models were trained on each individual subject. The IND models were trained on all other individual subjects except for the test subject. The SEMI models were only trained for walking speed and followed the IND structure but also adding a small portion of user specific data (30 secs from 0.4 m/s, 0.6 m/s, and 0.8 m/s each).

4.3.2 Training: Classification

Ambulation mode labels were generated using our finite state machine. Steady state steps (SS) were identified if the previous gait event (i.e. heel contact) remained in the same event. While transitional steps (TS) were identified if the previous gait event on the previous mode was different on the next mode (e.g. LW_EarlyStance to RA_EarlyStance – was labeled as RA). From our previous work, it was seen that XGBoost was the best algorithm to use for mode classification. A similar process was conducted of performing feature extraction and hyperparameter tuning for our data collected with the Open Source Leg. A more detailed description of the machine learning pipeline can be found in Chapter 2 [95]. One additional change made to our control system of our device was to include mode transition delays as seen in literature [44]. We found that incurring a 150 ms delay did not alter the user and did not perturb the user whilst walking. The optimal window size was found to be 250 ms and both DEP and IND model was found to use the following hyperparameters: learning rate of 0.1, number of estimators of 300, max depth of 3, lambda term of 0, and gamma term of 0.5.

4.3.3 Training: Regression

Two tasks were estimated in the real-time collect: slope/inclination angle and walking speed. Ground truth labels for the ramp circuits were based on the preset mapping as

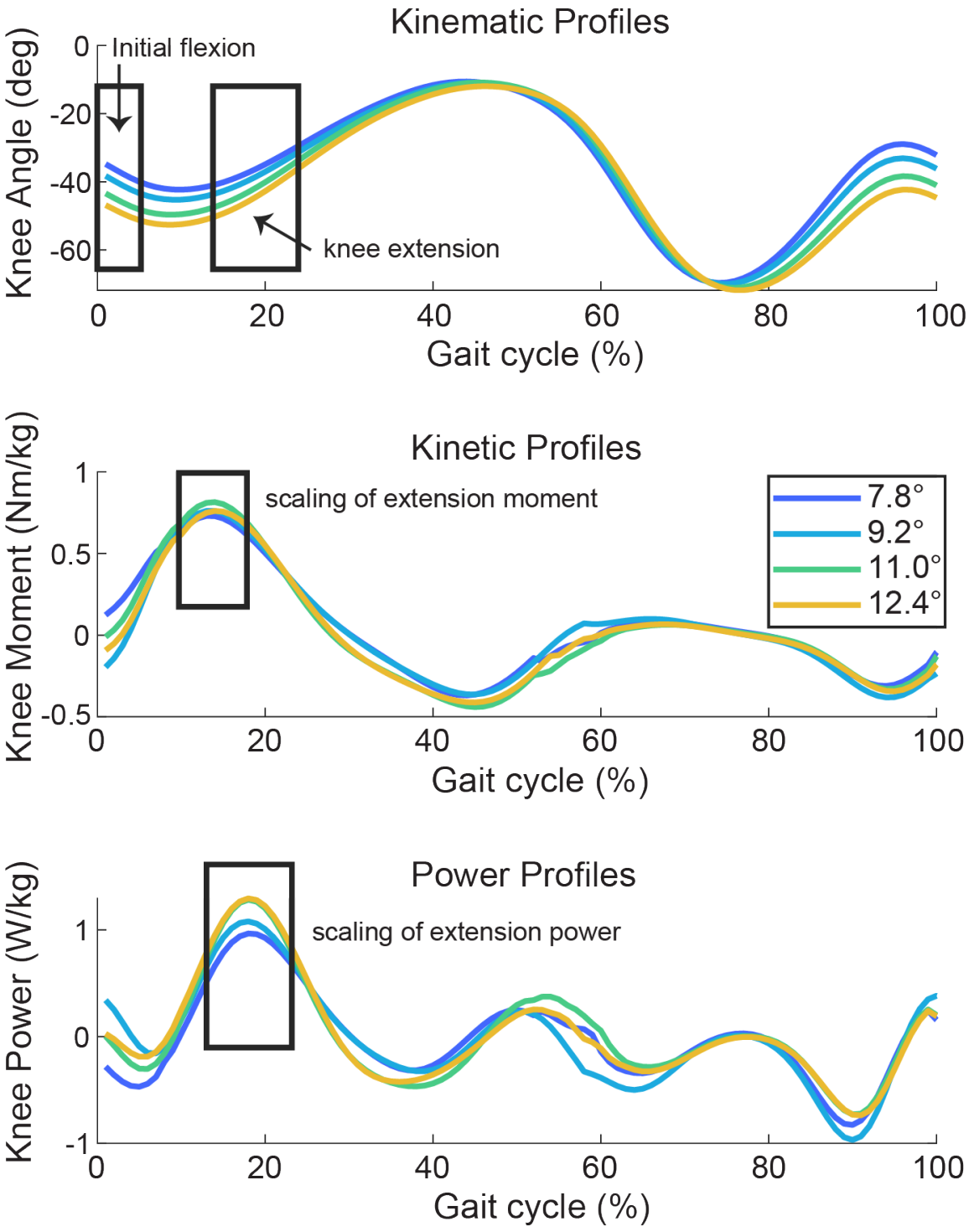

Figure 4.2: We used an open-source dataset that provides the locomotion biomechanics across different walking speeds, ramp angles, and even stair heights [94]. Specifically, we investigated how we could create scaling equations that follow similar patterns seen in healthy individuals. We looked at this for ramp ascent, and saw that the knee moment increased as slope angle increased. We took this information and made a scaling equation that would adjust the impedance parameter appropriately (i.e. knee stiffness). Similar methodologies were done for ramp descent and level walking (i.e. walking speed).

mentioned above. Walking speed profiles were generated using a custom MATLAB script that would send commands to the Bertec treadmill. The creation of both these models followed a similar pipeline seen in our previous work, where XGBoost was selected and allowed for continuous estimation of these environmental variables at 50 Hz. Detailed information can be found in Chapter 3 [76]. The optimal window size was found to be 500 ms and all 3 models (DEP, IND, and SEMI) used the following hyperparameters: learning rate of learning rate of 0.1, number of estimators of 300, max depth of 3, lambda term of 0, and gamma term of 0.5.

4.3.4 Real-Time Implementation

Custom scripts were made in our control architecture to perform real-time feature extraction on the prosthetic embedded sensors coupled with online prediction and estimation models depending on the context of locomotion. The primary performance metric these systems were classification error and RMSE for regression tasks. Although these metrics could be computed offline as a baseline comparison, this does not directly affect the control of the device. However, in real-time, when the prediction or estimation changes, the behavior of the prosthetic leg will change which will influence the gait of the user.

4.4 Statistical Analysis

We conducted three separate two-way repeated measures analysis of variance (ANOVA) to compare the performance for each machine learning task (mode classification, slope estimation, and speed estimation) , where the independent variables were the models (DEP/IND) and validation types (Offline/Real-Time). In the speed estimation statistical analysis, one more model was tested as one of the independent variables (DEP, IND, and SEMI). Across all tasks, the dependent variable was error (mode: %error, slope: RMSE (deg), and speed: RMSE (m/s))). In each analysis, an α = 0.05 and a Bonferroni post-hoc

correction was used to make pairwise comparisons to understand if there were statistical differences between each condition (Minitab 19.0, USA). Additionally, for mode classification, there was a 2-sided paired t-test (α=0.05) performed to quantify the relative change across models (DEP and IND) between offline and real-time results. The rationale behind this was to evaluate the validity of optimizing offline models and whether they would translate to similar real-time results.

4.5 Results

4.5.1 Mode Classification

Figure 4.3 shows the comparison of average error (% percent) across DEP and IND models from offline to real-time. The error was computed by taking the total number of incorrect steps across both steady-state steps and transitional steps over the total number of strides taken. The offline DEP model error was 5.24$\pm$0.54% and offline IND model error was 13.16$\pm$2.48%. The real-time DEP error was 21.86$\pm$3.29% while the real-time error IND error was 20.18$\pm$4.00%. There was a statistical difference overall between offline models and real-time models. Furthermore, there was a statistical difference between the offline DEP model and both real-time DEP and IND models. There was also a statistical difference found between the relative change in error across subjects between DEP and IND models from offline to real-time error. The relative change was calculated using Equation 4.1. The average relative change for the DEP models was 359.50$\pm$98.69% and for IND models was 61.82$\pm$25.82%.

$$RelativeChange = \frac{Real - TimeError - OfflineError}{OfflineError} \tag{4.1}$$

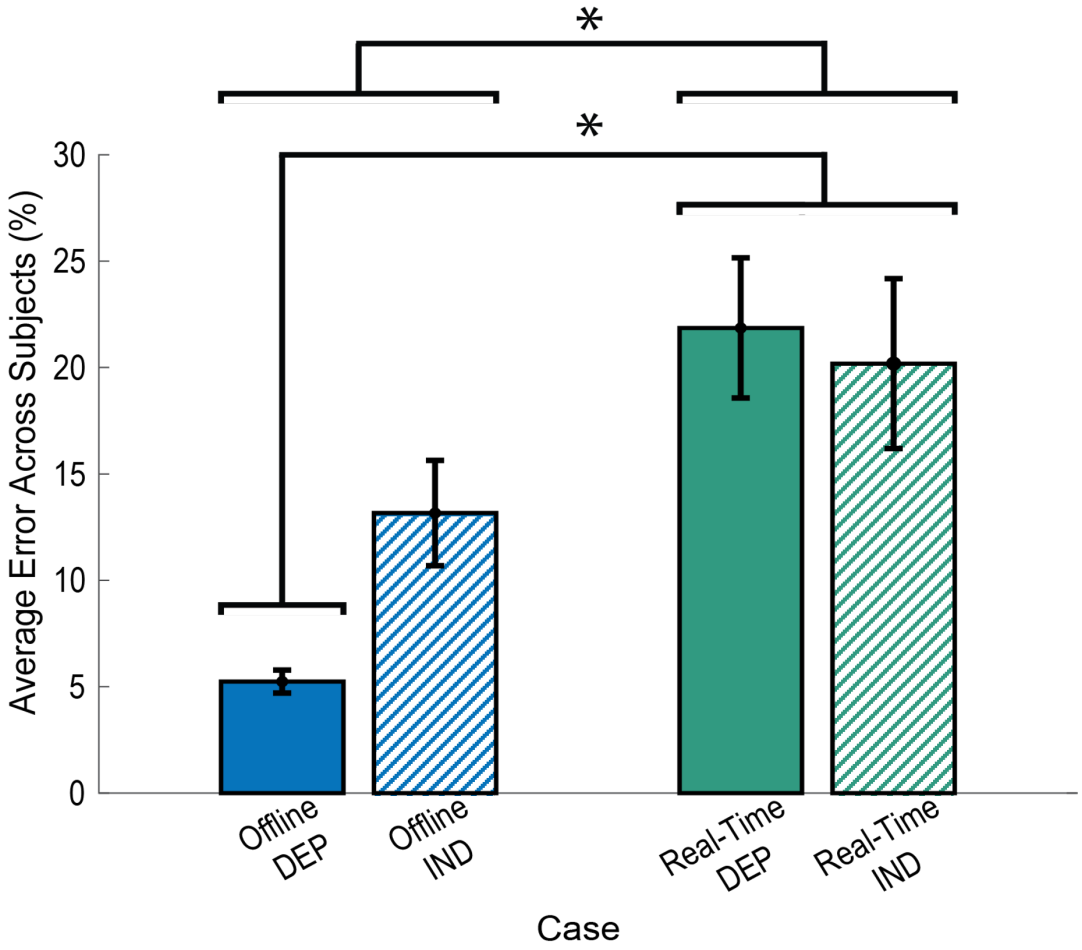

Figure 4.3: Average percent error across subjects (N=6) between offline models and real-time models for both dependent (DEP) and independent (IND) systems. Error bars represent $\pm$ standard error of the mean. Asterisks indicate statistical significance ($p<0.05$). Real-time errors are generally worse compared to offline models for both systems which is an expected result.

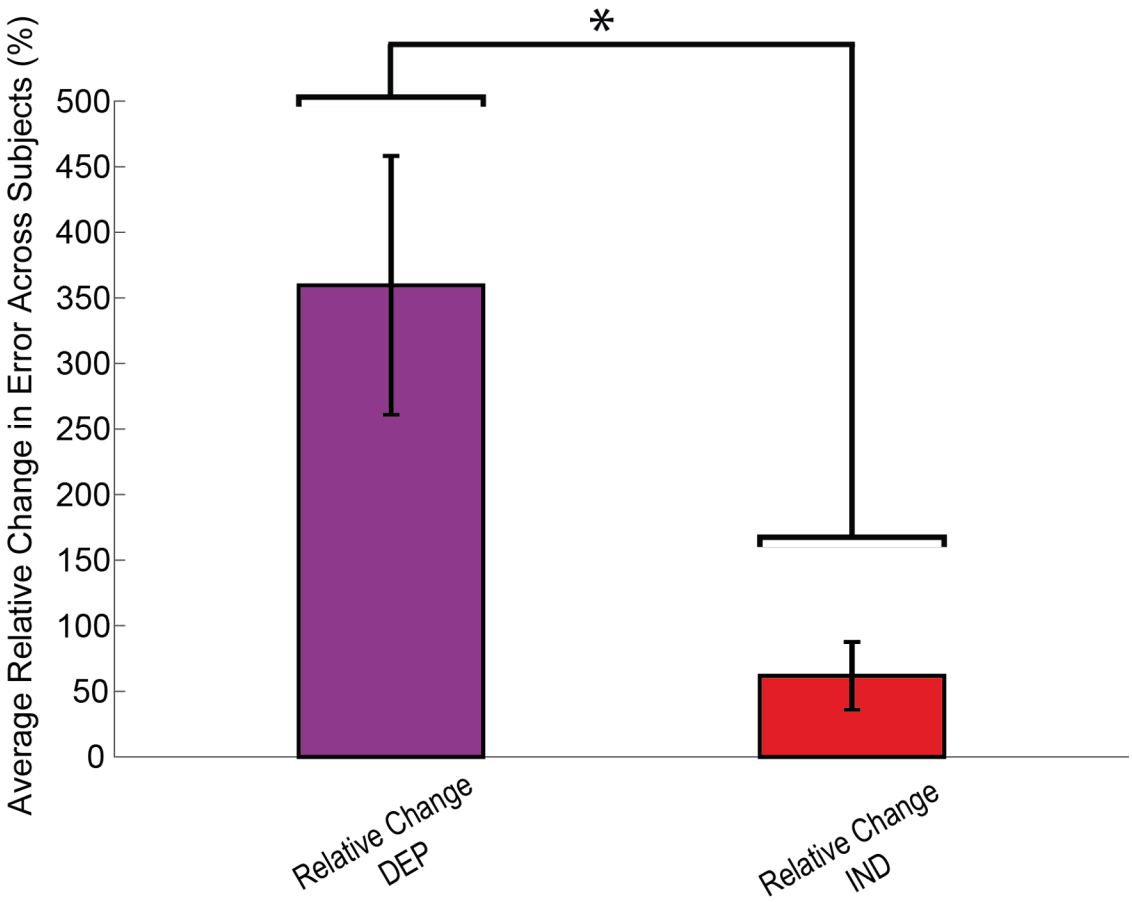

Figure 4.4: Average relative percentage change across subjects (N=6) between offline models and real-time models for both dependent (DEP) and independent (IND) systems. Error bars represent $\pm$ standard error of the mean. Asterisks indicate statistical significance ($p<0.05$). IND models show better promise of translating results from offline to real-time systems.

4.5.2 Slope Estimation

Figure 4.5 shows the comparison of average RMSE (deg) across DEP and IND models from offline to real-time. The offline DEP model error was 0.8531±0.0793 deg and offline IND model error was 1.1218±0.0841 deg. The real-time DEP error was 1.1995±0.0953 deg while the real-time error IND error was 1.0421±0.0555 deg. There was a statistical difference between the offline and real-time DEP models. Similarly, the average relative change for the DEP models was 46.97±20.27% and for IND models was -4.44±8.81%. However, no statistical difference was found between the relative change across both models.

4.5.3 Walking Speed Estimation

Figure 4.6 shows the comparison of average RMSE (m/s) across DEP, IND, and SEMI models from offline to real-time. The offline DEP model error was 0.0666±0.0074 m/s, the offline IND model error was 0.1003±0.0208 m/s, and the offline SEMI model was 0.0685±0.0050 m/s. The real-time DEP model error was 0.1054±0.0083 m/s, the real-time IND model error was 0.1144±0.0163 m/s, and the real-time SEMI model was 0.1051±0.0075 m/s. There was a statistical difference overall between offline models and real-time models, but no other statistical differences were found. Similarly, the average relative change for the DEP models was 67.72±21.69%, IND models was 21.76±12.16%, and for SEMI models 56.22±13.15%. However, no statistical difference was found between the relative change across all three models. Figure 4.7 shows an example of the tracking performance of a representative subject from the IND model on the staircase dynamic profile. The average RMSE was 0.0658 m/s.

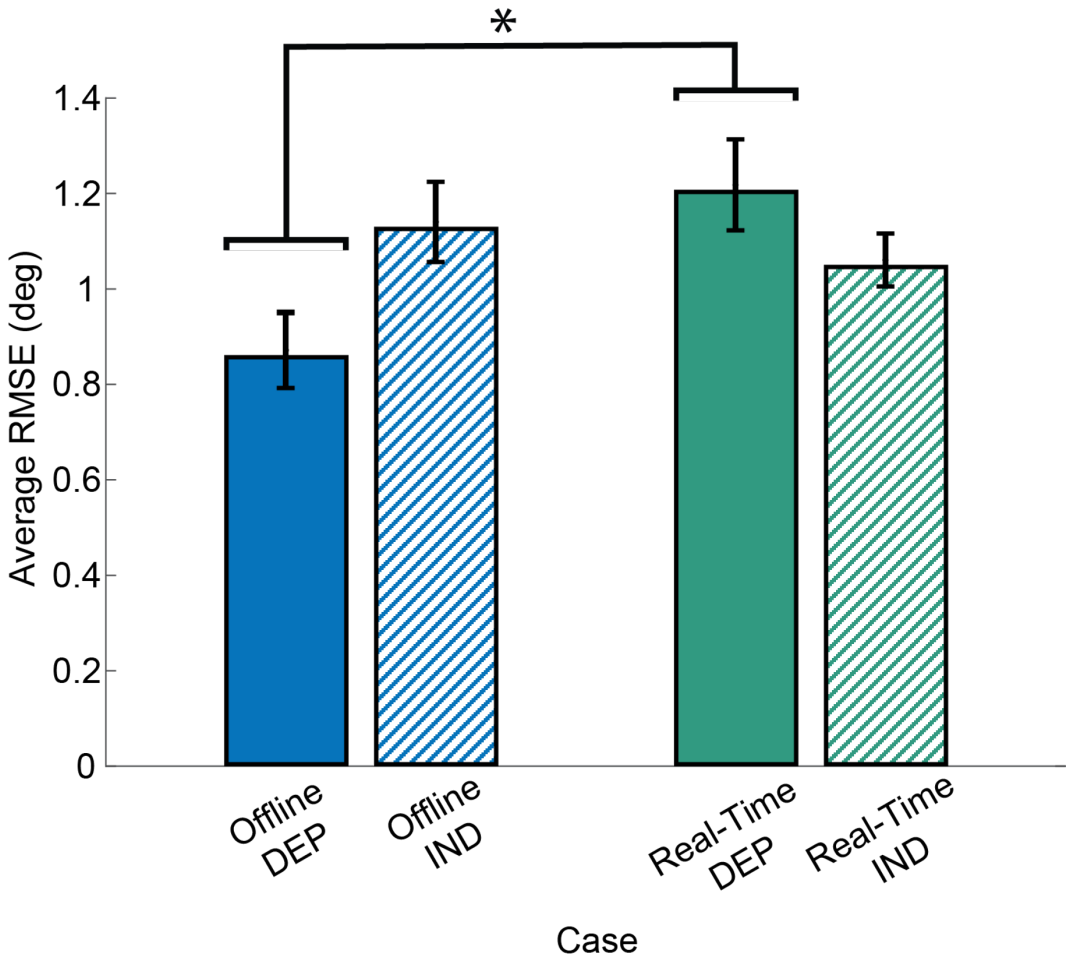

Figure 4.5: Average RMSE (deg) across subjects (N=6) between offline models and real-time models for both dependent (DEP) and independent (IND) systems. Error bars represent $\pm$ standard error of the mean. Asterisks indicate statistical significance ($p<0.05$). IND models show no degradation of error when going from offline to real-time, and in the context of slope estimation, the results are shown to improve.

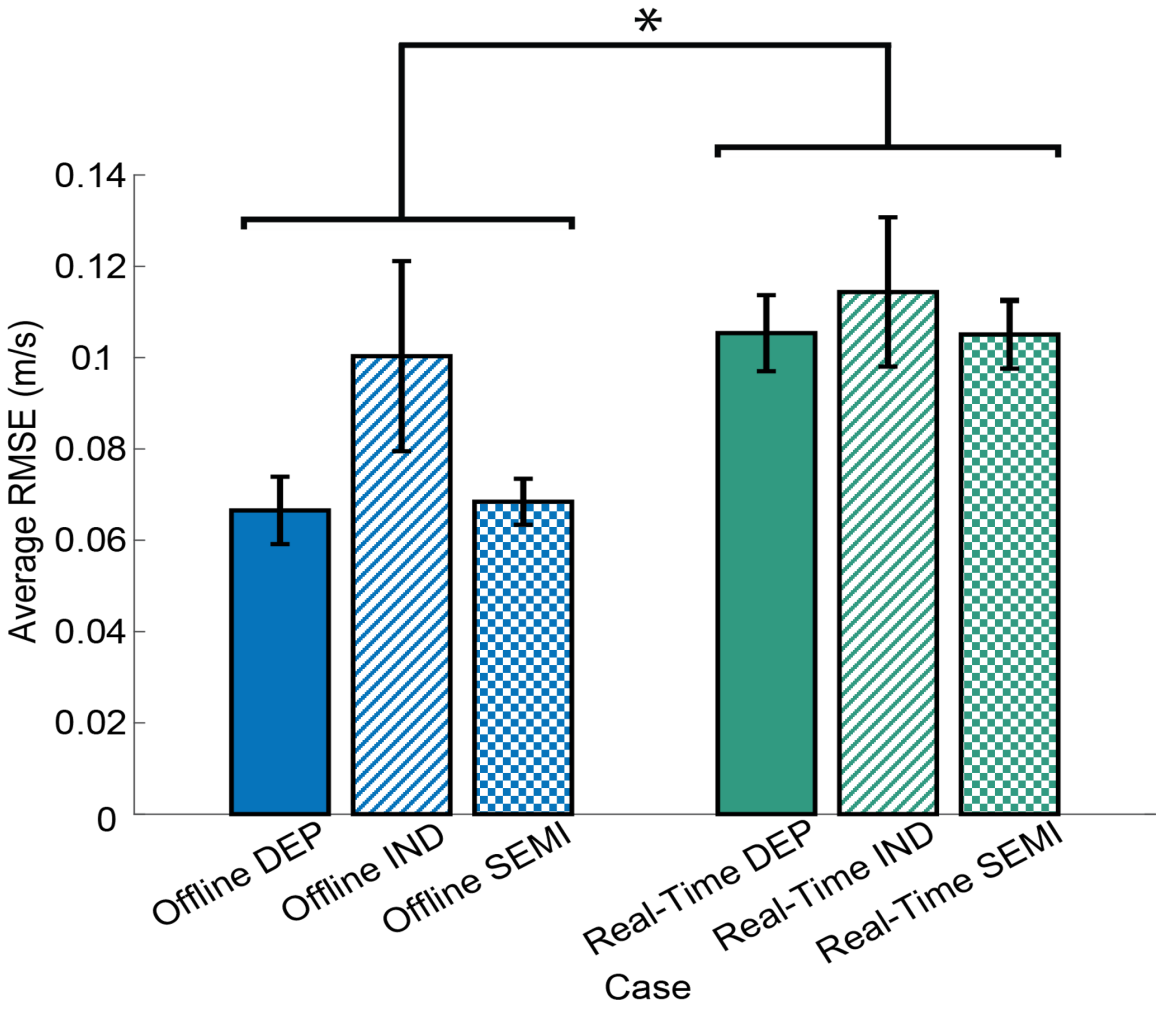

Figure 4.6: Average RMSE (m/s) across subjects (N=6) between offline models and real-time models for both dependent (DEP), independent (IND), and semi-independent (SEMI) systems. Error bars represent $\pm$ standard error of the mean. Asterisks indicate statistical significance ($p<0.05$).

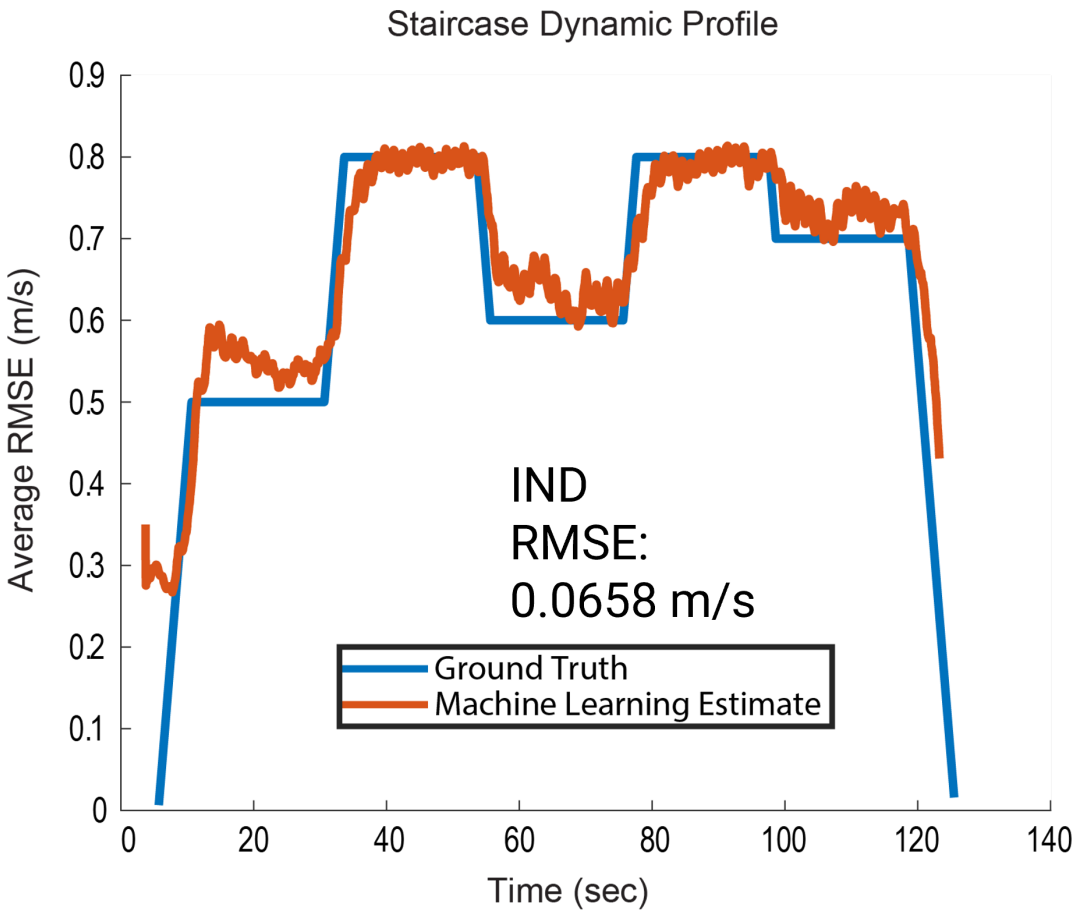

Figure 4.7: IND walking speed model tracking a dynamic trial (i.e. staircase profile) for one user. The RMSE of this trial was 0.0658 m/s.

4.6 Conclusions

The work described here in this chapter, to our knowledge, is the first clinical evaluation of a tiered classifier and regressor intent recognition system using embedded mechanical sensors on various slope angles and speeds contained with a powered knee and ankle prosthesis. Machine learning algorithms were utilized to take raw sensor information and predict and estimate different terrain contexts under different walking conditions. On average, the best result achieved in real-time mode classification was the IND model with an error of 20.18$\pm$4.00%. For real-time slope results, the IND model was best with an average RMSE of 1.0421$\pm$0.0555 deg. For real-time walking speed results, the SEMI and DEP models were best and achieved similar results with an average RMSE of 0.1052 m/s. These results serve as a baseline for real-time intent recognition systems to achieve in order to make these devices more clinically viable.

Our first hypothesis was accepted as we saw in general that real-time errors were worse than offline errors across tasks (more specifically in mode prediction and speed estimation). Our second hypothesis was rejected. We found that the relative improvement was worse for user DEP models compared to user IND models. Lastly, our third hypothesis was also rejected (i.e. a good thing) since we did not find a statistical difference between user IND and user DEP model's performance. The practical findings from this study indicate that the difference between errors from offline to real-time was smaller for IND compared to DEP systems. The focus of future studies should look to improve upon user-independent intent recognition systems as they will match closer to offline training results, due to its ability to capture both intra and inter subject variability across many different users. This also means that there does not need to be extra training sessions for each novel user to deploy these models.

One limitation of our study is that it is still unknown how many subjects must be pooled together to achieve generalizability. Although methods have been developed to

augment the dataset, it still unclear how to make these machine learning algorithms robust to differences and perturbations experienced in everyday walking. Trust and usage of a active device takes time, which allows the user to explore and understand how the device will help them. Although researchers need to create more intelligent controllers, they must also keep in mind that utilizing the device must be simple and easy to understand for end users to adopt this type of technology. By exploring and developing methods to overcome these limitations, this is one step closer to making these systems generalizable to the general population.

CHAPTER 5
BIOMECHANICAL COMPARISON OF HEALTHY, PASSIVE, AND POWERED PROSTHESIS GAIT

5.1 Background

In the current market, the most common prosthetic devices are passive or semi-active. These devices cannot provide net positive work during locomotion. Some of the passive devices apply a spring mechanism to store the energy at foot-ground impact and release the energy at toe-off phase. However, such strategies are not efficient and provide only a simple mechanism to support the load and achieve basic kinematic patterns [96]. The larger issue is that these devices can not replicate the kinetic characteristics of the missing limb. Simultaneously, the lack of knee-ankle joints increases the load of hip in walking which in turn increases the metabolic cost of the person and fatigue of the user. This leads to differences in gait parameters, asymmetry, and compensatory motions. One solution is to utilize an active/powered prostheses which can render positive power in knee and ankle joints. There is limited research in understanding how to use this power generation optimally to improve clinical and gait outcomes.

Although powered prostheses can be simply implemented by actuators, different controller strategies demonstrates different impact on the gait outcomes. Recent studies show the robustness of impedance controller in human locomotion, specifically with those wearing powered knee and ankle devices [13, 36, 25, 26, 76]. Impedance-based control allows for torques to be specified by tunable parameters coupled with environmental information (i.e. ankle angle). The controller can switch between these defined torque laws to define the motion of the prosthetic device for a given task [26]. Typically these change for different ambulation modes. Previous chapters were focused on determining

the correct mode, where as the controller here is meant to map the desired gait to programmable actions. This chapter provides results in discussion of how active prostheses can be enhanced to improve biomechanical function to lead to better user outcome measures which in the long term could improve quality of life. The analysis presented in this chapter looks at adapting the impedance controller to level walking, stairs, and ramps.

A full biomechanical analysis allows us to compare how the prosthesis affects the lower-limb joints. This analysis looks at kinematic, kinetic, power, and energy profiles to better understand the advantages of using active prostheses. Furthermore, this information can let us understand current limitations and provide insights into potential areas of improvement. The assessment of all the biomechanical profiles described above is scarce in the literature especially for different prostheses, specifically active, and for both stair and ramp ambulation [97, 98]. Most studies that compare biomechanics use passive prostheses which have limited functionality in more dynamic tasks. In prior literature, most studies have looked at commercially available devices to understand the kinematic and kinetic changes experience on both the prosthetic and intact sides [92, 99, 100, 101, 102, 103, 7]. Morgenroth et. al and Wolf et. al were the only studies to look at using a Power Knee to provide net positive work which showed results of reducing loading on the intact side hip. Similarly, Kaufman et al. looked at gait asymmetry in level walking using microprocessor-controlled prosthetic knees, noting that improvements in gait symmetry may lead to improved long-term health outcomes [104]. In addition, Lawson et al. observed kinematic joint profiles in stairs for a single subject with TFA [105]. Finally, Ledoux et al. looked at stair ascent kinematics and kinetics for the prosthesis side only [106, 107].

With this motivation, we studied the locomotion in level walking, stairs, and ramps to compare the biomechanics for individuals with transfemoral amputation (TFA) using commercial passive prostheses to a research-grade active prosthesis. The focus of this

chapter was to investigate the analysis of kinematics, kinetics, mechanical energy for the prosthetic side and the intact side. As it has been noted in previous literature, an active prosthesis is expected to improve the patterns of kinematic response in the sense of motion profiles that resemble those of individuals without amputation [100, 108, 109]. We hypothesized that with an active prosthesis the intact side joint loads and energy expenditure will be lower compared to passive prostheses. Secondly, we hypothesized that with active prostheses, users would exhibit more symmetric locomotion comparable to able-bodied individuals. Furthermore, we evaluated the biomechanical response at different inclination angles while scaling assistance as a function of slope angle in ramp ascent. Finally, by comparing this to data from healthy subjects from [94], this chapter discusses the limitations of current active prostheses. Note the work on stair ambulation and level walking presented in this chapter was led by my collaborator Dr. Jonathan Camargo. Specifically, he was first author lead on the submitted manuscript for the stair ambulation comparison between powered and passive prostheses.

5.2 Robotic Devices

Two devices were utilized to compare the biomechanical profiles of both the prosthetic and intact sides. The first device (EPIC leg) is described in more detail in Chapter 2 and 3. Specifically this device has 2 actuated joints in the sagittal plane and a passive inversion/eversion degree of freedom. For details on the design and validation, the reader can refer to [75, 76]. The second device is the Open Source Leg (OSL), designed by University of Michigan. The device can provide active power in knee and ankle joints in sagittal plane. For details on the design and validation, the reader can refer to [17, 18]. The EPIC leg was used in our stair ambulation study, while the OSL was used in our ramp ambulation and level walking protocols. The main reasons for using a different device was adaptability to user height, weight of the device, and ease of control.

Custom OpenSim models were created for both active devices (Figure 5.3). OpenSim

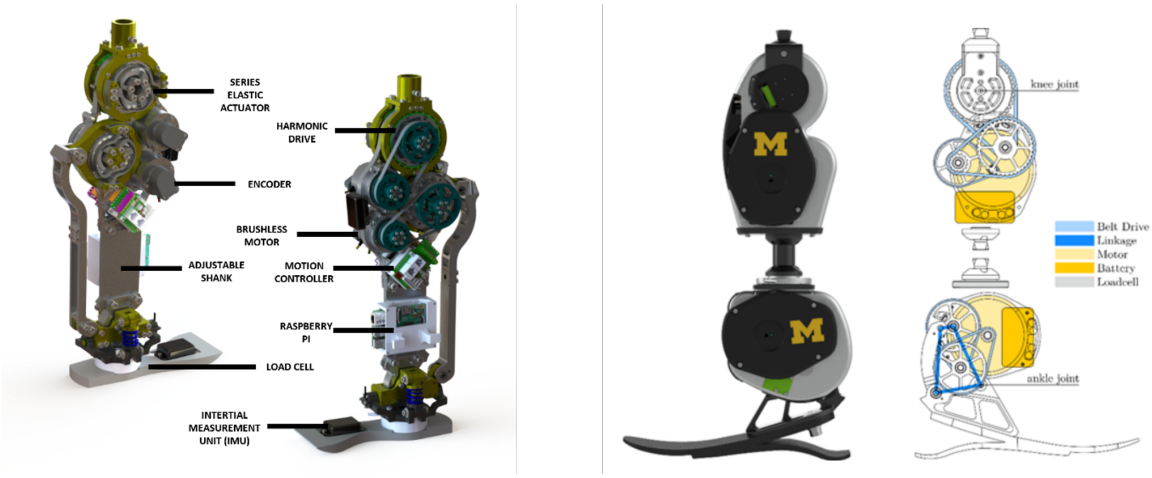

Figure 5.1: EPIC leg device originally designed from AMBER Lab from California Institute of Technology. Open Source Leg (OSL) concept was designed by Neurobionics lab from University of Michigan. Both of these devices were manufactured in house at the mechanical engineering machine shop at Georgia Tech. Active knee and ankle prosthesis device with 6 embedded sensors (2 encoders, 3 IMUs, and 1 6-DOF loadcell)

	EPIC Leg	OSL
Peak Torque	~72 Nm (Knee) ~105 Nm (Ankle)	~150 Nm (Knee) ~178 Nm (Ankle)
Active ROM (Extension/Flexion)	~ 70˚ (Knee) -40˚ ~ 25˚ (Ankle)	~120˚ (Knee) ~30˚ (Ankle)
Passive ROM (Inversion/Eversion)	-5˚ ~ 5˚ (Ankle)	N/A
Device Weight	~8 kg	~4.1 kg

Figure 5.2: EPIC leg and OSL comparison of torque, range of motion, and device weight.

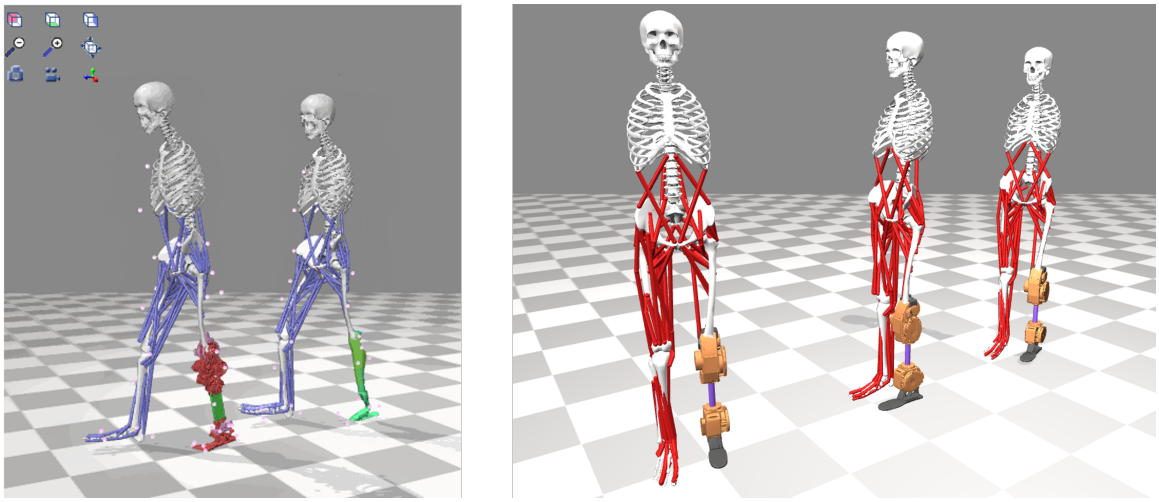

Figure 5.3: OpenSim models created for the EPIC leg and OSL. Custom models were generated to incorporate more accurate mass and inertial properties. Custom models were made for both left and right sides for individuals with transfemoral amputation.

is an open-source biomechanics platform useful for computing inverse kinematics and kinetics using motion capture and forceplate data. The rationale for creating custom models were to better incorporate mass and inertial properties to generate more accurate results compared to able-bodied skeletal models. An automated biomechanics pipeline was designed and built to compute biomechanical information for each joint. The new modified model can be used to render a full-body biomechanics analysis from motion capture and ground reaction force (GRF) data. With a same fashion, a modified model for passive prosthesis is utilized for passive full-body biomechanics analysis. Scaling, inverse kinematics and inverse dynamics were computed using these models in OpenSim with MoCapTools toolbox [110]. The biomechanical profiles were used to compute user outcome metrics of symmetry, temporal parameters, and energy distribution across joints.

5.3 Comparisons of Active and Passive Prostheses: Stair Ascent Ambulation

5.3.1 Protocol Design

Individuals with unilateral transfemoral amputation (N=7 subjects, one female, six males, age 49$\pm$14 years, height: 1.77$\pm$0.07m, mass: 87.3$\pm$16.5 kg) provided written, informed

consent for this study under the Georgia Institute of Technology Institutional Review Board. Subjects performed stair ascent tasks using an active knee-ankle prosthesis under four different stair configurations within the range of the Americans with Disabilities Act (ADA): 10.2 cm (4in), 12.7 cm (5in), 15.2 cm (6in), 17.8 cm (7in). The same subjects also performed the task while using their clinically prescribed passive prostheses at the nominal height configuration of 15.2 cm. We recorded motion capture data using infrared markers (Vicon. Ltd., Oxford, UK) and ground reaction force using force plates (Bertec, Ohio, USA), located on each step of the staircase. After a session of training and tuning of the impedance parameters, supervised by a certified prosthetist, the subjects were instructed to perform five repetitions of ascending and descending the stairs under each prosthetic condition [26]. Users were instructed to minimize the use of handrails during the ambulation tasks.

5.3.2 Statistical Analysis

A statistical comparison of passive and active results was conducted using a one-way repeated-measures ANOVA for each symmetrical measure. The independent variables were device type (active/passive prostheses) and the dependent variables were spatiotemporal parameters (stance time/swing time). A Bonferroni post hoc analysis to determine pairwise differences with a significance level of α = 0.05. For the analysis of the energy profiles, paired t-tests were run comparing both the total energy of the active and passive data to able-bodied individuals (α = 0.05). For the analysis of the knee moment scaling, linear regression was performed to determine a relation with respect to the stair height. The significance of the regression equations was tested with an F-test. Furthermore, a Wilcoxon signed rank test was performed on the PEQ-MS results comparing active and passive prostheses.

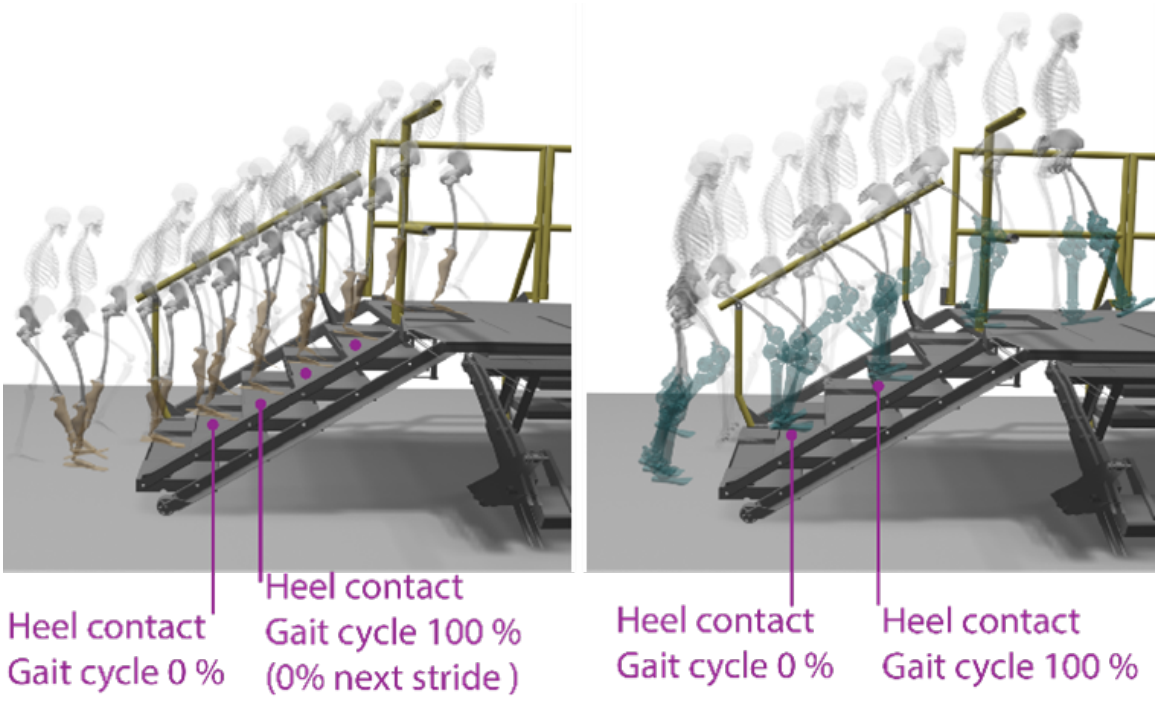

Figure 5.4: Experimental protocol. Using an active prosthesis, subjects performed a stair ascent for different configurations of stair height (10.2cm-17.8cm). Subjects performed the same task using their regular passive prosthesis at the intermediate height (15.2cm). Skeletal models of individual with passive prosthesis (left) and active prosthesis (right) performing a stair ascent task. The stair consisted of 6 steps of adjustable height. Subjects with active prosthesis performed step-over-step locomotion in ascent, with passive prosthesis the locomotion is step-to-step. For stair descent locomotion is step-over step.

5.3.3 Results

Biomechanical profiles of joint kinematics, kinetics, and power profiles were generated for the passive and powered devices. While using the active prosthesis, the kinematic profiles of the limb resemble that of the able-bodied subjects in both the prosthetic (Figure 5.5) and intact sides (Figure 5.6). For the prosthetic side, the hip matches the kinematic profile of able-bodied individuals with motion peaks at -6.2±3.4 deg and a reduced flexion of 42.4±7.2 deg. The active knee allows for 46.4±7.4 degrees of knee flexion angle at heel-contact, as well as producing clearance motion in the swing phase with peak flexion of 63.0±9.1 degrees. The active ankle provides dorsiflexion of 14.2±3.0 deg during the stance phase and plantar flexion at the end of the stance with a peak of 10.3±4.5 deg. Subjects with passive prosthesis could not perform step-over-step gait in stair ascent without excessive effort or significant handrail usage. Thus, we evaluated the step-to-step gait as a more representative locomotion pattern for everyday situations with a passive prosthesis. In contrast to the active prosthesis, the passive prostheses showed a reduced peak knee flexion angle of 8.2±5.1deg during the swing phase and reduced hip motion in the range of 3.1±10.0 deg extension and -20.4±7.2 deg flexion. The ankle showed some level of dorsiflexion of 8.4±3.0 deg during mid-stance due to the elastic deformation of the foot as weight loading increases.

The powered prosthesis showed peak moments significantly lower than those of able-bodied subjects. However, in comparison to the passive prosthesis, we observed a significant assistive moment at the knee, producing a peak extension moment around 0.56±0.17 Nm/kg during the early stance phase. The ankle produced a peak plantarflexion moment at push-off of 0.41±0.10 Nm/kg. These corresponded to 75% (knee) and 34% (ankle) of the able-bodied peak moments, respectively.

In terms of symmetry and temporal characteristics (Figure 5.7), the velocity of the task (ascended stair steps per minute) is significantly higher for the active condition ($p<0.05$) compared to the passive condition but significantly lower than able-bodied subjects

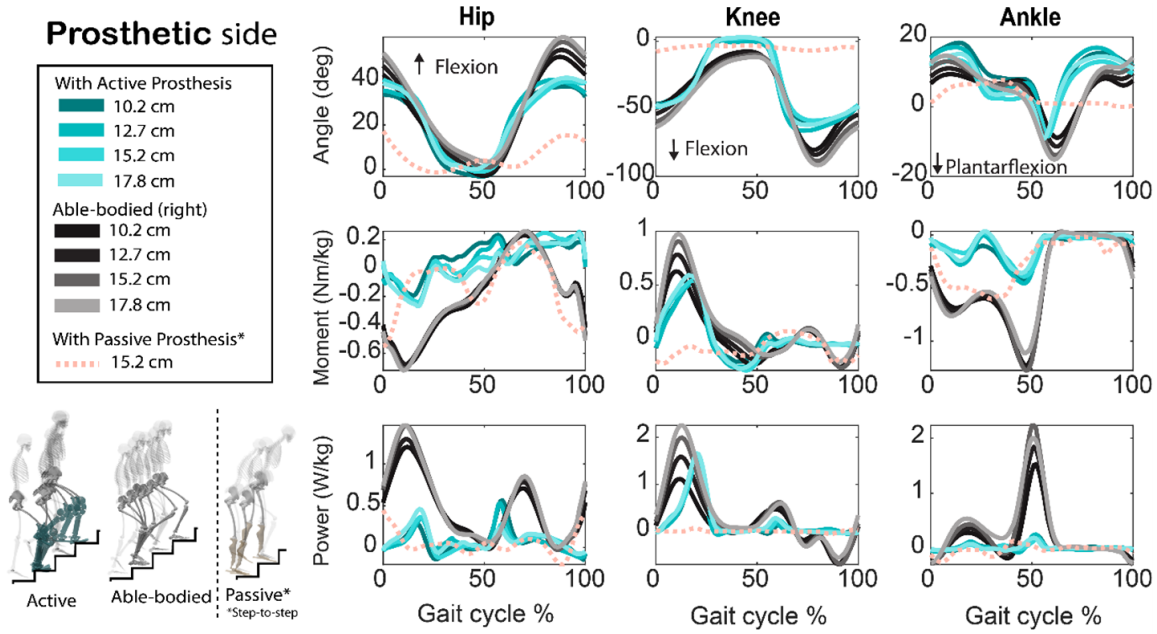

Figure 5.5: Average kinematic, kinetic, and mechanical power profiles of the hip, knee, and ankle during stair ascent on the prosthetic side at different stair height configurations for healthy subjects' right side (black) and subjects with transfemoral amputation wearing an active prosthesis (blue). The profile with passive prostheses in step-to-step gait at the nominal height of 152mm is included as a reference of comparison (pink).

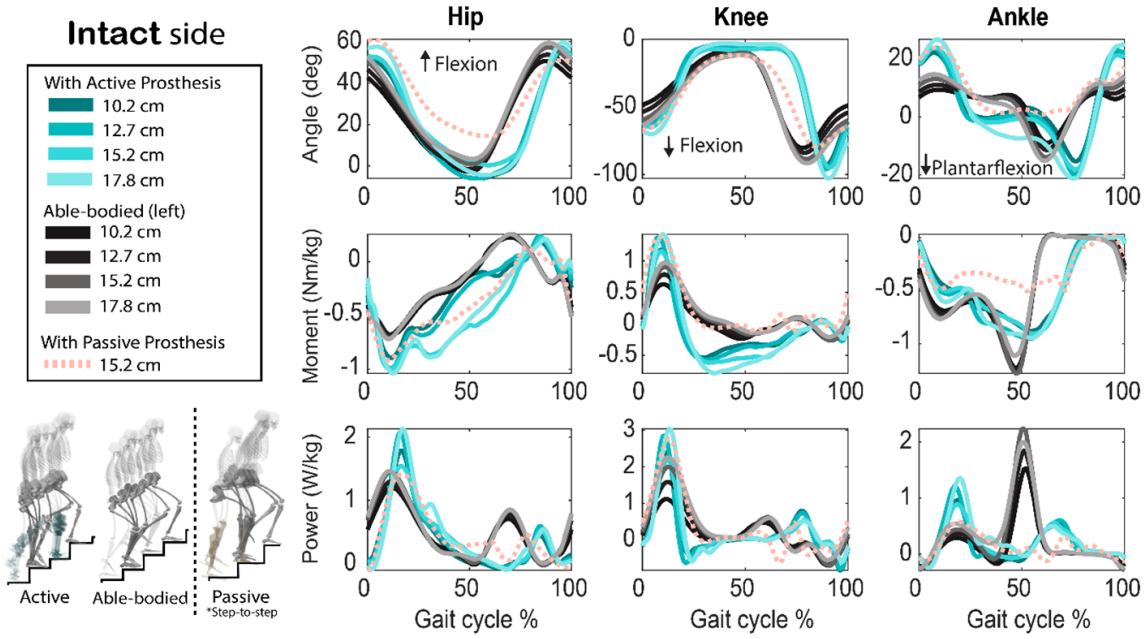

Figure 5.6: Average kinematic, kinetic, and mechanical power profiles of the hip, knee, and ankle during stair ascent on the intact side at different stair height configurations for healthy subjects' right side (black) and subjects with transfemoral amputation wearing an active prosthesis (blue). The profile with passive prostheses in step-to-step gait at the nominal height of 152mm is included as a reference of comparison (pink).

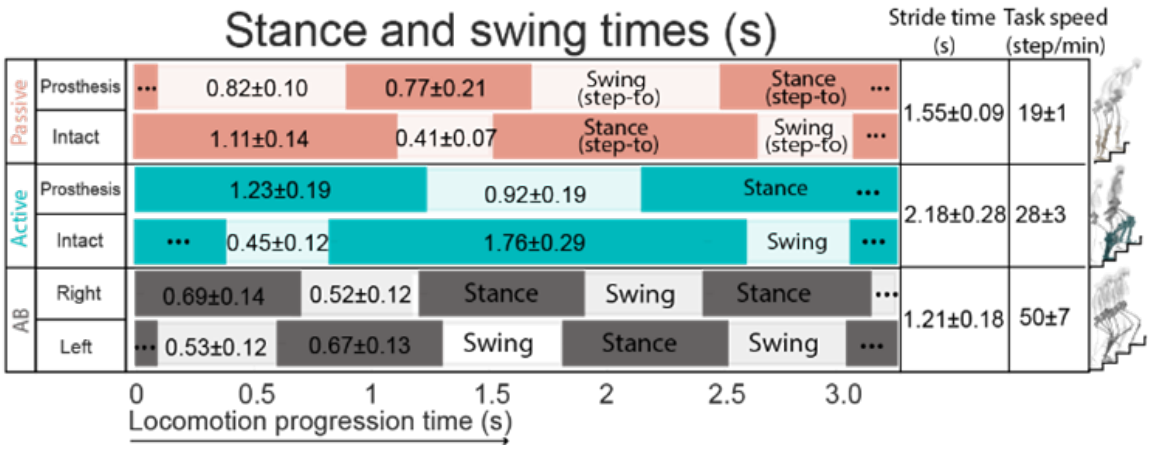

Figure 5.7: Temporal characteristics of stair ascent wearing an active prosthesis, passive prostheses, and reference data for able-bodied (AB) subjects. Stance times (dark color) and swing times (light color) ± standard deviation is presented in sequence, showing alternating support on the intact and prosthetic side. Note that with the passive prostheses, the subject executes two strides to achieve the same progression as a single stride with the active.

($p<0.05$). The step-to-step nature of the gait for the passive prosthesis reduces the task speed and increases the asymmetry. The stance time ASI was -35.6% for passive. Swing time presented an ASI of 65.9%. This means that subjects spent more time on the intact side for both types of prostheses.

Figure 5.8 presents the energy distribution of the stair ascent task where the pie-chart size is scaled to the total positive energy. Both active and passive prostheses increased the total positive energy compared to the able body ($p<0.05$). However, with the passive prosthesis, the prosthetic side provides negligible net energy at the knee and ankle joints, with most of the total energy provided by the knee and hips of the intact side. The energy from the active prosthesis is concentrated at the knee with 12.4% of the total energy, a similar ratio to 16% found in the able-bodied subjects. Passive prostheses showed an increase ($p<0.05$) in the requirements of total positive mechanical energy with respect to active.

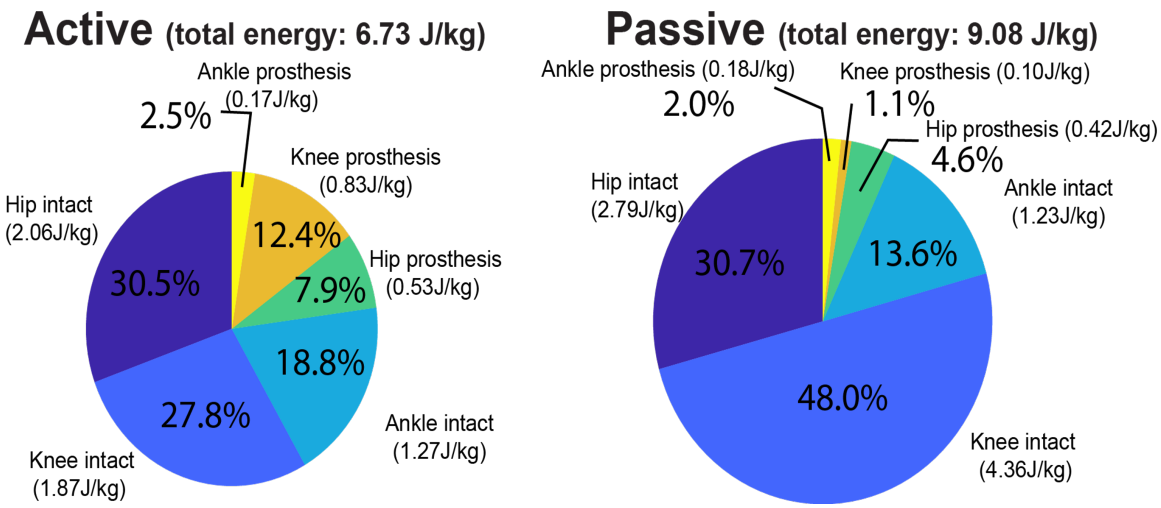

Figure 5.8: Average positive energy distribution for stair ascent comparing individuals with transfemoral amputation with the active prosthesis compared to the passive prosthesis. The distribution for passive prostheses is calculated for a step-to-step gait.

5.3.4 Stair Ascent: Modulation of Knee Torque as function of Stair Height

During stair ascent walking, the increase in the peak knee moment of the able-bodied subjects during the stance phase is influenced by the increase in the stair height ($p<0.05$). We suggest that future control solutions could use the effects of locomotion context found in able-bodied individuals to incorporate into scaling priors in the impedance control framework. Here we demonstrated this idea by using the able-bodied peak knee moment to determine a linear regression model to the stair's height and estimate the influence of stair height on the changes in knee moment given by the slope of the regression equation Figure 5.9. This slope could be used as a scaling factor for the stiffness in the impedance control. Taking the nominal knee stiffness on early stance (k), which was tuned at the nominal stair height (152 mm), we can affect the output moment at the knee by increasing (or decreasing) the stiffness by a factor that is a function of the change in stair height relative to the nominal tuning configuration and the constant scaling ratio (α) (see Equation 5.1).

$$k_{scaled} = k_{nominal}(1 + \alpha \cdot \delta h) \tag{5.1}$$

5.3.5 Qualitative Results: Stair Ascent

The PEQ-MS (prosthetic evaluation questionnaire - mobility scale) results showed improved performance with the active prosthesis over the passive prosthesis in both stair ascent (Active: 3.35 ± 0.61; Passive: 2.71 ± 1.10, scale: 1-5). Stair ascent was found to be statistically significant ($W = 48.0$, ($p<0.05$)).

5.4 Comparisons of Active and Passive Prostheses: Ramp Ascent Ambulation

5.4.1 Protocol Design

The ramp experiment protocol consisted a total of nine individuals with transfemoral amputation (TFA) subjects (2 females, 7 males) who provided written, informed consent for this study under the Georgia Institute of Technology Institutional Review Board. Subjects performed ramp ascent and descent tasks using the active knee-ankle prosthesis and their owned clinically prescribed passive prostheses. For research grade active device (OSL), subjects completed a training and tuning session to ensure comfort and fit (Figure 5.10). Subjects were instructed to conduct five full trials of ramp ascent and descent under four slope angle conditions. The experiment used an adjustable terrain park with four different preset ramp angles: 7.8°, 9.2°, 10.8° to 12.4°. Additionally, the experiment utilized a motion capture system (Vicon. Ltd., Oxford, UK) and ground reaction forceplates (Bertec, Ohio, USA) located at the center of the ramp. Users were only asked to walk on their passive device for a nominal slope angle of 10.8°. Users were instructed to minimize the use of handrails during the ambulation tasks.

5.4.2 Ramp Ascent Scaling

Using a healthy biomechanics reference dataset as a baseline, we designed a scaling equation (Equation 5.2) that would scale knee assistance in ramp ascent in the early stance portion of the gait cycle as a function of inclination angle [94]. From the healthy profiles,

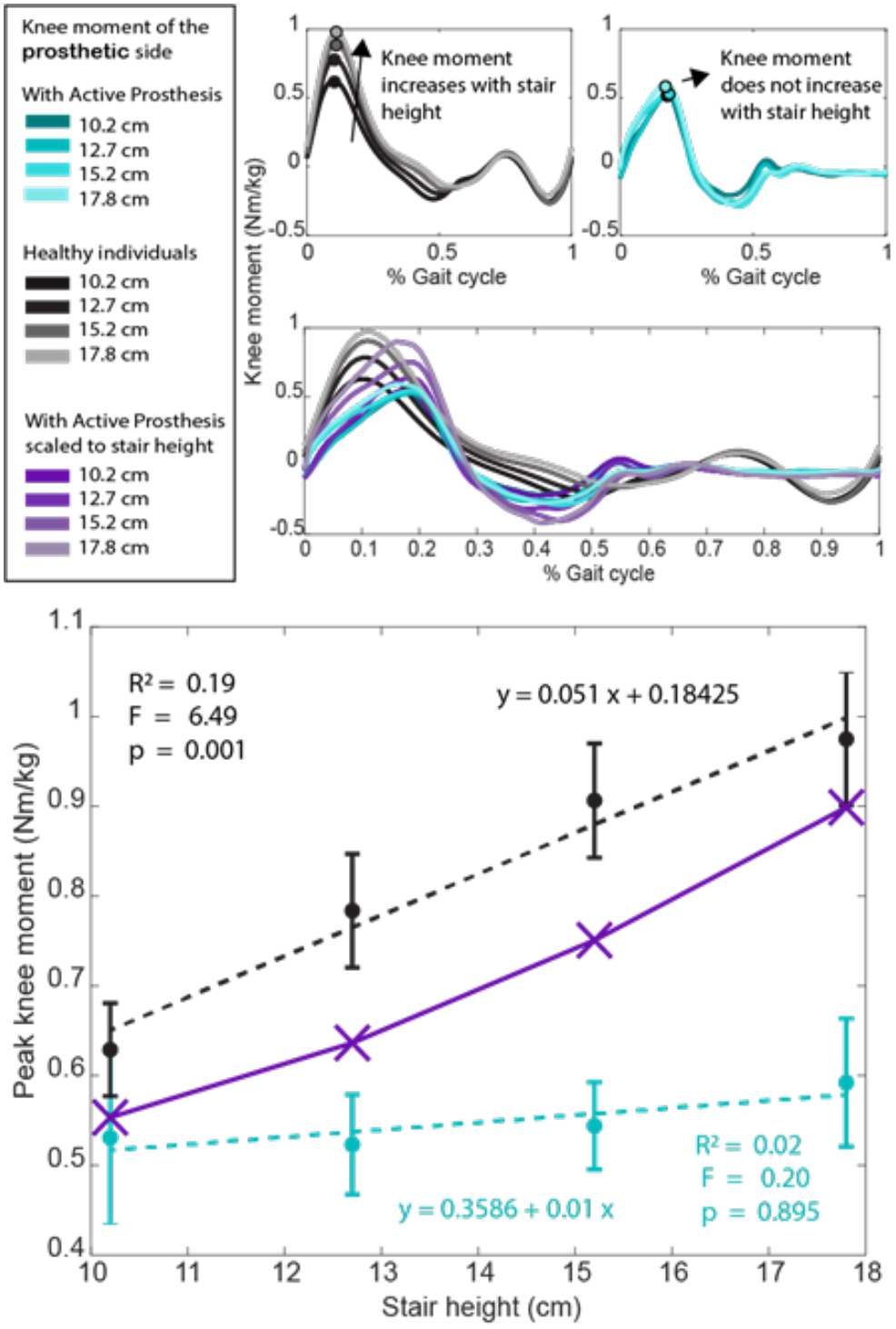

Figure 5.9: Knee moment during stair ascent task for able-bodied subjects and individuals with transfemoral amputation using a passive prosthesis and an active prosthesis. Able-bodied subjects exhibit modulation of knee moment for a change in condition of the stair height. Knee moment modulation for different conditions of stair height.

Figure 5.10: Experimental protocol using Open Source Leg (OSL) on ramp ascent. The powered device scales knee assistance as a function of slope angle throughout early stance.

it can be seen that knee torque scales and hence allowing for this behavior, we hypothesized that this would lead to more symmetric profiles of gait between the prosthetic and intact sides.

$$\tau_{scaled} = k_{scaled}(\tilde{\theta} - \theta_{eq}) - b\tilde{\dot{\theta}}, with\ k_{scaled} = k_{nominal}(1 + \alpha \cdot \delta slope) \tag{5.2}$$

5.4.3 Statistical Analysis

A statistical comparison of passive and active results was conducted using a 2-way repeated-measures ANOVA. The independent variables were device type (active or passive prosthesis) and six lower limb joints (hip, knee, and ankle on both intact and prosthesis side). The dependent variable was the mechanical energy. A Bonferroni post hoc analysis was performed to compare pairwise comparisons with a significance level of α = 0.05.

5.4.4 Outcome Metrics

We evaluated the temporal and symmetry metrics for ramp ascent locomotion. We found that on average, users spent 58.9% in stance phase on the prosthesis compared to 70.6% in stance phase on their intact side. For the passive device, we found that users spent 58.6% in stance phase on their prosthesis side and 68.7% in stance phase on their intact side. This implies that users regardless of prosthesis, spend more time on their intact side, but not they do not differ between passive or active device. Furthermore, asymmetry index was calculated to evaluate symmetry for scalar measurements [111]. Equation 5.3 maps 0% as symmetric and $\pm$100% as total asymmetry. The active stance ASI is -0.1488 $\pm$ 0.0660 and the active swing ASI is 0.3773 $\pm$ 0.1311. The passive stance ASI is -0.0513 $\pm$ 0.0199 and passive swing ASI is 0.3786 $\pm$ 0.1113. Although statistical tests were not performed, these results indicate that subjects still spend more time on the intact side for both types of prostheses.

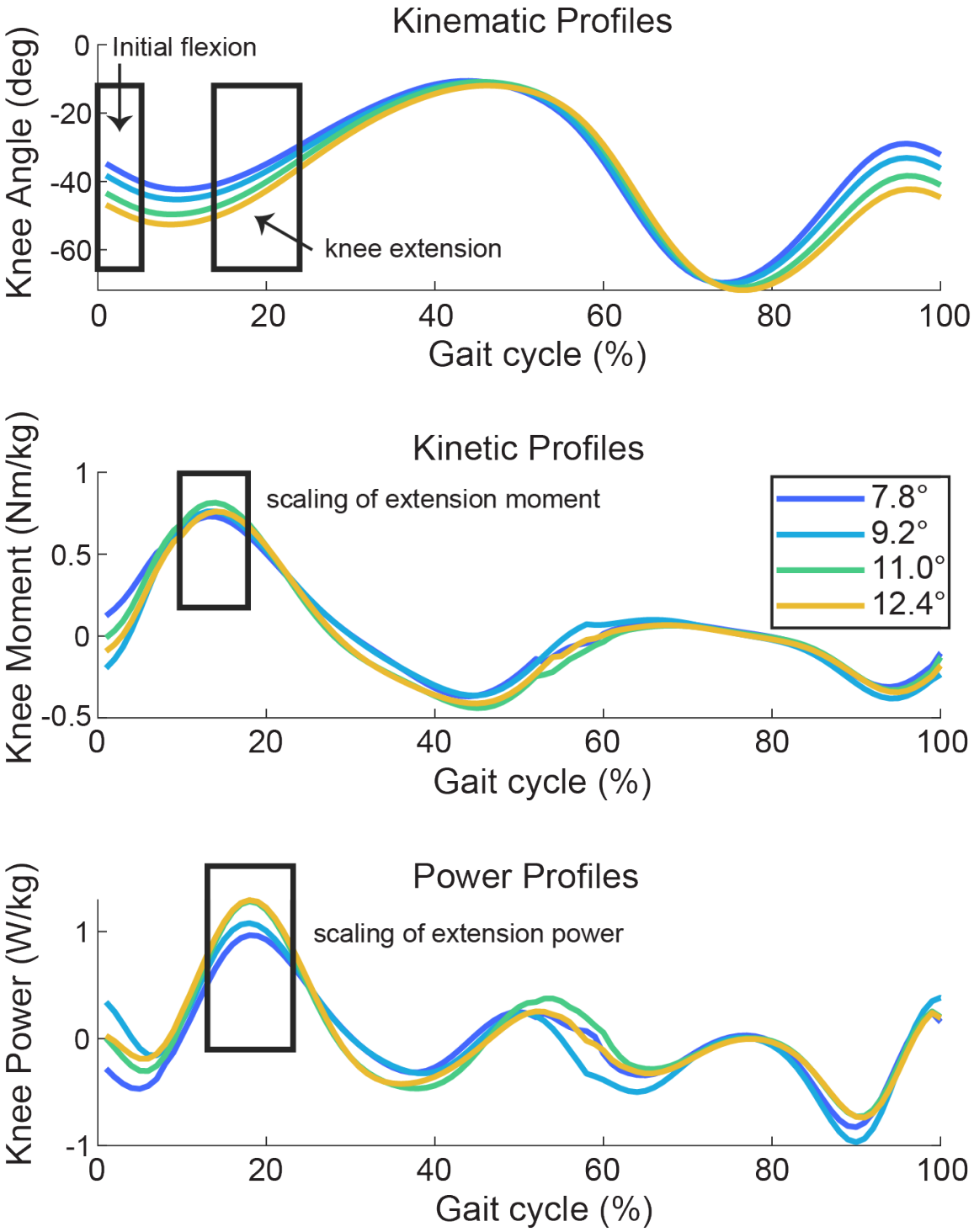

Figure 5.11: Healthy dataset of the knee joint across kinematic, kinetic, and power plots. Knee shows scaling of extension moment in early stance of the gait cycle. Hence a scaling equation was designed to provide a similar torque assistance pattern compared to the biological signal.

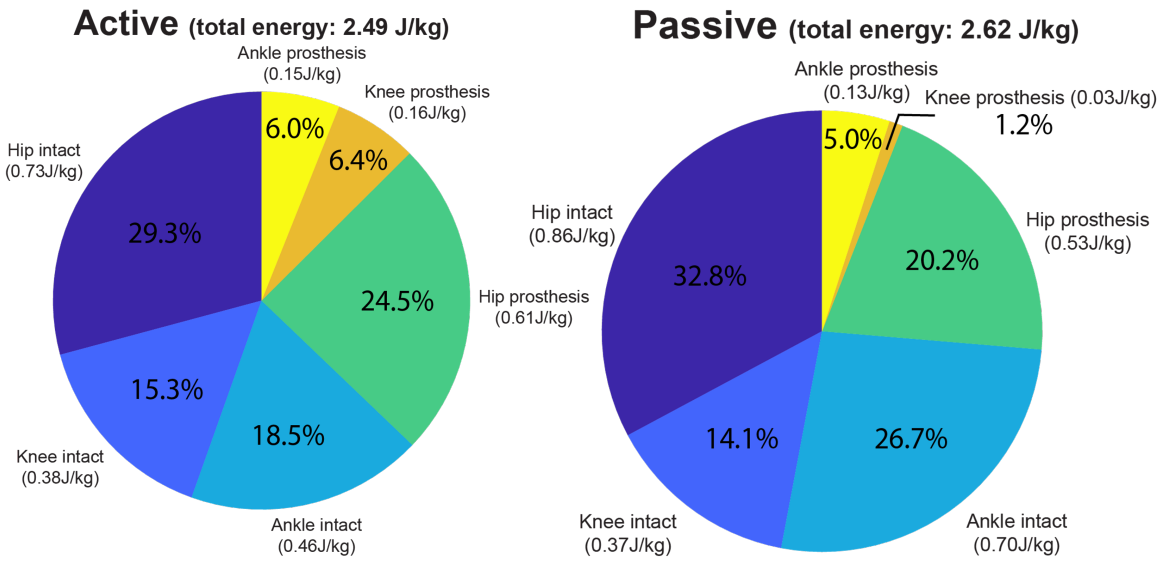

Figure 5.12: Average positive energy distribution for ramp ascent comparing individuals with transfemoral amputation with the active prosthesis compared to the passive prosthesis.

$$ASI = 2 * \frac{(x\_prosthesis - x\_intact)}{(x\_prosthesis + x\_intact)} \tag{5.3}$$

Figure 5.12 shows the energy distribution of the ramp ascent task where the area of the circle is scaled to total amount of energy. Passive prostheses show an increase in total mechanical energy required compared to the active device. However, our active prosthesis still does not match when compared to healthy subjects [94]. With the active prosthesis, it can be seen that hip joint energy on the intact side is reduced compared to the passive device but no statistical difference was found. Furthermore, the majority of total energy is provided by the knee and hip intact side during ramp ascent ambulation. Although minimal handrail usage was instructed for users wearing the active device, we still noticed users utilizing for balance and support purposes. We quantified on average that for ramp ascent, users utilized the handrail to support 9.40% of their body weight, while in ramp descents, handrail usage was 10.27%.

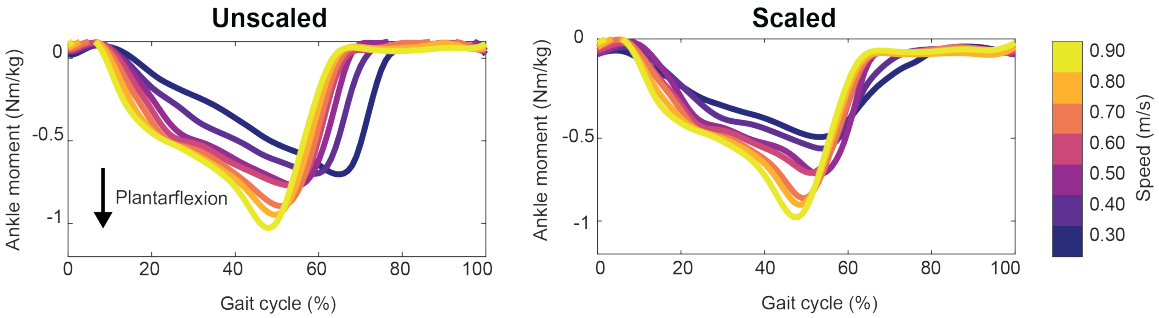

Figure 5.13: Average ankle moment at each condition of walking speed across three subjects. The baseline control (Unscaled) is not aware of the walking speed. The scaled control uses the walking speed information to modulate the ankle stiffness, resulting in scaled plantarflexion moment.

5.5 Comparisons of Active and Passive Prostheses: Level Walking Ambulation

5.5.1 Protocol Design

The preliminary experiment consisted of N=3 healthy male adults, ages (45 yr, 53 yr, 69 yr), height (1.84 m,1.76 m,1.98 m), mass (65.6 kg, 86.5 kg, 104.0 kg). Subjects were instrumented with 46 motion capture markers (Vicon. Ltd., Oxford, UK) using the OSL markerset (Figure 5.3). Ground reaction forces were recorded using force plates (Bertec, Ohio, USA) located in the instrumented treadmill. All the subjects provided informed consent, and the study was approved by the Georgia Institute of Technology IRB. Subjects walked at 0.3-0.8 m/s, with increments of 0.1 m/s during one minute per each speed.

5.5.2 Statistical Analysis

No statistical tests were evaluated for this walking speed comparison due to the small number of subject samples (N=3).

5.5.3 Scaled vs Unscaled Assistance

Ankle stiffness was scaled as a function of walking speed. The difference between the scaled and unscaled controllers was evident for the lower speeds (0.3 m/s and 0.4m/s). Using the context information of the walking speed provides a consistent modulation of the

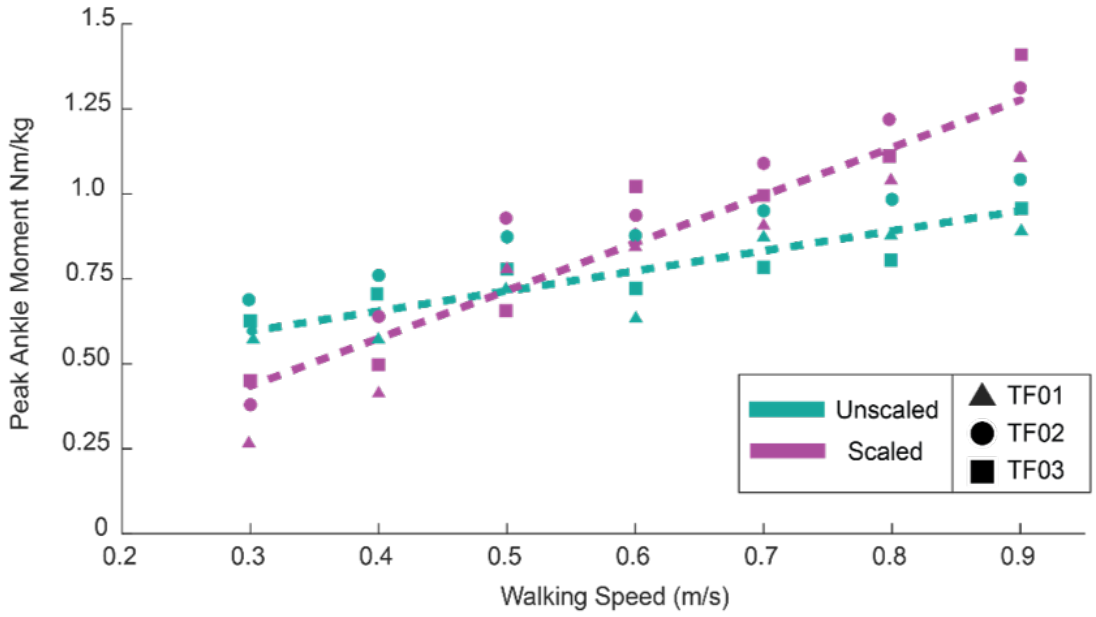

Figure 5.14: Peak ankle moment at each condition of walking speed across three subjects. A regression line is fit to display trend of scaled vs unscaled assistance.

ankle plantarflexion torque that gradually reduces the push-off torque for slower walking. This phenomenon can be seen in the scattered plot of the peak ankle moment as a function of walking speed (Figure 5.14). The effect of this change in ankle moment translated to an improved timing of ankle plantarflexion within the gait cycle. Figure 5.13 presents the ankle kinematics of the prosthesis. For the unscaled case, an unnecessarily high ankle stiffness in the stance phase produces a higher impedance at the ankle, producing a slower dorsiflexion process and delaying the transition to the swing phase. The scaled controller can reduce the ankle moment, achieving a lower ankle impedance and correcting the timing of the plantarflexion event. Furthermore, we found an average reduction of 24.9% in the asymmetry index (Equation 5.3) when applying the scaled control in the lower speed (0.3 m/s).

5.6 Conclusions

We presented the bilateral biomechanics of the user, energetic distribution plots, and asymmetry measures with a powered knee and ankle prosthesis. We also showed scaling equations that were developed across contexts. We found that the active prosthesis significantly improves the symmetry of the kinematic profiles for all the joints and the symmetry of the knee kinetics ($p<0.05$) for stair ascent. With the active leg, the results show the reduction of energetic contribution from the intact side ($p<0.05$). A similar result was also see in the energetic comparison between active and passive devices for ramp ascent. However, a fundamental difference in the kinetics of the active prosthesis with respect to able-bodied subjects was the scaling of the knee moment during the stair ascent task. With peak moment increasing 8.5% for a 1 cm increase in stair height, able-bodied subjects adapt better to a more challenging task, whereas the active leg maintains a nominal torque. To show proof of concept, we implemented the modulation with respect to a context variable. We observed that adjusting the ankle stiffness as a function of the walking speed could drive the resulting biomechanics closer to healthy subjects. By correcting the timing and intensity of ankle plantarflexion for the range of lower speeds, the scaled strategy provides a more consistent response in the walking with better waveform and asymmetry indices. This modulation type could further smooth the response and provide a biological adaptation to the terrain context. Using this information, controllers could scale according to the terrain characteristics, which may lead to a better symmetry between the intact and the prosthetic side.

However, there is still a gap to be addressed for future controllers to make these devices comparable to able-bodied subjects. Although we applied scaling assistance at both the knee and ankle joints, there are still some limitations to be addressed for future studies. Anecdotally, subjects have a hard time adjusting to changes in gait patterns that they have been accustomed to when using a passive device (ex. early stance knee flexion). There

is also a need to allow for users to trust the device and learn how to appropriately use the device to get maximal benefit. The modulation of parameters is key to provide smooth response and provide adaptation to different terrain contexts. By optimally figuring out how to provide scaling at key locations in the gait cycle, this could improve common clinical and gait metrics, which in turn could improve user's ability to walk and function at more dynamic tasks.

CHAPTER 6

CONCLUSIONS

The overall objective of this dissertation was to develop intent recognition systems that could be deployed in real-time to assist and enhance user's locomotion compared to current state-of-the-art devices. Furthermore, this work generated a reproducible pipeline that could be replicated for different wearable robotics, not just powered prostheses. Throughout this dissertation, we were able to make several research contributions to the field in adding intelligence to powered prostheses. First, we used a novel machine learning algorithm that could detect the user's intent based on the embedded sensors in a powered prosthesis. The novelty of this approach was its ability to generalize across unseen terrain configurations (i.e. mode classification could operate on a range of different stair height and slope angles) for both user-dependent and user-independent settings (Chapter 2). Secondly, we developed an offline pipeline that could continuously estimate environmental parameters such as walking speed or slope angle compared to once-per-gait-cycle updates (Chapter 3). We were able to show that these algorithms were robust to different ranges of walking speed but also that they could track dynamic profiles to emulate more real-world behaviors. The main takeaway from this dissertation was the ability to deploy these intent recognition systems in real-time for different users. This work took previous offline studies and combined to allow for direct modulation of assistance during different terrain contexts. Two main points resulted from this in which, 1) user-independent systems do not have a significant reduction of error between offline and real-time implementation compared to user-dependent systems, and 2) real-time intent recognition systems can be embedded onto a powered device making it one step closer to clinical acceptance (Chapter 4). Lastly, we quantified the biomechanical effects of active prostheses compared to passive devices (Chapter 5). Understanding how these devices,

and in general wearable robotics, impact the user is key in order to allow this research to improve the quality of lives for individuals with gait impairment.

There are several topics that have resulted from these studies that must be considered which range from limitations on current intent recognition systems, cognitive loads, biomechanical effects, and adoption to real-world settings. Future directions can be split into two categories: technical and qualitative feedback. From a technical perspective, there is still a need to develop algorithms that can be robust to user variability across various days of walking, different gait patterns, and more unstructured movements (i.e. shuffling of feet, navigating through obstacles, etc.). The accuracy of these systems need to be much higher in order to avoid fall risk with a powered device. Although the developed intent recognition systems in this dissertation show improved results, there are still limitations to generalizability. A need for having a large dataset is a must in order to capture preferences of walking across individuals with transfemoral amputation. Furthermore, making intent recognition systems more robust to walking patterns and perturbations is a critical need. Although we can show methods of improvement of predicting and estimating tasks, this is still not near functional. There must be virtually no errors especially in mode classification in order for these devices to be used in real-world settings. Future studies should look into exploring deep learning techniques, building adaptive machine learning frameworks that can combine new user data coupled with pre-trained models, and looking into methods of improving/maximizing the learnability of the data set. One limitation of machine learning techniques is that the prediction or estimation is only as good as the data it was trained upon. Other methods that do not require ground truth labels could be explored to approach detecting user intent from a different perspective. Lastly, regardless of how well offline results perform, there must be real-time testing performed to truly understand how to improve the interaction between the user and robotic device. From a qualitative view, the need to properly tune and train users to use the powered prosthesis is critical for the performance of the device. Trust of

the device is one of the harder challenges to overcome. Future research directions need to improve control of these wearable devices to handle variable gait patterns that are present in common everyday tasks.

From the biomechanical results presented in this dissertation, there are trends towards more symmetric gait and energy distributions. From a user's perspective, having a device that can reduce the load on their intact side can improve overall functionality to do more tasks and not exert large amounts of energy. Translational research from able-bodied gait is an important aspect of wearable robotics in general to improve gait mobility. The cognitive load of individuals must also be reduced to not have to consciously think about how they are walking across a variety of tasks. Future studies should explore quantifying this variable on users while using a robotic device. If users have to spend too much time or effort to get the intended functionality of the device, this can reduce motivation and potentially lead to abandonment of this technology. It is imperative that researchers, not only develop the technical aspects of designing and controlling these devices, but create a better user interface to promote human-robot symbiosis. From qualitative feedback that we have received from subjects, the device when functional feels very similar to their intact side. In order for individuals to use these devices, embodiment and understanding of how the device works is key in order to provide seamless assistance.

Lastly, for these devices to be used in the community setting, there are three main thrusts of research that must be made: hardware, control, and biomechanical validation. The overall goal is to identify user intent, adjust control strategies for assisting the user during real-world community ambulation. From a user's perspective, the device must be easy-to-use, robust to different movements, and durable. By incorporating the information learned from this dissertation and future research directions, intelligent prostheses can help enhance mobility to various locomotion tasks compared to currently available devices.

The body of work described in this dissertation has meaningful impact to the clinical populations and in general the advancement of powered prosthetic technology.

Specifically in clinical settings, the intent recognition systems developed through this dissertation should generalizability to multiple walking modes and within context changes (i.e. multiple stair heights and inclination angles.) Another impact of this work is to show that user-independent models can be useful and deployed in real-time. This methodology results in a reduction of many hours of training required for each new user wanting to wear a smart device. Biomechanical advantages of using powered prostheses, can alleviate the burden on users' intact joints resulting in increased ability to walk more, reduce the cognitive load from the user due to the nature of automatic detection of user intent, and even improving overall quality of life. In the context of prosthetic technology, the controllers developed here are shown to allow for these systems to adapt to the environment. As current hardware continues to improve in terms of providing high torques coupled with a low profile weight, intuitive functionality of the device must also be developed. The work described here showed methods of adapting these devices to dynamic changes and making them one step closer to clinical acceptance. The benefit of developing intelligent controllers goes beyond just powered prostheses and in general can be applied to wearable robotics. Research in these fields can be life-changing for individuals with gait impairments. This dissertation here serves as a stepping stone to further enhance intelligent controllers to be able to decipher user intent and ultimately restore functionality as close as possible to the biological limb.

REFERENCES

[1] K. Ziegler-Graham, E. J. MacKenzie, P. L. Ephraim, T. G. Travison, and R. Brookmeyer, "Estimating the Prevalence of Limb Loss in the United States: 2005 to 2050," *Archives of Physical Medicine and Rehabilitation*, vol. 89, no. 3, pp. 422–429, Mar. 2008.

[2] S. K. Au, J. Weber, and H. Herr, "Powered Ankle–Foot Prosthesis Improves Walking Metabolic Economy," *IEEE Transactions on Robotics*, vol. 25, no. 1, pp. 51–66, Feb. 2009.

[3] K. A. Ingraham, N. P. Fey, A. M. Simon, and L. J. Hargrove, "Assessing the relative contributions of active ankle and knee assistance to the walking mechanics of transfemoral amputees using a powered prosthesis," *PLOS ONE*, vol. 11, no. 1, p. 0 147 661, Jan. 2016.

[4] M. J. Highsmith *et al.*, "Low back pain in persons with lower extremity amputation: A systematic review of the literature," *The Spine Journal*, vol. 19, no. 3, pp. 552–563, Mar. 2019.

[5] L. Nolan and A. Lees, "The functional demands on the intact limb during walking for active trans-femoral and trans-tibial amputees," *Prosthetics and Orthotics International*, vol. 24, no. 2, pp. 117–125, Aug. 2000.

[6] R. Gailey, K. Allen, J. Castles, J. Kucharik, and M. Roeder, "Review of secondary physical conditions associated with lower-limb amputation and long-term prosthesis use," vol. 45, no. 1, 2008.

[7] D. C. Morgenroth, M. Roland, A. L. Pruziner, and J. M. Czerniecki, "Transfemoral amputee intact limb loading and compensatory gait mechanics during down slope ambulation and the effect of prosthetic knee mechanisms," *Clinical Biomechanics*, vol. 55, pp. 65–72, Jun. 2018.

[8] P. F. Pasquina *et al.*, "Special Considerations for Multiple Limb Amputation," *Current Physical Medicine and Rehabilitation Reports*, vol. 2, no. 4, pp. 273–289, 2014.

[9] M. R. Tucker *et al.*, *Control strategies for active lower extremity prosthetics and orthotics: A review*, Jan. 2015.

[10] J. L. Johansson, D. M. Sherrill, P. O. Riley, P. Bonato, and H. Herr, "A Clinical Comparison of Variable-Damping and Mechanically Passive Prosthetic Knee Devices," *American Journal of Physical Medicine & Rehabilitation*, vol. 84, no. 8, pp. 563–575, Aug. 2005.

[11] J. A. Kent, K. Z. Takahashi, and N. Stergiou, "Uneven terrain exacerbates the deficits of a passive prosthesis in the regulation of whole body angular momentum in individuals with a unilateral transtibial amputation," *Journal of Neuroengineering and Rehabilitation*, vol. 16, no. 1, p. 25, Feb. 2019.

[12] M. K. Shepherd and E. J. Rouse, "The VSPA Foot: A Quasi-Passive Ankle-Foot Prosthesis With Continuously Variable Stiffness," *IEEE Transactions on Neural Systems and Rehabilitation Engineering*, vol. 25, no. 12, pp. 2375–2386, Dec. 2017.

[13] F. Sup, A. Bohara, and M. Goldfarb, "Design and control of a powered transfemoral prosthesis," *International Journal of Robotics Research*, vol. 27, no. 2, pp. 263–273, Feb. 2008, From Duplicate 3 (Design and control of a powered transfemoral prosthesis - Sup, F; Bohara, A; Goldfarb, M) 0278-3649.

[14] B. E. Lawson, J. Mitchell, D. Truex, A. Shultz, E. Ledoux, and M. Goldfarb, "A robotic leg prosthesis: Design, control, and implementation," *IEEE Robotics and Automation Magazine*, vol. 21, no. 4, pp. 70–81, Dec. 2014.

[15] T. Elery, S. Rezazadeh, C. Nesler, J. Doan, H. Zhu, and R. Gregg, "Design and benchtop validation of a powered knee-ankle prosthesis with high-torque, low-impedance actuators," *IEEE Int. Conf. Robot. Automat.*, pp. 2788–2795, 2018.

[16] A. M. El-Sayed, N. A. Hamzaid, and N. A. Abu Osman, "Technology efficacy in active prosthetic knees for transfemoral amputees: A quantitative evaluation," *TheScientificWorldJournal*, vol. 2014, p. 297 431, 2014.

[17] A. F. Azocar, S. Member, L. M. Mooney, L. J. Hargrove, and E. J. Rouse, "Design and characterization of an open-source robotic leg prosthesis," in *2018 7th IEEE International Conference on Biomedical Robotics and Biomechatronics (Biorob)*, 2018, pp. 111–118, ISBN: 978-1-5386-8182-4.

[18] A. F. Azocar, L. M. Mooney, J. F. Duval, A. M. Simon, L. J. Hargrove, and E. J. Rouse, "Design and clinical implementation of an open-source bionic leg," *Nature Biomedical Engineering*, vol. 4, no. 10, pp. 941–953, Oct. 2020.

[19] M. E. Carney, T. Shu, R. Stolyarov, J.-F. Duval, and H. M. Herr, "Design and Preliminary Results of a Reaction Force Series Elastic Actuator for Bionic Knee and Ankle Prostheses," *IEEE Transactions on Medical Robotics and Bionics*, vol. 3, no. 3, pp. 542–553, Aug. 2021.

[20] H. Zhao, E. Ambrose, and A. D. Ames, "Preliminary results on energy efficient 3D prosthetic walking with a powered compliant transfemoral prosthesis," in *2017 IEEE International Conference on Robotics and Automation (ICRA)*, 2017, pp. 1140–1147, ISBN: 978-1-5090-4633-1.

[21] J. M. Caputo and S. H. Collins, "An experimental robotic testbed for accelerated development of ankle prostheses," *Proceedings - IEEE International Conference on Robotics and Automation*, pp. 2645–2650, 2013.

[22] C. D. Hoover, G. D. Fulk, and K. B. Fite, "The design and initial experimental validation of an active myoelectric transfemoral prosthesis," *Journal of Medical Devices*, vol. 6, no. 1, p. 011 005, 2012.

[23] E. C. Martinez-Villalpando, L. Mooney, G. Elliott, and H. Herr, "Antagonistic active knee prosthesis. A metabolic cost of walking comparison with a variable-damping prosthetic knee," *Annual International Conference of the IEEE Engineering in Medicine and Biology Society. IEEE Engineering in Medicine and Biology Society. Annual International Conference*, vol. 2011, pp. 8519–8522, 2011.

[24] S. Rezazadeh, D. Quintero, N. Divekar, and R. D. Gregg, "A phase variable approach to volitional control of powered knee-ankle prostheses," 2018, pp. 2292–2298.

[25] N. Hogan, "Impedance control: An approach to manipulation: Part III-applications," *Journal of Dynamic Systems, Measurement and Control, Transactions of the ASME*, vol. 107, no. 1, pp. 17–24, 1985.

[26] A. M. Simon *et al.*, "Configuring a powered knee and ankle prosthesis for transfemoral amputees within five specific ambulation modes," *PLoS ONE*, vol. 9, no. 6, e99387, 2014.

[27] M. Liu, F. Zhang, P. Datseris, and H. H. Huang, "Improving finite state impedance control of active-transfemoral prosthesis using dempster-shafer based state transition rules," *Journal of Intelligent and Robotic Systems: Theory and Applications*, vol. 76, no. 3-4, pp. 461–474, Dec. 2014.

[28] M. F. Eilenberg, H Geyer, and H Herr, "Control of a powered ankle-foot prosthesis based on a neuromuscular model," *IEEE Transactions on Neural Systems and Rehabilitation Engineering*, vol. 18, no. 2, pp. 164–173, 2010.

[29] D. Quintero, D. J. Villarreal, D. J. Lambert, S. Kapp, and R. D. Gregg, "Continuous-phase control of a powered knee-ankle prosthesis: Amputee experiments across speeds and inclines," *IEEE Transactions on Robotics*, pp. 1–16, 2018.

[30] V. Azimi, T. Shu, H. Zhao, E. Ambrose, A. D. Ames, and D. Simon, "Robust control of a powered transfemoral prosthesis device with experimental verification," *Proceedings of the American Control Conference*, pp. 517–522, 2017.

[31] N Aghasadeghi, Z Huihua, L Hargrove, A Ames, E Perreault, and T Bretl, "Learning impedance controller parameters for lower-limb prostheses," in *2013 IEEE/RSJ International Conference on Intelligent Robots and Systems*, Tokyo, Japan, 2013.

[32] S.-K. Wu, G. Waycaster, and X. Shen, "Electromyography-based control of active above-knee prostheses," *Control Engineering Practice*, vol. 19, no. 8, pp. 875–882, Aug. 2011.

[33] H. Huang, F. Zhang, L. J. Hargrove, Z. Dou, D. R. Rogers, and K. B. Englehart, "Continuous locomotion-mode identification for prosthetic legs based on neuromuscular - Mechanical fusion," *IEEE Transactions on Biomedical Engineering*, vol. 58, no. 10 PART 1, pp. 2867–2875, Oct. 2011.

[34] A. J. Young, A. M. Simon, N. P. Fey, and L. J. Hargrove, "Intent recognition in apowered lower limb prosthesis using time history information," *Annals of Biomedical Engineering*, vol. 42, no. 3, pp. 631–641, Mar. 2013.

[35] A Young, A Simon, and L Hargrove, "A training method for locomotion mode prediction using powered lower limb prostheses," *IEEE Transactions on Neural Systems and Rehabilitation Engineering*, vol. 22, no. 3, pp. 671–677, 2014.

[36] H. A. Varol, F. Sup, and M. Goldfarb, "Multiclass real-time intent recognition of a powered lower limb prosthesis," *IEEE Transactions on Biomedical Engineering*, vol. 57, no. 3, pp. 542–551, Mar. 2010.

[37] J. A. Spanias, A. M. Simon, S. B. Finucane, E. J. Perreault, and L. J. Hargrove, "Online adaptive neural control of a robotic lower limb prosthesis," *Journal of Neural Engineering*, vol. 15, no. 1, p. 016 015, Feb. 2018.

[38] L. J. Hargrove *et al.*, "Intuitive control of a powered prosthetic leg during ambulation: A randomized clinical trial," *JAMA : the journal of the American Medical Association*, vol. 313, no. 22, pp. 2244–2252, 2015.

[39] A. J. Young and L. J. Hargrove, "A classification method for user-independent intent recognition for transfemoral amputees using powered lower limb prostheses," *IEEE Transactions on Neural Systems and Rehabilitation Engineering*, vol. 24, no. 2, pp. 217–225, Feb. 2016.

[40] Y. Ding, I. Galiana, C. Siviy, F. A. Panizzolo, and C. Walsh, *IMU-based Iterative Control for Hip Extension Assistance with a Soft Exosuit*, Stockholm, Sweden, 2016.

[41] A. M. Sabatini, "Kalman-filter-based orientation determination using inertial/magnetic sensors: Observability analysis and performance evaluation," *Sensors (Basel, Switzerland)*, vol. 11, no. 10, pp. 9182–9206, 2011.

[42] H. Huang, T. A. Kuiken, and R. D. Lipschutz, "A Strategy for Identifying Locomotion Modes Using Surface Electromyography," *IEEE Transactions on Biomedical Engineering*, vol. 56, no. 1, pp. 65–73, Jan. 2009.

[43] A. J. Young, A. M. Simon, and L. J. Hargrove, "A training method for locomotion mode prediction using powered lower limb prostheses," *IEEE Transactions on Neural Systems and Rehabilitation Engineering*, vol. 22, no. 3, pp. 671–677, 2014.

[44] A. M. Simon *et al.*, "Delaying ambulation mode transition decisions improves accuracy of a flexible control system for powered knee-ankle prosthesis," *IEEE Transactions on Neural Systems and Rehabilitation Engineering*, vol. 25, no. 8, pp. 1164–1171, 2017.

[45] A. J. Young, L. H. Smith, E. J. Rouse, and L. J. Hargrove, "A comparison of the real-time controllability of pattern recognition to conventional myoelectric control for discrete and simultaneous movements," *Journal of Neuroengineering and Rehabilitation*, vol. 11, 2014, Times Cited: 0.

[46] J. A. Brantley, T. P. Luu, S. Nakagome, and J. L. Contreras-Vidal, "Towards the development of a hybrid neural-machine interface for volitional control of a powered lower limb prosthesis," in *2017 International Symposium on Wearable Robotics and Rehabilitation (WeRob)*, IEEE, Nov. 2017, pp. 1–1, ISBN: 978-1-5386-4377-8.

[47] J. M. Canino and K. B. Fite, "Haptic feedback in lower-limb prosthesis: Combined haptic feedback and EMG control of a powered prosthesis," *2016 IEEE EMBS International Student Conference: Expanding the Boundaries of Biomedical Engineering and Healthcare, ISC 2016 - Proceedings*, pp. 1–4, May 2016.

[48] K. H. Ha, H. A. Varol, and M. Goldfarb, "Volitional control of a prosthetic knee using surface electromyography," *IEEE transactions on bio-medical engineering*, vol. 58, no. 1, pp. 144–151, Jan. 2011.

[49] F. Zhang, M. Liu, and H. Huang, "Effects of locomotion mode recognition errors on volitional control of powered above-knee prostheses," *IEEE Transactions on Neural Systems and Rehabilitation Engineering*, vol. 23, no. 1, pp. 64–72, Jan. 2015.

[50] A. Sabatini, C. Martelloni, S. Scapellato, and F. Cavallo, "Assessment of walking features from foot inertial sensing," *IEEE Transactions on Biomedical Engineering*, vol. 52, no. 3, pp. 486–494, Mar. 2005.

[51] F. Sup, H. A. Varol, and M. Goldfarb, "Upslope Walking With a Powered Knee and Ankle Prosthesis: Initial Results With an Amputee Subject," *IEEE Transactions on Neural Systems and Rehabilitation Engineering*, vol. 19, no. 1, pp. 71–78, Feb. 2011.

[52] J.-S. Hu, K.-C. Sun, and C.-Y. Cheng, "A Kinematic Human-Walking Model for the Normal-Gait-Speed Estimation Using Tri-Axial Acceleration Signals at Waist Location," *IEEE Transactions on Biomedical Engineering*, vol. 60, no. 8, pp. 2271–2279, Aug. 2013.

[53] I. Kang, P. Kunapuli, H. Hsu, and A. J. Young, "Electromyography (EMG) Signal Contributions in Speed and Slope Estimation Using Robotic Exoskeletons," *IEEE ... International Conference on Rehabilitation Robotics: [proceedings]*, vol. 2019, pp. 548–553, Jun. 2019.

[54] B. Dauriac, X. Bonnet, H. Pillet, and F. Lavaste, *Estimation of the walking speed of individuals with transfemoral amputation from a single prosthetic shank-mounted IMU - Boris Dauriac, Xavier Bonnet, Helene Pillet, Francois Lavaste, 2019*, https://journals.sagepub.com/doi/full/10.1177/0954411919858468.

[55] J. M. Czerniecki and D. C. Morgenroth, "Metabolic energy expenditure of ambulation in lower extremity amputees: What have we learned and what are the next steps?" *Disability and Rehabilitation*, pp. 1–9, 2015.

[56] E. J. Rouse, L. M. Mooney, E. C. Martinez-villalpando, H. M. Herr, and M. Ieee, "Clutchable series-elastic actuator : Design of a robotic knee prosthesis for minimum energy consumption," *2013 IEEE International Conference on Rehabilitation Robotics*, no. 1122374, 2013.

[57] A. M. Simon, N. P. Fey, K. A. Ingraham, S. B. Finucane, E. G. Halsne, and L. J. Hargrove, "Improved weight-bearing symmetry for transfemoral amputees during standing up and sitting down with a powered knee-ankle prosthesis," *Archives of Physical Medicine and Rehabilitation*, vol. 97, no. 7, pp. 1100–1106, Jul. 2016.

[58] H. M. Herr and A. M. Grabowski, "Bionic ankle–foot prosthesis normalizes walking gait for persons with leg amputation," *Proceedings of the Royal Society B: Biological Sciences*, vol. 279, no. 1728, pp. 457–464, Feb. 2012.

[59] E. Russell Esposito, J. M. Aldridge Whitehead, and J. M. Wilken, "Step-to-step transition work during level and inclined walking using passive and powered ankle–foot prostheses," *Prosthetics and Orthotics International*, vol. 40, no. 3, pp. 311–319, Jun. 2016.

[60] B. Y. Su, J. Wang, S. Q. Liu, M. Sheng, J. Jiang, and K. Xiang, "A cnn-based method for intent recognition using inertial measurement units and intelligent

lower limb prosthesis," *IEEE Transactions on Neural Systems and Rehabilitation Engineering*, vol. 27, no. 5, pp. 1032–1042, May 2019.

[61] R. B. Woodward, J. A. Spanias, and L. J. Hargrove, "User intent prediction with a scaled conjugate gradient trained artificial neural network for lower limb amputees using a powered prosthesis," in *Proceedings of the Annual International Conference of the IEEE Engineering in Medicine and Biology Society, EMBS*, vol. 2016-Octob, Institute of Electrical and Electronics Engineers Inc., Oct. 2016, pp. 6405–6408, ISBN: 978-1-4577-0220-4.

[62] L. J. Hargrove, K. Englehart, and B. Hudgins, "A comparison of surface and intramuscular myoelectric signal classification," *IEEE Transactions on Biomedical Engineering*, vol. 54, no. 5, pp. 847–853, May 2007.

[63] D. Nielsen, "Tree boosting with XGBoost why does XGBoost win "Every" machine learning competition?" NTNU, Tech. Rep., 2016.

[64] B. Semiz, S. Hersek, D. C. Whittingslow, L. A. Ponder, S. Prahalad, and O. T. Inan, "Using knee acoustical emissions for sensing joint health in patients with juvenile idiopathic arthritis: A pilot study," *IEEE Sensors Journal*, vol. 18, no. 22, pp. 9128–9136, 2018.

[65] H. Lu, M. Pinaroc, M. Lv, S. Sun, H. Han, and R. C. Shah, "Locomotion recognition using XGboost and neural network ensemble," in *UbiComp/ISWC 2019- - Adjunct Proceedings of the 2019 ACM International Joint Conference on Pervasive and Ubiquitous Computing and Proceedings of the 2019 ACM International Symposium on Wearable Computers*, Association for Computing Machinery, Inc, Sep. 2019, pp. 757–760, ISBN: 978-1-4503-6869-8.

[66] Y. Ye, C. Liu, N. Zemiti, and C. Yang, "Optimal feature selection for EMG-Based finger force estimation using LightGBM model," in *2019 28th IEEE International Conference on Robot and Human Interactive Communication, RO-MAN 2019*, Institute of Electrical and Electronics Engineers Inc., Oct. 2019, ISBN: 978-1-72812-622-7.

[67] A. Kadrolkar and F. C. Sup, "Intent recognition of torso motion using wavelet transform feature extraction and linear discriminant analysis ensemble classification," *Biomedical Signal Processing and Control*, vol. 38, pp. 250–264, Sep. 2017.

[68] T. Chen and C. Guestrin, "XGBoost: A scalable tree boosting system," in *Proceedings of the ACM SIGKDD International Conference on Knowledge Discovery and Data Mining*, vol. 13-17-Augu, Association for Computing Machinery, Aug. 2016, pp. 785–794, ISBN: 978-1-4503-4232-2. arXiv: 1603.02754.

[69] S. Ben Taieb and R. J. Hyndman, "A gradient boosting approach to the Kaggle load forecasting competition," *International Journal of Forecasting*, vol. 30, no. 2, pp. 382–394, Apr. 2014.

[70] R. Mitchell and E. Frank, "Accelerating the XGBoost algorithm using GPU computing," *PeerJ Computer Science*, vol. 2017, no. 7, e127, Jul. 2017.

[71] N. Shawen *et al.*, "Fall detection in individuals with lower limb amputations using mobile phones: Machine learning enhances robustness for real-world applications," *JMIR mHealth and uHealth*, vol. 5, no. 10, e151, Oct. 2017.

[72] C. Wang, X. Wu, Y. Ma, G. Wu, and Y. Luo, "A flexible lower extremity exoskeleton robot with deep locomotion mode identification," *Hindawi*, p. 9, 2018.

[73] F. Peng, W. Peng, and C. Zhang, "Evaluation of sEMG-Based feature extraction and effective classification method for gait phase detection," in *Communications in Computer and Information Science*, vol. 1006, Springer Verlag, Nov. 2019, pp. 138–149, ISBN: 9789811379857.

[74] S. Nakagome, T. P. Luu, Y. He, A. S. Ravindran, and J. L. Contreras-Vidal, "An empirical comparison of neural networks and machine learning algorithms for EEG gait decoding," *Scientific Reports*, vol. 10, no. 1, pp. 1–17, Dec. 2020.

[75] K. Bhakta, J. Camargo, and A. J. Young, "Control and experimental validation of a powered knee and ankle prosthetic device," in *ASME 2018 Dynamic Systems and Control Conference, DSCC 2018*, vol. 1, American Society of Mechanical Engineers (ASME), Nov. 2018, ISBN: 978-0-7918-5189-0.

[76] K. Bhakta, J. Camargo, P. Kunapuli, L. Childers, and A. Young, "Impedance control strategies for enhancing sloped and level walking capabilities for individuals with transfemoral amputation using a powered multi-joint prosthesis," *Military Medicine*, vol. 185, no. Supplement_1, pp. 490–499, Jan. 2020.

[77] K. Englehart and B. Hudgins, "A robust, real-time control scheme for multifunction myoelectric control," *IEEE Transactions on Biomedical Engineering*, vol. 50, no. 7, pp. 848–854, 2003.

[78] S Martin and D Macisaac, "Innervation zone shift with changes in joint angle in the brachial biceps," vol. 16, pp. 144–148, 2006.

[79] R. L. Waters and S. Mulroy, "The energy expenditure of normal and pathologic gait," *Gait & Posture*, vol. 9, no. 3, pp. 207–231, Jul. 1999.

[80] Q. Li, M. Young, V. Naing, and J. M. Donelan, "Walking speed estimation using a shank-mounted inertial measurement unit," *Journal of Biomechanics*, vol. 43, no. 8, pp. 1640–1643, 2010.

[81] B. Mariani, C. Hoskovec, S. Rochat, C. Büla, J. Penders, and K. Aminian, "3D gait assessment in young and elderly subjects using foot-worn inertial sensors," *Journal of Biomechanics*, vol. 43, no. 15, pp. 2999–3006, Nov. 2010.

[82] K Aminian, B Najafi, C Bula, P. F. Leyvraz, and P Robert, "Spatio-temporal parameters of gait measured by an ambulatory system using miniature gyroscopes.," *Journal of Biomechanics*, vol. 35, no. 5, pp. 689–699, 2002, have ProCite field[38]: 21953078.

[83] Z. He and W. Zhang, "Estimation of Walking Speed Using Accelerometer and Artificial Neural Networks," in *Computer Science for Environmental Engineering and EcoInformatics*, Y. Yu, Z. Yu, and J. Zhao, Eds., ser. Communications in Computer and Information Science, Berlin, Heidelberg: Springer, 2011, pp. 42–47, ISBN: 978-3-642-22691-5.

[84] H. Vathsangam, B. A. Emken, D. Spruijt-Metz, and G. Sukhatme, "Toward free-living walking speed estimation using Gaussian Process-based Regression with on-body accelerometers and gyroscopes," *2010 4th International Conference on Pervasive Computing Technologies for Healthcare*, 2010.

[85] S. Zihajehzadeh and E. J. Park, "Regression Model-Based Walking Speed Estimation Using Wrist-Worn Inertial Sensor," *PLOS ONE*, vol. 11, no. 10, e0165211, Oct. 2016.

[86] R. S. McGinnis *et al.*, "A machine learning approach for gait speed estimation using skin-mounted wearable sensors: From healthy controls to individuals with multiple sclerosis," *PLoS One*, vol. 12, no. 6, Jun. 2017, Publisher Copyright: © 2017 McGinnis et al. This is an open access article distributed under the terms of the Creative Commons Attribution License, which permits unrestricted use, distribution, and reproduction in any medium, provided the original author and source are credited.

[87] S. Byun, H. J. Lee, J. W. Han, J. S. Kim, E. Choi, and K. W. Kim, "Walking-speed estimation using a single inertial measurement unit for the older adults," *PLOS ONE*, vol. 14, no. 12, e0227075, Dec. 2019.

[88] A Soltani, *A. Soltani, H. Dejnabadi, M. Savary, and K. Aminian, "Real-world gait speed estimation using wrist sensor: A. personalized approach," IEEE J. Biomed. Health Inform., vol. 24, no. 3, pp. 658–668, Mar. 2020. - Google Search.*

[89] G. Bastas, J. J. Fleck, R. A. Peters, and K. E. Zelik, "IMU-based gait analysis in lower limb prosthesis users: Comparison of step demarcation algorithms," *Gait and Posture*, vol. 64, pp. 30–37, Jul. 2018.

[90] C. Duraffourg, X. Bonnet, B. Dauriac, and H. Pillet, "Real Time Estimation of the Pose of a Lower Limb Prosthesis from a Single Shank Mounted IMU," *Sensors (Basel, Switzerland)*, vol. 19, no. 13, p. 2865, Jun. 2019.

[91] P. Probst, A.-L. Boulesteix, and B. Bischl, "Tunability: Importance of Hyperparameters of Machine Learning Algorithms," p. 32,

[92] M. Bellmann, T. Schmalz, E. Ludwigs, and S. Blumentritt, "Immediate Effects of a New Microprocessor-Controlled Prosthetic Knee Joint: A Comparative Biomechanical Evaluation," *Archives of Physical Medicine and Rehabilitation*, vol. 93, no. 3, pp. 541–549, Mar. 2012.

[93] R. B. Woodward, A. M. Simon, E. A. Seyforth, and L. J. Hargrove, "Real-Time Adaptation of an Artificial Neural Network for Transfemoral Amputees using a Powered Prosthesis," *IEEE Transactions on Biomedical Engineering*, pp. 1–1, 2021.

[94] J. Camargo, A. Ramanathan, W. Flanagan, and A. Young, "A comprehensive, open-source dataset of lower limb biomechanics in multiple conditions of stairs, ramps, and level-ground ambulation and transitions," *Journal of Biomechanics*, vol. 119, p. 110 320, Apr. 2021.

[95] K. Bhakta, J. Camargo, L. Donovan, K. Herrin, and A. Young, "Machine Learning Model Comparisons of User Independent amp; Dependent Intent Recognition Systems for Powered Prostheses," *IEEE Robotics and Automation Letters*, vol. 5, no. 4, pp. 5393–5400, Oct. 2020.

[96] K. Lechler and K Kristjansson, "The importance of additional mid swing toe clearance for amputees. Canadian Prosthetics & Orthotics Journal.," Oct. 2019.

[97] H. Hobara *et al.*, "Lower extremity joint kinematics of stair ascent in transfemoral amputees," *Prosthetics and Orthotics International*, vol. 35, no. 4, pp. 467–472, Dec. 2011.

[98] T. Schmalz, S. Blumentritt, and B. Marx, "Biomechanical analysis of stair ambulation in lower limb amputees," *Gait & posture*, vol. 25, no. 2, pp. 267–278, 2007.

[99] X. Bonnet, C. Villa, I. Loiret, F. Lavaste, and H. Pillet, "Distribution of joint work during walking on slopes among persons with transfemoral amputation," *Journal of Biomechanics*, vol. 129, p. 110 843, Dec. 2021.

[100] E. J. Wolf, V. Q. Everding, A. L. Linberg, B. L. Schnall, J. M. Czerniecki, and J. M. Gambel, "Assessment of transfemoral amputees using C-Leg and Power Knee for ascending and descending inclines and steps," *The Journal of Rehabilitation Research and Development*, vol. 49, no. 6, p. 831, Jun. 2012.

[101] Z. M. Abdulhasan, A. J. Scally, and J. G. Buckley, "Gait termination on a declined surface in trans-femoral amputees: Impact of using microprocessor-controlled limb system," *Clinical Biomechanics*, vol. 57, pp. 35–41, Aug. 2018.

[102] M. P. Mileusnic, L. Rettinger, M. J. Highsmith, and A. Hahn, "Benefits of the Genium microprocessor controlled prosthetic knee on ambulation, mobility, activities of daily living and quality of life: A systematic literature review," *Disability and Rehabilitation: Assistive Technology*, vol. 16, no. 5, pp. 453–464, Jul. 2021.

[103] Y. Okita *et al.*, "Intra-individual biomechanical effects of a non-microprocessor-controlled stance-yielding prosthetic knee during ramp descent in persons with unilateral transfemoral amputation," *Prosthetics and Orthotics International*, vol. 43, no. 1, pp. 55–61, Feb. 2019.

[104] K. R. Kaufman, S. Frittoli, and C. A. Frigo, "Gait asymmetry of transfemoral amputees using mechanical and microprocessor-controlled prosthetic knees," *Clinical Biomechanics (Bristol, Avon)*, vol. 27, no. 5, pp. 460–465, Jun. 2012.

[105] B Lawson, A Varol, A Huff, E Erdemir, and M Goldfarb, "Control of stair ascent and descent with a powered transfemoral prosthesis," *IEEE Transactions on Neural Systems and Rehabilitation Engineering*, vol. 21, no. 466-473, 2013.

[106] E. D. Ledoux, B. E. Lawson, A. H. Shultz, H. L. Bartlett, and M. Goldfarb, "Metabolics of stair ascent with a powered transfemoral prosthesis," *Annual International Conference of the IEEE Engineering in Medicine and Biology Society. IEEE Engineering in Medicine and Biology Society. Annual International Conference*, vol. 2015, pp. 5307–5310, 2015.

[107] E. D. Ledoux and M. Goldfarb, "Control and evaluation of a powered transfemoral prosthesis for stair ascent," *IEEE Transactions on Neural Systems and Rehabilitation Engineering*, vol. 25, no. 7, pp. 917–924, 2017.

[108] A. Parri *et al.*, "Whole Body Awareness for Controlling a Robotic Transfemoral Prosthesis," *Frontiers in Neurorobotics*, vol. 11, p. 25, 2017.

[109] M. J. Highsmith, J. T. Kahle, and L. Stephanie, *Kinetic Differences Using a Power Knee and C-Leg While itting Down and Standing Up: A Case Report. JPO: Journal of Prosthetics and Orthotics*.

[110] J. Camargo, A. Ramanathan, N. Csomay-Shanklin, and A. Young, "Automated gap-filling for marker-based biomechanical motion capture data," *Computer Methods in Biomechanics and Biomedical Engineering*, vol. 23, no. 15, pp. 1180–1189, Nov. 2020.

[111] L. Nolan, A. Wit, K. Dudziñski, A. Lees, M. Lake, and M. Wychowañski, "Adjustments in gait symmetry with walking speed in trans-femoral and trans-tibial amputees," *Gait & Posture*, vol. 17, no. 2, pp. 142–151, Apr. 2003.

VITA

Krishan Bhakta was born November 21, 1996 and is from Santa Fe, New Mexico. He did his bachelor's in mechanical engineering at New Mexico Tech and joined the PhD program in mechanical engineering at Georgia Tech as a graduate research assistant. He joined the EPIC lab to develop wearable robots that could help people. He loves to learn and is always excited to talk with people about different ideas/projects. Outside of his professional career, he is an avid sports fan. He plays basketball in his spare time and will always have time for a game of pick-up.